Charles University in Prague

Faculty of Science

Department of Physical and Macromolecular Chemistry

PH.D. THESIS

Multireference Brillouin-Wigner Coupled Clusters Method with Connected Triple Excitations

Ondřej Demel

Abstract

The multireference Brillouin-Wigner coupled clusters method with connected triple excitations has been developed and implemented in the ACES II program. This method provides an accurate description of both the static and dynamic correlation, and is thus suitable for chemical systems with quaside-generacies, e.g. in cases of bond breaking, studies of larger sections of potential energy surface, and systems with multi-determinantal character like diradicals.

The connected triples were included in both iterative and noniterative way. The iterative approach is more rigorous and conceptually straightforward, but computationally more demanding than the noniterative one.

The iterative inclusion of connected triples was done in two successive steps. First, in the MR BWCCSDTα method, all terms except for the disconnected and unlinked ones in the T_3 equation have been included. Second, the missing terms were included to obtain the MR BWCCSDT method.

The noniterative inclusion of connected triples was based on triples correction to matrix elements of the effective Hamiltonian, which yield the total energy by diagonalization. In the MR BWCCSD(T_d) method only the diagonal elements of effective Hamiltonian are corrected, wheres in MR BWCCSD(T) method correction is performed for all the elements. In all cases, the triples correction is done after the size-extensivity correction.

In order to assess the performance of the newly developed methods, following four systems were studied: low lying electronic states of the oxygen molecule, C_{2v} insertion pathway of Be to H_2, singlet-triplet gaps of methylene and silylene, and the automerization barrier of cyclobutadiene.

Acknowledgment

Table of contents

6

Chapter 1

Introduction

1.1 Historical review

There is little doubt that the coupled clusters method is today one of the most commonly used ab initio methods in quantum chemistry. The reason behind its success is the size extensivity and high accuracy compared to other methods with comparable computational demands.

The basic idea of the approach is the exponential ansatz with the cluster operator, which leads both to the size-extensivity and to the inclusion of the dominant part of tetraexcitations even when the cluster operator is truncated to biexcitations.

The coupled clusters method was first proposed by Coester and Kümmel [1–3] for atomic nuclei. Their main inspiration was the concept of the exponential ansatz of wavefunction, proposed for the description of the bound state by Gell-Mann and Low [4] and Hubbard [5]. This lead to the idea to calculate directly the cluster amplitudes instead of perturbation contributions to the energy.

It was introduced into the world of quantum chemistry in 1966 by Čížek [6], who was also the first who derived the explicit form of the cluster equations. His work contained a general formulation of coupled clusters theory, as well as an illustrative example of the CPMET method, which is today denoted as CCD. However, the complexity of the theoretical aspects of the method prevented it for years from becoming widespread.

Great progress was achieved in late seventies due to the availability of work station computers. First general codes for the CCD method were presented simultaneously in 1978 by groups of Rodney J. Bartlett [7] and John

A. Pople [8]. Since then, the coupled clusters method has been included into vast majority of quantum chemistry programs.

The CCD method was extended by the inclusion of connected singles into CCSD [9]. Soon it became clear, that in order to achieve higher accuracy, it is necessary to include connected triple excitations. Tetraexcitations, which are the most important contribution after biexcitations, were sufficiently included even at the CCD level due to the exponential ansatz, while the role of connected quadruples is generally very small. However, for triexcitations the connected triples constitute the main contribution.

The full inclusion of connected triples, i.e. the CCSDT method [10–14], was found to be computationally too expensive for most of the systems, due to the n^8 scaling. Therefore, suitable approximations, both iterative [10, 11, 15–17] and noniterative [16, 18–24], were formulated. Among these, the most successful became the CCSD(T) method [20–23] with the n^7 scaling and balanced treatment of the fourth and fifth order contributions to the energy.

After the connected triples, also the inclusion of connected quadruples [25, 26] and pentuples [27] has been performed. A procedure for general truncation of the cluster operator has been also developed [28].

More detailed historical reviews can be found in [29–33].

1.2 Multireference coupled clusters methods

As for today, the CCSD and CCSD(T) methods are widespread and commonly used for small and medium sized systems. However, like other single reference approaches, standard coupled clusters method gives rather poor performance for systems with quasi-degenerate boundary orbitals, unless very high excitations are included in the cluster operator. These quasidegenerate systems are often encountered in many problems of great chemical interest, particularly in cases of breaking of chemical bond, calculations of larger sections of potential energy surface, and studies of states with a multideterminantal character, like diradicals. In these situations, it is highly desirable and convenient to use a multireference scheme.

The generalization of coupled clusters approach to the multireference scheme has therefore become a subject of interest. However, the task is conceptually rather difficult, due to the fact, that the generalization of the exponential ansatz to the multireference case is not unique. Furthermore, these

9

methods often suffer from high complexity of working equations, extremely large computational demands, intruder state problems, or size-inextensivity.

There are several groups of multireference coupled clusters methods. In the Fock space or valence universal methods [34–40] there is only one cluster operator for all the reference configurations. In the case of the Hilbert space methods [41–46], each of the reference configurations has its own cluster operator. The latter group is then divided into the state specific and state universal subgroups. The state universal methods study all the electronic states within the given model space at once and all the eigenvalues of the effective Hamiltonian have a physical meaning. For state specific methods [47,48], one state is studied at time, only the selected eigenvalue has a physical meaning, and the remaining ones are purely artificial.

All these approaches use the effective Hamiltonian formalism. The cluster amplitudes are found by solving the Bloch equation. The energy is obtained as a eigenvalue of the nonhermitian effective Hamiltonian matrix. For majority of these methods is also characteristic the intermediate normalization of the projected wavefunctions.

Besides these multireference coupled clusters methods, there exist also other state specific approaches which are not based on the Hilbert or Fock space formalism. Some of these methods use basically a single reference formalism with the inclusion of a subset of important higher excitations. This can be performed in a standard way [49, 50], or implicitly [51–57], or using so called externally corrected approaches, which can be divided into amplitude [58–63] or energy [64–66] type. The latter of these approaches is closely related to the renormalized CCSD(T) method [67,68]. In connection to indirect multireference coupled clusters methods are also often mentioned the equation of motion (EOM) [69–72] and similarity transformed equation of motion (STEOM) coupled clusters methods [73–76]. Between multireference coupled clusters and configuration interaction lie the multireference linear CC (MR LCCM) method [77], multireference averaged quadratic CC (MR AQCC) method [78–80], multireference averaged coupled pair (MR ACPF) method [81], and multireference coupled electron pair approximation (MR CEPA) [82].

The multireference Brillouin-Wigner coupled clusters method is one of the Hilbert space state specific methods. It was proposed by Hubač, Čársky, and Mášik [83–85], who also developed a pilot implementation for calculations with two reference functions. An efficient implementation in the ACES II program, which allows to perform calculations with an arbitrary number of references including open shell ones, has been implemented by Pittner et.

al. [86–89]. The main advantages of this approach are the linear scaling of its computational complexity with the number of reference configurations and avoidance of intruder states due to the denominator shift. The most important drawback of this scheme is the size-inextensivity of the method. Therefore, various size-extensivity corrections have been developed [90–92].

The implementation of MR BWCC method enabled investigation of numerous chemical systems. These included studies of singlet-triplet gaps in methylene, silylene, twisted ethylene [93], tetramethylethylene [86], alkylcarbenes [94] and trimethylenemethane [95]. Further studies investigated the potential curves and surfaces of oxygen [96], fluorine [87], iodine bromide [97], beryllium hydride [88], calcium carbide [98] and beryllium carbide [99] . Among the studies of moderately sized systems are the automerization barrier of cyclobutadiene [100] and the Bergman reaction [101].

1.3   Why connected triples?

The studies mentioned above numerically verified the ability of the MR BWCC method to include the static correlation at a very satisfactory level. However, as the MR BWCC method was developed only with inclusion of connected singles and doubles (i.e. MR BWCCSD method), it was often found that the inclusion of dynamic correlation is far from quantitative.

A very good example of this behavior was the study of the low lying electronic states of the oxygen molecule [96]. The calculations were performed using the standard Dunnings's cc-pVTZ basis set [102]. The model space was spanned by four reference configurations formed within the π_g antibonding orbitals occupied by two electrons. The spectroscopic constants were obtained by Dunham's type polynomial expansion of the potential curves.

MR BWCCSD provides good values of most of the spectroscopic constants. However, the vibrational frequency is sensitive to the potential energy curve in the vicinity of the equilibrium geometry, and, therefore, it is sensitive to the description of dynamic correlation, with the static correlation playing only a minor role. The vibrational frequency is here overestimated by approximately 100 cm^{-1}. This difference is not caused by the basis set used, since the vibrational frequency increases with the size of the basis set. On the other hand, standard single reference CCSD(T) method provides a value only 10 cm^{-1} above the experiment.

The accuracy of the vibrational frequencies obtained is even lower for the excited states. The vibrational frequencies are overestimated by approx-

imately 120 wavenumbers for the $a^1\Delta_g$ state and 145 cm^{-1} for $b^1\Sigma_g^+$ state. The situation is improved when additional four reference configurations are used, but the improvement is not large enough and it is clear that the description of static correlation itself is not sufficient without an accurate inclusion of dynamic correlation.

For higher accuracy it is therefore inevitable to improve the description of dynamic correlation. That implies the inclusion of connected triples to the expansion of the cluster operator.

The first multireference coupled clusters method with connected triples was the MR CCSD(T) by Balková and Bartlett [46], which was based on the state universal Rayleigh-Schrödinger coupled clusters method by Kucharski and Bartlett [42]. Recently, there has been a great progress in this field and several new approaches emerged. These include the state-universal coupled clusters method with diagonal perturbative triples correction by Li and Paldus [103, 104], the Fock space multireference coupled clusters method with noniterative triples by Vaval, Pal and Mukherjee [105], and with full connected triples by Musial and Bartlett [106].

1.4   The subject and aim of the thesis

Like in the case of single reference coupled clusters method, there are several ways how to include connected triple excitations. The rigorous approach is based on explicit inclusion of connected triples within the cluster operator. That requires solving the cluster amplitude equations for connected triples. As these equations are solved iteratively, it is said that the connected triples are included iteratively.

However, the full inclusion of connected triples is computationally very demanding. It is therefore necessary to make further approximations which would include the dominant part of triples contribution at a limited computational cost. Therefore methods, where the connected triples are included only perturbatively in one step at the end of the calculation, were developed. Such methods are called noniterative.

The iterative inclusion of connected triples is rigorous and more reliable. However, because of much lower computational demands, the noniterative methods can be used for significantly larger systems, and CCSD(T) is thus commonly used in applications.

The aim of this work is, as already mentioned, to develop and imple-

ment the multireference Brillouin-Wigner coupled clusters method with the inclusion of connected triple excitations in both the iterative and noniterative manner. The main task is to develop the MR BWCC generalization of the standard CCSD(T), which would be capable of treating moderately sized systems. Moreover, for the assessment of the performance of the noniterative method, it is necessary to have a method with iterative inclusion of connected triples.

The first part of this work introduces the theoretical background used throughout the thesis. It includes techniques commonly used in quantum chemistry as well as the most important ab initio methods, relevant to this work. Special attention is, of course, paid to the coupled clusters approach, the inclusion of connected triples for single reference coupled clusters method and to the multireference Brillouin-Wigner coupled clusters method.

The next two chapters are the center of the thesis and include the description of the newly developed methods. The second part discusses the iterative approach towards the inclusion of connected triples to the MR BWCC method, while the third part concerns the noniterative triples corrections to MR BWCCSD.

Finally, the last chapter consists of applications of these methods. The basic aim of all these studies is to assess the performance of the newly developed methods.

Chapter 2

Theory

The aim of this chapter is to make a short review of the theoretical background of ab initio quantum chemistry methods, that are important for the discussion of multireference Brillouin-Wigner coupled clusters method with connected triples. Special attention is paid to the coupled clusters method and particularly to the inclusion of connected triple excitations, state specific multireference Brillouin-Wigner coupled clusters method, and the perturbational analysis of the coupled clusters wavefunction. Further details about these methods can be found in [107–114].

Throughout the text, the following notation is used. Unless stated otherwise, indices i, j, k, ... correspond to occupied orbitals, indices a, b, c, ... to virtual orbitals and indices p, q, r, ... to orbitals not a priori occupied or virtual.

2.1   Basic concepts

2.1.1   The reference and exact wavefunction. The wave operator

The restriction of the variational trial wavefunction to one Slater's determinant or one spin-adapted combination of them is the nature of the Hartree--Fock method. However, the exact wavefunction follows no such restriction, and therefore the solution of the Hartree-Fock equations is generally not equal to the exact wavefunction. The difference between the exact nonrelativistic energy, in a given basis set, and the Hartree-Fock energy is called correlation energy.

A vast majority of the post-Hartree-Fock methods uses the single determinant wavefunction as a reference function, i.e. the starting point of further calculations in the search of the exact wavefunction. Formally, the transition from the reference wavefunction Φ to the exact wavefunction Ψ is performed by the wave operator $\hat{\Omega}$

$$\Psi = \hat{\Omega}\Phi. \tag{2.1}$$

Once the wave operator is known, the exact wavefunction is easily obtained from this equation. Of course, the determination of the wave operator is as complicated as the determination of the exact wavefunction.

Furthermore, let us define the projection operator to the reference state $\hat{P}$ and its orthogonal complement $\hat{Q}$

$$\Phi = \hat{P}\Psi, \tag{2.2}$$
$$\Psi = \hat{P}\Psi + \hat{Q}\Psi. \tag{2.3}$$

Let us assume, that the exact wavefunction fulfills the intermediate normalization

$$\langle \Phi \mid \Psi \rangle = 1. \tag{2.4}$$

Single reference methods are those which take as the reference one Slater's determinant. The multireference methods start from a linear combination of several of them.

2.1.2 Second quantization

The second quantization is an alternative representation of quantum mechanics. It is often described as the "occupation number representation", since the quantum mechanical states are described by occupation numbers with respect to a given system of orthonormal one-particle functions. The main advantages of this approach are automatically correct symmetry of the wavefunction with respect to exchange of identical particles and the possibility of diagrammatic representation of the basic quantities of this formalism, which enables derivation of rules to simplify calculations.

Let $|k_i\rangle$ be a general complete set of orthonormal one-particle wavefunctions. Then the space of the wavefunctions for a system of N identical particles is constructed within the N-th tensor power of one-particle spaces. In quantum chemistry, the studied particles are electrons. The one-electron wavefunctions $|k_i\rangle$ are spin orbitals, usually obtained from a Hartree–Fock

calculation. The N-electron wavefunctions are described by linear combinations of Slater's determinants formed within this basis set.

The elementary operators within the second quantization theory are the creation and annihilation operators. All other operators are constructed from these elementary operators. The creation operator formally creates a particle in a state described by requested one-particle wavefunction. The annihilation operator annihilates an particle.

In an orthonormal basis set, the hermitian conjugate of the creation operator $\hat{a}_p^\dagger$ is the corresponding annihilation operator $\hat{a}_p$ and vice versa.

$$(\hat{a}_p)^\dagger = \hat{a}_p^\dagger \tag{2.5}$$

$$(\hat{a}_p^\dagger)^\dagger = \hat{a}_p \tag{2.6}$$

Properties of these operators are defined in a way to satisfy the symmetry requirement on the wavefunction. For fermions, which have antisymmetric wavefunctions, the anticommutation relations

$$\{\hat{a}_p^\dagger, \hat{a}_q\} \equiv \hat{a}_p^\dagger \hat{a}_q + \hat{a}_q \hat{a}_p^\dagger = \delta_{pq} \tag{2.7}$$

$$\{\hat{a}_p^\dagger, \hat{a}_q^\dagger\} = \{\hat{a}_p, \hat{a}_q\} = 0 \tag{2.8}$$

must therefore be obeyed.

Unlike the operators in the standard formulation of quantum mechanics, the creation and annihilation operators do not conserve the particle number. However, it is possible to construct from them number conserving combinations, for example the excitation operator $a_q^\dagger a_p$, which excites a particle from p-th state to q-th, and the number operator $a_p^\dagger a_p$ which gives the occupation number in p-th state.

As stated before, the N-electron state is represented by a set of occupation numbers. Let us define the vacuum state $|0\rangle$ as the state with all occupation numbers equal to zero. Let us also assume, that the vacuum state is normalized.

Any N-electron state can be constructed from the vacuum state by applying N creation operators on the vacuum, generating electrons in N different spin orbitals corresponding to the requested state.

The second quantization representation of the operators corresponding to physical observables depends on the number of particles involved in the

16

respective interaction. For one–body and two–body operators, which are common in quantum mechanics, we have

$$\hat{O}_1 = \sum_{pq} \langle p \mid O_1 \mid q \rangle \, \hat{a}_p^\dagger \hat{a}_q, \tag{2.9}$$

and

$$\hat{O}_2 = \sum_{pqrs} \langle pq \mid O_2 \mid rs \rangle \, \hat{a}_p^\dagger \hat{a}_q^\dagger \hat{a}_s \hat{a}_r. \tag{2.10}$$

The calculation of expectation values of operators is thus reduced to determination of vacuum mean values of products of creation and annihilation operators, because of the nature of second quantization representation of both the state vectors and operators.

For the reduction of the number of creation and annihilation operators, it is very convenient to introduce the concept of Fermi vacuum. Instead of the "true" vacuum $\mid 0 \rangle$, we choose the Slater's determinant of the reference Hartree-Fock state as the new vacuum and then redefine the creation and annihilation operators via the hole-particle formalism. Here, the creation operators generating a particle in a spin orbital, occupied in the Slater's determinant of the ground state, are taken as annihilation operators destroying the corresponding hole. Similarly, the annihilation operator destroying a particle in an occupied orbital are considered to be creation operators generating a hole. As can be easily verified, this redefinition does not affect the anticommutation relation of these operators.

Normal products, contractions, and their diagrammatic representation

A normal product $N\{\ldots\}$ of creation and annihilation operators is defined as the product of these operators whose order in the product is rearranged in such a way, that all the creation operators stand on the left from all the annihilation operators, multiplied by the sign of the permutation corresponding to the rearrangement

$$N\{\hat{a}_p^\dagger \hat{a}_q \hat{a}_r^\dagger \hat{a}_s \ldots\} = (-1)^P \hat{a}_p^\dagger \hat{a}_r^\dagger \ldots \hat{a}_q \hat{a}_s \ldots \tag{2.11}$$

Note that although the normal product of any number $n > 2$ of creation and annihilation operators can, in general, be expressed in different forms, all these forms are equivalent, due to the anticommutation relations (2.7).

A contraction of two operators is then defined as the difference between their product and normal product

$$\overline{\hat{A}\hat{B}} = \hat{A}\hat{B} - N\{\hat{A}\hat{B}\} \tag{2.12}$$

From the definition, we obtain the following formulas for contraction of two operators:

$$\overline{\hat{a}_p^\dagger \hat{a}_q^\dagger} = \overline{\hat{a}_p \hat{a}_q} = 0 \tag{2.13}$$

$$\overline{\hat{a}_p^\dagger \hat{a}_q} = 0 \tag{2.14}$$

$$\overline{\hat{a}_p \hat{a}_q^\dagger} = \delta_{pq} \tag{2.15}$$

This means, that a contraction of two second quantized operators is always a number, and as such it can be dealt with.

A vacuum mean value of a normal product of any nonzero number of creation and annihilation operators vanishes, since either an annihilation operator on the right acts on the vacuum state, or there is no annihilation operator at all, which also leads to zero. According to Wick's theorem, any product of second quantized operators can be expressed as their normal product plus the normal products with all possible contractions. A contraction is a number, and as such it can be taken out of the mean value. All normal products, except for the fully contracted ones, have zero contribution to the vacuum mean value. By this procedure we are able to express vacuum mean values in terms of fully contracted terms only, as all the remaining terms vanish. Since a contraction of creation and annihilation operator are either zero or equal to a Kronecker delta symbol, the vacuum mean value itself is a linear combination of products of Kronecker's deltas.

For expectation values of operators this leads to tensor contraction of the indices from different matrix elements of respective operators of physical quantities. These expressions can be represented diagrammatically. This approach has been introduced by Feynman in quantum field theory and has become widespread in many parts of theoretical physics.

The matrix elements of operators of physical quantities are represented by vertices and contractions of creation and annihilation operators by internal lines connecting the vertices. The total number of lines outgoing from a vertex corresponding to a n-body operator is equal to $2n$, which is the total number of creation and annihilation operators within its representation.

18

Figure 2.1: An example of connected and disconnected, linked and unlinked diagrams

Connected diagram   Unlinked diagram

Disconnected linked diagram
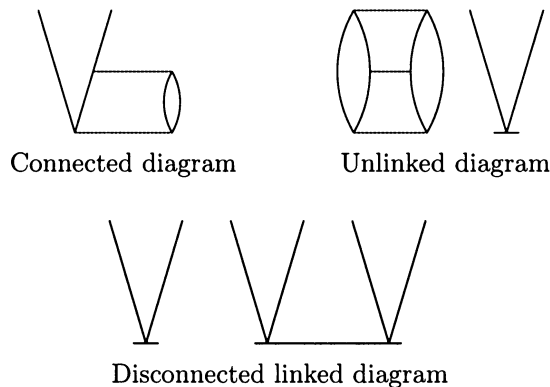
These lines are either internal, corresponding to contractions as mentioned above, or external.

The diagrammatic techniques thus provide a graphical representation of the respective formulas. Furthermore, there are simple rules how to translate the diagrams back to the algebraic formulas in which all the contractions were already performed and the expressions thus simplified. There are several classes of diagrams. Under connected diagrams we understand such ones, where all the vertices are connected with one another through the internal or interaction lines. Those that do not fulfill this criterion are called disconnected. As linked we denote all connected diagrams, as wall as such disconnected diagrams, where each of its connected components has at least one pair of external lines. Examples of diagrams belonging to these three classes are shown in Figure 2.1.

There are many types of different diagrammatic schemes. The most commonly used ones are the Goldstone's [115], Hugenholtz's [116], and Brandow's [117] diagrams used in perturbation and coupled clusters theory. In this text, the Brandow's diagrams will be used. The details are given in the respective chapters.

Hamiltonian in the second quantization

In quantum theory, the Hamiltonian plays a crucial role for the description of the system. For a system consisting of electrons and atomic nuclei, the non-relativistic Hamiltonian has a one-electron, two-electron components, and a

term not depending on electron coordinates. The one-electron part includes the electron kinetic energy and electron-nuclei potential energy, whereas the two-electron part consists of the electron-electron interaction energy. Within the Born-Oppenheimer approximation, atomic nuclei are considered stationary, and the nuclei-nuclei interaction is a constant and forms the part of Hamiltonian independent of the position of the electrons. As such, it does not influence the eigenfunctions of Hamiltonian and, therefore will be omitted in further discussion.

Using the formalism of second quantization, the Hamiltonian can be written as

$$\hat{H} = \hat{H}_1 + \hat{H}_2 = \sum_{pq} h_{pq} \hat{a}_p^\dagger \hat{a}_q + \frac{1}{2} \sum_{pqrs} \langle pq \mid rs \rangle \hat{a}_p^\dagger \hat{a}_q^\dagger \hat{a}_s \hat{a}_r, \qquad (2.16)$$

where the Hamiltonian was divided into one– and two–electron parts. Here, h_{pq} is a matrix element of the one–electron part of Hamiltonian, and $\langle pq \mid rs \rangle$ a matrix element of the two–electron component

$$\langle pq \mid rs \rangle = \int \chi_p^*(1) \chi_q^*(2) \frac{1}{r_{12}} \chi_r(1) \chi_s(2) dx_1 dx_2 \qquad (2.17)$$

Using the Fermi vacuum instead of physical vacuum, the Hamiltonian can be written in a normal product form

$$\hat{H} = \langle \Phi \mid \hat{H} \mid \Phi \rangle + \hat{H}_{N1} + \hat{H}_{N2} \qquad (2.18)$$

where $\hat{H}_{N1}$ and $\hat{H}_{N2}$ are given by

$$\hat{H}_{N1} = \sum_{pq} f_{pq} N\{\hat{a}_p^\dagger \hat{a}_q\} \qquad (2.19)$$

$$\hat{H}_{N2} = \frac{1}{2} \sum_{pqrs} \langle pq \mid rs \rangle N\{\hat{a}_p^\dagger \hat{a}_q^\dagger \hat{a}_s \hat{a}_r\}. \qquad (2.20)$$

Here, f_{pq} are matrix elements of the Fock matrix, and the integrals $\langle pq \mid rs \rangle$ were defined above.

2.1.3 Size extensivity

A quantum chemistry method is called size-extensive, if it yields the energy, which is for a system, consisting of n identical noninteracting subsystems, directly proportional to n.

20

A method is size-consistent, if it correctly describes the dissociation of the system, i.e. the energy of noninteracting subsystems is equal to the sum of the energies of the respective subsystems.

Methods, that are based on diagrammatic expansion with only connected diagrams, are automatically size-extensive. However, they are not always size-consistent, unless the orbitals used are localized. On the other hand, some multireference methods are size-consistent without being size-extensive.

2.2 Configuration interaction

The configuration interaction method expands the wavefunction as a linear combination of Slater's determinants formed from Hartree-Fock orbitals, and optimizes variationally the expansion coefficients.

It is based on the fact, that any antisymmetric many electron wavefunction can be expressed in this form, as long as the basis set of one electron functions is complete. The expansion coefficients, and therefore the exact wavefunction, are then obtained variationally by minimization of the total energy.

However, the calculations with a complete basis set of one electron functions are impossible, and results for the complete basis set are accessible only through extrapolation. Therefore, we obtain the "exact" wavefunction and "exact" energy only within a given basis set.

The Slater's determinants in the expansion are classified by the rank of their excitation with respect to the Slater's determinant of the reference wavefunction Φ. This corresponds to the wave operator in the form

$$\hat{\Omega}_{CI} = 1 + \sum_i \hat{C}_i = 1 + \hat{C}_1 + \hat{C}_2 + \hat{C}_3 + \ldots, \qquad (2.21)$$

where $\sum_i \hat{C}_i$ is a linear combination of all excitation operators corresponding to excitation of i electrons.

$$\hat{C}_1 = \sum_{ia} c_i^a \hat{a}_a^\dagger \hat{a}_i \qquad (2.22)$$

$$\hat{C}_2 = \sum_{i<j} \sum_{a<b} c_{ij}^{ab} \hat{a}_a^\dagger \hat{a}_b^\dagger \hat{a}_j \hat{a}_i \qquad (2.23)$$
$$\ldots$$

Here, the $c_{i\ldots}^{a\ldots}$ coefficients are the unknowns. The calculation is performed by the diagonalization of the Hamiltonian matrix whose elements are given

by $H_{pq} = \langle \Phi_p | H | \Phi_q \rangle$, where the indices p and q run over all Slater's determinants in the expansion. There are several techniques for evaluation of the elements of the CI matrix, including Slater's rules, second quantization, and the unitary group theory.

The correlation energy is given by

$$\Delta E = \sum_{ijab} c_{ij}^{ab} \langle \Phi | \hat{H} | \Phi_{ij}^{ab} \rangle. \tag{2.24}$$

Although the energy depends directly only on expansion coefficients of biexcited Slater's determinants, the other excitations interact with biexcitations and influence thus the energy as well.

Even with an incomplete basis set, the total number of Slater's determinants or its spin adapted combinations is generally too high. For K spatial orbitals, n electrons and spin S, the total number of spin-adapted functions is $\frac{2S+1}{K+1} \binom{K+1}{n/2-S} \binom{K+1}{n/2-S+1}$ [118]. Therefore, some truncation of the expansion of the wave operator (2.21) is inevitable. The equation (2.24) suggests that the dominant contribution to the correlation energy comes from the biexcited determinants. Also, the role of monoexcitations and tetraexcitations is significant.

Therefore, the most commonly used truncation is that with monoexcitations and biexcitations (the CISD method). However, unlike the full configuration interaction, these limited expansions lead to size-inextensivity of the method. This inextensivity is usually reduced by a a posteriori correction, usually the Davidson correction.

The advantage of the CI method is its variational nature, which guarantees that the energy obtained is always an upper bound of the exact energy. The disadvantages include high computational demands and the lack of size-extensivity for limited CI.

2.3 Perturbation methods

The perturbation theory is based on partitioning of the Hamiltonian into an unperturbed Hamiltonian $\hat{H}_0$ and perturbation $\hat{V}$

$$\hat{H} = \hat{H}_0 + \hat{V} \tag{2.25}$$

We assume, that the eigenfunctions and eigenvalues of the unperturbed Hamiltonian $\hat{H}_0$ are known and that the perturbation is "small" compared

to $\hat{H}_0$. The perturbation theory then provides a way to find the solution of the perturbed Schrödinger equation.

For the rest of this chapter, we introduce the following notation. Let Ψ be the wavefunction of the ground state of the Hamiltonian $\hat{H}$ with the exact energy E. Let Φ be the ground state of the unperturbed Hamiltonian $\hat{H}_0$ with energy E_0.

2.3.1 Perturbation expansion of energy and wavefunction

Let z be an arbitrary complex number. Using the partitioning of the Hamiltonian (2.25), the stationary Schrödinger equation yields

$$(z - \hat{H}_0)\Psi = (z - E + \hat{V})\Psi. \tag{2.26}$$

Assuming that the inverse of the operator $(z - E + \hat{V})$ exists, and using the definition of the $\hat{Q}$ operator (2.3), we obtain an infinite perturbation expansion of the wavefunction

$$\Psi = \sum_{n=0}^{\infty} \Psi^{[n]} = \sum_{n=0}^{\infty} \left(\frac{\hat{Q}}{z - \hat{H}_0}(z - E + \hat{V}) \right)^n \Phi, \tag{2.27}$$

where $\Psi^{[n]}$ is the n-th order contribution to the wavefunction and the expression $\frac{\hat{Q}}{z - \hat{H}_0}$ is called resolvent.

The perturbation expansion of the correlation energy is then

$$\Delta E = \sum_{n=0}^{\infty} \Delta E^{[n]} = \sum_{n=0}^{\infty} \langle \Phi \mid \hat{V} \left(\frac{\hat{Q}}{z - \hat{H}_0}(z - E + \hat{V}) \right)^n \mid \Phi \rangle, \tag{2.28}$$

and for the wave operator we obtain

$$\hat{\Omega} = \sum_{n=0}^{\infty} \Omega^{[n]} = \sum_{n=0}^{\infty} \left(\frac{\hat{Q}}{z - \hat{H}_0}(z - E + \hat{V}) \right)^n. \tag{2.29}$$

These expansions are in principle infinite. In practical calculations the expansions are usually limited only to the first few contributions. However, it is possible to sum up certain types of contributions to infinite order.

The variable z is in principle an arbitrary complex number. However, for some particular choice of z the expansions are very convenient. The two most common choices of z are the exact energy E and the unperturbed energy E_0. The former scheme is called Brillouin-Wigner perturbation theory, and the latter Rayleigh-Schrödinger perturbation theory.

2.3.2 Rayleigh-Schrödinger expansion

The more commonly used approach is the Rayleigh-Schrödinger expansion. Since the unperturbed energy is known apriori, the resolvent has a very simple form

$$R_0 = \frac{\hat{Q}}{E_0 - \hat{H}_0}.\tag{2.30}$$

However, the presence of the energy in the $(E_0 - E + \hat{V})$ term gives rise to so called bracketing, or renormalization, terms

$$\Psi^{[n]} = R_0 \hat{V} \Psi^{[n-1]} - \sum_{\kappa=1}^{n-1} E^{[\kappa]} R_0 \Psi^{[n-\kappa]},\tag{2.31}$$

where the energy $E^{[n]}$ is given by

$$E^{[n]} = \langle \Phi \mid \hat{V} \mid \Psi^{[n-1]} \rangle = \langle \Phi \mid \hat{V} \mid \hat{\Omega}^{[n-1]} \Phi \rangle.\tag{2.32}$$

By using the equations (2.31) and (2.32) recursively, the formula for the n-th order energy contribution $E^{[n]}$ has generally the form

$$E^{[n]} = \langle \Phi \mid \hat{V} (R_0 \hat{V})^{n-1} \mid \Phi \rangle + \text{renormalization terms}\tag{2.33}$$

The first term is called the principal term, which has a simple general formula. The latter term, the renormalization part of the formula, includes a rapidly growing number of contributions. However, employing the diagrammatic approach, the formula can be limited to the principle part, as long as the unlinked diagrams are excluded from the principal part and the exclusion principle violating terms [119–124] are included. By EPV diagrams we mean such expressions, in which two summation indices, corresponding to adjacent creation or annihilation operators, have the same value. The first condition is the essence of the linked cluster theorem, which also guarantees the size-extensivity of the method.

The wave operator fulfills the Bloch equation [125]

$$[\hat{\Omega}\hat{H}_0 - \hat{H}_0\hat{\Omega}]\hat{P} = \hat{V}\hat{\Omega}\hat{P} - \hat{\Omega}\hat{P}\hat{V}\hat{\Omega}\hat{P},\tag{2.34}$$

which is fully equivalent to the Schrödinger equation.

2.3.3 Brillouin-Wigner expansion

In the Brillouin-Wigner perturbation theory, the constant z is chosen to be the exact energy E. Therefore, no bracketing terms are present. However, the exact energy remains in the resolvent, and this approach has thus to be used iteratively, which is inconvenient for standard perturbation calculations. However, in combination with other iterative approaches (for example coupled clusters theory), this scheme becomes useful.

Within this scheme, the wave operator fulfills the Bloch's equation

$$\hat{\Omega} = 1 + \hat{B}\hat{V}\hat{\Omega}, \tag{2.35}$$

where $\hat{B} = \frac{\hat{Q}}{E - \hat{H}_0}$ is the Brillouin-Wigner resolvent.

Since the formula for energy includes also the unlinked contributions, the Brillouin-Wigner perturbation theory is not size-extensive.

2.3.4 Møller-Plesset perturbation theory

So far, the discussion concerned a general partitioning of the Hamiltonian. In quantum chemistry, one usually employs the Møller-Plesset partitioning. In this scheme, the Hamiltonian of the unperturbed system includes the Hartree-Fock energy and the contribution of diagonal Fock matrix elements. The perturbation is then obtained as the difference between $\hat{H}$ and $\hat{H}_0$. In the second quantization form this reads

$$\hat{H}_0 = \langle \Phi \mid H \mid \Phi \rangle + \sum_p f_{pp} N\{\hat{a}_p^\dagger \hat{a}_p\} \tag{2.36}$$

$$\hat{V}_N = \sum_{p \neq q} f_{pq} N\{\hat{a}_p^\dagger \hat{a}_q\} + \hat{H}_{N2}, \tag{2.37}$$

As the reference state, the Hartree-Fock wavefunction is used. Because of the Brillouin theorem, for restricted or unrestricted Hartree-Fock reference functions the off-diagonal elements of the Fock matrix are zero, and therefore the first term in $\hat{V}_N$ vanishes. However, for restricted open shell Hartree-Fock or other types of orbitals, both terms are nonzero and have to be considered. This conclusion is valid also in the coupled clusters theory.

Rayleigh-Schrödinger perturbation method with the Møller-Plesset partitioning is automatically size-extensive and invariant with respect to orbital rotations among occupied or among virtual orbitals, at all orders of perturbation expansion.

Figure 2.2: Diagrammatic representation of $\hat{H}_N$
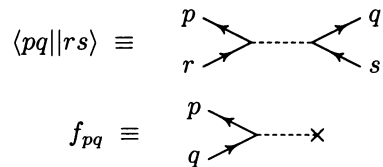
The diagrammatic representation of $\hat{H}_N$ is shown in Figure 2.2. The number of vertexes is equal to the order of perturbation theory. The vertexes are connected by internal lines to obtain a connected diagram. Each internal line is assigned a summation index. Diagrams corresponding to energy have no external lines. A numerical factor is assigned to each diagram, depending on the number of hole lines, loops and symmetry of the diagram. Details can be found in literature, eg. [107, 109–111].

2.4   Coupled clusters method

2.4.1   Cluster operator and cluster amplitudes

In the coupled clusters approach the wave operator is chosen in the form of the exponential ansatz

$$\hat{\Omega}_{CC} = e^{\hat{T}}, \tag{2.38}$$

where the cluster operator $\hat{T}$ is a linear combination of excitation operators. Therefore, the cluster operator can be divided according to the rank of excitation

$$\hat{T} = \hat{T}_1 + \hat{T}_2 + \hat{T}_3 + \cdots, \tag{2.39}$$

where $\hat{T}_1$ includes contributions from monoexcitations, $\hat{T}_2$ from biexcitations, $\hat{T}_3$ from triexcitations, etc.

$$\hat{T}_1 = \sum_{i,a} t_i^a \, \hat{a}_a^\dagger \, \hat{a}_i \tag{2.40}$$

$$\hat{T}_2 = \sum_{i<j} \sum_{a<b} t_{ij}^{ab} \, \hat{a}_a^\dagger \, \hat{a}_b^\dagger \, \hat{a}_j \, \hat{a}_i \tag{2.41}$$

The expansion coefficients t_i^a, t_{ij}^{ab}, ... are called clusters amplitudes. They are a priori unknown and their determination leads to determination of the

wave operator, and therefore the wavefunction. The cluster amplitudes are chosen to be totally antisymmetric in both occupied and virtual orbital indices, which is possible due to the anticommutation of the creation and annihilation operators.

Let us use the partitioning of Hamiltonian to $\langle \Phi \mid \hat{H} \mid \Phi \rangle$ and remaining terms $\hat{H}_N$. Then, we obtain for the correlation energy

$$\Delta E = \langle \Phi \mid \hat{H}_N e^{\hat{T}} \mid \Phi \rangle_C = \langle \Phi \mid \hat{H}_N \left(\hat{T}_1 + \frac{1}{2}\hat{T}_1^2 + \hat{T}_2 \right) \mid \Phi \rangle_C. \tag{2.42}$$

The C index indicates that only contributions from connected diagrams are included.

The number of cluster amplitudes in the full cluster operator is the same as the number of CI coefficients. Again, the number of cluster amplitudes is too large, and therefore a truncation of the cluster operator is inevitable. Commonly used truncations are listed in Table 2.1, as well as the scaling of the computational demands of the respective methods. The number of occupied orbitals is denoted as n_o and the number of virtual orbital as n_v.

Table 2.1: Examples of truncation of the cluster operator

Method	Cluster operator	Scaling of the method
CCD	$\hat{T} = \hat{T}_2$	$(n_o)^2(n_v)^4$
CCSD	$\hat{T} = \hat{T}_1 + \hat{T}_2$	$(n_o)^2(n_v)^4$
CCSDT	$\hat{T} = \hat{T}_1 + \hat{T}_2 + \hat{T}_3$	$(n_o)^3(n_v)^5$
CCSDTQ	$\hat{T} = \hat{T}_1 + \hat{T}_2 + \hat{T}_3 + \hat{T}_4$	$(n_o)^4(n_v)^6$

2.4.2 Cluster equations

As stressed before, the cluster amplitudes are the unknowns. They are obtained by projection of the equation

$$e^{-\hat{T}} \hat{H}_N e^{\hat{T}} \Phi = \Delta E \Phi \tag{2.43}$$

to monoexcited, biexcited, etc. Slater's determinants Φ_i^a, Φ_{ij}^{ab} etc..

$$\langle \Phi_i^a \mid e^{-\hat{T}} \hat{H}_N e^{\hat{T}} \mid \Phi \rangle_C = 0 \tag{2.44}$$

$$\langle \Phi_{ij}^{ab} \mid e^{-\hat{T}} \hat{H}_N e^{\hat{T}} \mid \Phi \rangle_C = 0 \tag{2.45}$$

$$\cdots$$

27

The first of these equations is called the T_1 equation, the second T_2 equation, etc. The number of the cluster equations is equal to the number of clusters amplitudes. The cluster equations are nonlinear in the cluster amplitudes, and thus an iterative approach to their solution is used. We separate the part of the expression linear in the respective cluster amplitudes and put it to the left hand side, while the remaining terms are kept on the right hand side of the equation. For T_1 and T_2 equations we get

$$t_i^a(\text{new}) = \frac{1}{D_i^a}\langle\Phi_i^a \mid \hat{V}_N e^{\hat{T}(\text{old})} \mid \Phi\rangle_C \qquad (2.46)$$

and

$$t_{ij}^{ab}(\text{new}) = \frac{1}{D_{ij}^{ab}}\langle\Phi_{ij}^{ab} \mid \hat{V}_N e^{\hat{T}(\text{old})} \mid \Phi\rangle_C \qquad (2.47)$$

Here, the denominators D_i^a and D_{ij}^{ab} are combinations of the diagonal elements of the Fock matrix

$$D_i^a = f_{ii} - f_{aa} \qquad (2.48)$$
$$D_{ij}^{ab} = f_{ii} + f_{jj} - f_{aa} - f_{bb} \qquad (2.49)$$

and in general

$$D_{ij\ldots}^{ab\cdots} = f_{ii} + f_{jj} + \ldots - f_{aa} - f_{bb} - \ldots \qquad (2.50)$$

The initial guess of the cluster amplitudes is taken as

$$t_i^a = \frac{f_{ia}}{D_i^a} \qquad (2.51)$$

$$t_{ij}^{ab} = \frac{\langle ij \mid ab\rangle}{D_{ij}^{ab}} \qquad (2.52)$$

with cluster amplitudes corresponding to higher excitations equal to zero. This corresponds to setting $\hat{T} = 0$ in the right hand side of the cluster equation in the zero-th iteration.

The diagrammatic representation of cluster amplitudes is given in Figure 2.3. The representation of $\hat{H}_N$ is the same as in the perturbation theory. Diagrams in T_1 equation have one pair of external lines, in T_2 two pairs etc.

2.4.3 Comparison of CI and CC approaches

Let us compare the expansion of the wave operator within the scheme of coupled clusters and configuration interaction. By the expansion of the exponential ansatz of the coupled clusters wave operator (2.38) and its comparison

Figure 2.3: Diagrammatic representation of the cluster operator
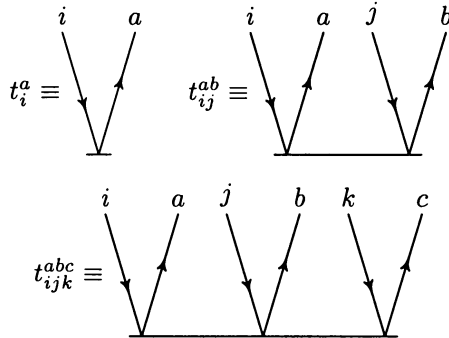
with the CI-like form (2.21) we obtain

$$\hat{C}_1 = \hat{T}_1 \tag{2.53}$$

$$\hat{C}_2 = \hat{T}_2 + \frac{1}{2}\hat{T}_1^2 \tag{2.54}$$

$$\hat{C}_3 = \hat{T}_3 + \hat{T}_1\hat{T}_2 + \frac{1}{3!}\hat{T}_1^3 \tag{2.55}$$

$$\hat{C}_4 = \hat{T}_4 + \frac{1}{2}\hat{T}_2^2 + \frac{1}{2}\hat{T}_1^2\hat{T}_2 + \hat{T}_1\hat{T}_3 + \frac{1}{4!}\hat{T}_1^4 \tag{2.56}$$

. . .

From these equations it is clear that both approaches are equivalent, if no truncation is applied. However, the coupled cluster scheme includes contributions from higher excitations than a configuration interaction at the same level of truncation. For $\hat{T}$ with all excitations up to the rank n the first n contributions $\hat{C}_1, \ldots, \hat{C}_n$ contributions are included exactly, while the higher excitations only partially.

For example, at the CCSD level, only the monoexcitations and biexcitations are included fully. However, there are nonzero contributions to triexcitations and particularly tetraexcitations, i.e. the most important contributions beyond biexcitations. Consequently, the performance of CCSD is only slightly worse than that of CISDTQ, although its computational cost is comparable with CISD.

Further advantage of the coupled clusters scheme, when compared to CI, is the size-extensivity of the method. The drawback is, that it cannot be effectively performed as a variational method, since that would lead to an infinite diagrammatic expansion of cluster equations.

2.4.4 Perturbational analysis of coupled clusters approach

The coupled clusters method and the perturbation theory are two distinct approaches to post-Hartree-Fock calculations. However, there is a clear link between the two approaches, although not as obvious as in the case of coupled clusters and configuration interaction.

In this section, this relationship is discussed. The aim is to obtain perturbation theory expressions in terms of cluster amplitudes, and vice versa expressions for cluster amplitudes in terms of Fock matrix elements and $\langle pq \mid rs \rangle$ integrals.

In the perturbation theory, the wave operator is represented by the expansion

$$\hat{\Omega} = \sum_i \hat{\Omega}^{[i]}. \tag{2.57}$$

It is very convenient to separate the i-th order operator $\hat{\Omega}^{[i]}$ into several different classes

$$\hat{\Omega}^{[i]} = \hat{\Omega}_1^{[i]} + \hat{\Omega}_2^{[i]} + \ldots + \hat{\Omega}_{2k}^{[i]} \tag{2.58}$$

Here, $\hat{\Omega}_k^{[i]}$ corresponds to the part of $\hat{\Omega}^{[i]}$ which involves only a k-tuple substitution of the reference Slaters determinant.

Then, $\hat{\Omega}_k$ (the sum of $\hat{\Omega}_k^{[i]}$ over all orders i) can be expressed using the coupled cluster formalism by

$$\hat{\Omega}_k = \hat{T}_k + \sum_{\{n_j\}} \prod_{j=1}^p \frac{1}{n_j!} \hat{T}_j^{n_j}, \tag{2.59}$$

where the summation runs over p-tuples $\{n_j\}_{j=1}^p$, where $p < k$, $1 \le n_j \le k$ and $\sum_{j=1}^p j n_j = k$. This provides the link between the perturbation theory and the coupled clusters formalism.

The initial guess of cluster amplitudes, already shown in (2.51), is $t_i^a = \frac{f_{ia}}{D_i^a}$ for connected singles, and $t_{ij}^{ab} = \frac{\langle ij|ab \rangle}{D_{ij}^{ab}}$ for connected doubles. These expressions are identical to the first order contribution $\hat{\Omega}^{[1]}$ of the perturbation expansion of the wave operator.

By inserting the initial guess of cluster amplitudes into cluster equations, one generates higher order terms of the expansion. Using this approach, the perturbation expansion of cluster amplitudes is obtained. Therefore, the cluster amplitudes can be in principle expressed by expressions including only elements of Fock matrix and two-electron integrals.

Let us write the cluster operator and its components in the form of perturbation expansion

$$\hat{T}_q = \hat{T}_q^{[1]} + \hat{T}_q^{[2]} + \hat{T}_q^{[3]} + \ldots, \tag{2.60}$$

where $\hat{T}_q$ stands for either the whole cluster operator or any of its components.

In the first order of perturbation theory, only connected singles and doubles yield nonzero contributions. Furthermore, when we restrict ourselves to the Hartree-Fock reference function, $\hat{T}_1^{[1]}$ vanishes, due to the Brillouin theorem. In the following text, we will for simplicity adopt this restriction. Using equation (2.59), the contributions to the wave operators in first three orders of the perturbation theory are given by

$$\hat{\Omega}^{[1]} = \hat{T}_2^{[1]} \tag{2.61}$$

$$\hat{\Omega}^{[2]} = \hat{T}_2^{[2]} + \hat{T}_1^{[2]} + \hat{T}_3^{[2]} + \frac{1}{2}\hat{T}_2^{[1]}\hat{T}_2^{[1]} \tag{2.62}$$

$$\hat{\Omega}^{[3]} = \hat{T}_2^{[3]} + \hat{T}_1^{[3]} + \hat{T}_3^{[3]} + \hat{T}_1^{[2]}\hat{T}_2^{[1]} + \tag{2.63}$$
$$+ \hat{T}_4^{[3]} + \hat{T}_2^{[1]}\hat{T}_2^{[2]} + \frac{1}{3!}\hat{T}_2^{[1]}\hat{T}_2^{[1]}\hat{T}_2^{[1]}$$

where we have used

$$\hat{T}_3^{[1]} = \hat{T}_4^{[1]} = \hat{T}_4^{[2]} = \hat{T}_1^{[1]} = 0. \tag{2.64}$$

The diagrammatic representation of the first and second order contributions to the cluster operator are shown in Figure 2.4. The correspondence between perturbation theory and coupled clusters diagrams is established by the factorization of the denominators [109].

As shown before, the correlation energy contributions are given by (2.32).

$$E^{[n]} = \langle \Phi \mid \hat{V} \mid \hat{\Omega}^{[n-1]}\Phi \rangle \tag{2.65}$$

When we restrict ourselves to the Hartree-Fock reference function, the perturbation $\hat{V}_N$ includes only contributions from the $\langle ij \mid ab \rangle$ integrals. Using this and the fact, that $\langle ij \mid ab \rangle = D_{ij}^{ab}t_{ij}^{ab[1]}$, this equation can be, after performing all the contractions, rewritten as

$$E^{[n]} = \sum_{ijab} D_{ij}^{ab}t_{ij}^{ab[1]}t_{ij}^{ab[n-1]} \tag{2.66}$$

This equation provides an effective computational way for calculating $E^{[2]}$ and $E^{[3]}$. However, in the fourth order, the situation becomes more

Figure 2.4: First and second order perturbation contributions to the cluster operator
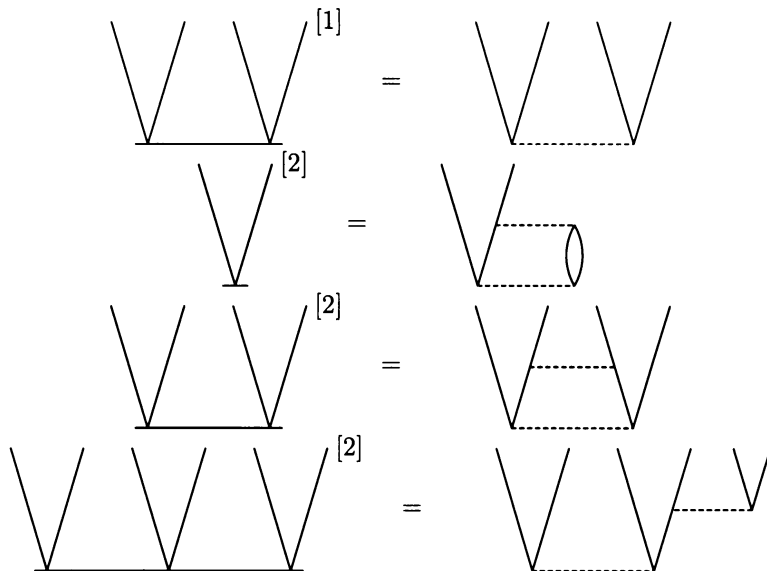
Figure 2.5: Diagrammatic representation of $E_S^{[4]}$
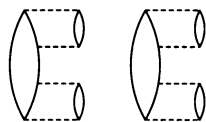
complicated, because of the complexity of $\hat{T}_2^{[3]}$. It is therefore very convenient to use the Wigner's rule, which states that using the wavefunction exact to the n-th order of perturbation theory, it is possible to obtain the energy exact to the $(2n + 1)$-th order.

The third order part of connected doubles, $\hat{T}_2^{[3]}$, is formed in the first two iterations of the cluster equations. In the first iteration, only connected doubles are nonzero. However, in the second iteration, even connected singles and triples, and also disconnected quadruples from $\hat{T}_2^2$ emerge.

It is thus convenient to divide the fourth order energy $E^{[4]}$ into parts corresponding to single, double, triple, and quadruple excitations $E_S^{[4]}$, $E_D^{[4]}$, $E_T^{[4]}$ and $E_Q^{[4]}$. The diagrammatic representation of these terms is presented in Figures 2.5, 2.6, 2.7 and 2.8.

Figure 2.6: Diagrammatic representation of $E_{\mathrm{D}}^{[4]}$
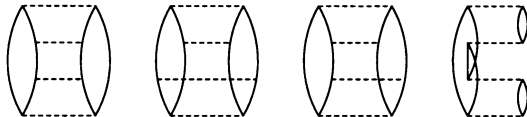
Figure 2.7: Diagrammatic representation of $E_{\mathrm{T}}^{[4]}$
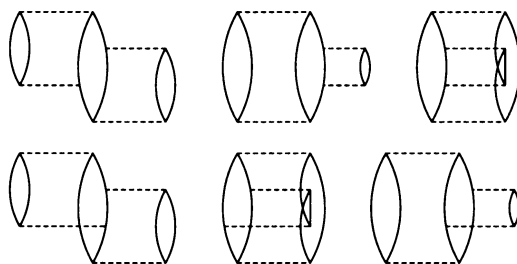
The $E_{\mathrm{S}}^{[4]}$ comes from $\hat{T}_1^{[2]}$ being substituted in $\hat{V}_N \hat{T}_1$ term in the T_2 equation. The effective way of evaluation of this term is

$$E_{\mathrm{S}}^{[4]} = \sum_{ia} D_i^a t_i^{a[2]} t_i^{a[2]} \tag{2.67}$$

where the $2n + 1$ rule [126, 127] has been used.

Similarly, the $E_{\mathrm{D}}^{[4]}$ term originates from $\hat{T}_2^{[2]}$ being inserted into the $\hat{V}_N \hat{T}_2$ term of the right hand side of T_2 equation, and $E_T^{[4]}$ from $\hat{T}_3^{[2]}$ being inserted into the $\hat{V}_N \hat{T}_2$ term.

$$E_{\mathrm{D}}^{[4]} = \sum_{i>j} \sum_{a>b} D_{ij}^{ab} t_{ij}^{ab[2]} t_{ij}^{ab[2]} \tag{2.68}$$

$$E_{\mathrm{T}}^{[4]} = \sum_{i>j>k} \sum_{a>b>c} D_{ijk}^{abc} t_{ijk}^{abc[2]} t_{ijk}^{abc[2]} \tag{2.69}$$

The $E_{\mathrm{Q}}^{[4]}$ comes from $\frac{1}{2}\hat{T}_2^{[1]}\hat{T}_2^{[1]}$, however, there is no convenient $2n+1$ rule for this term.

From the computational point of view, the determination of $E_{\mathrm{S}}^{[4]}$ scales as n^5, $E_{\mathrm{D}}^{[4]}$ as n^6 and $E_{\mathrm{T}}^{[4]}$ as n^7. The computational cost of $E_{\mathrm{Q}}^{[4]}$ can be reduced

33

Figure 2.8: Diagrammatic representation of $E_Q^{[4]}$
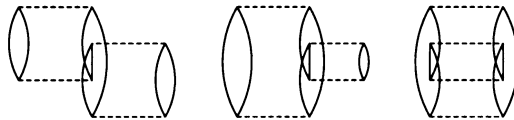
from n^8 to n^6 by the vertical factorization technique [7, 128]. The CCSD energy includes $E_S^{[4]}$, $E_D^{[4]}$ and $E_Q^{[4]}$ contributions, while missing $E_T^{[4]}$.

In the fifth order of the perturbation theory, the situation is even more complicated. The diagrams are classified by the excitation rank at two levels, i.e. between the second and the third, and between the third and the fourth vertex. The 15 resulting classes of energy contributions are denoted as $E_{SS}^{[5]}$, $E_{SD}^{[5]}$, $E_{ST}^{[5]}$, $E_{DS}^{[5]}$, $E_{DD}^{[5]}$, $E_{DT}^{[5]}$, $E_{DQ}^{[5]}$, $E_{Tdc}^{[5]}$, $E_{TD}^{[5]}$, $E_{TT}^{[5]}$, $E_{TQ}^{[5]}$, $E_{Qdc}^{[5]}$, $E_{QT}^{[5]}$, $E_{QQ}^{[5]}$, and $E_{dc}^{[5]}$. Among these, there are two pairs of identical contributions, that are hermitian conjugates of each other: $E_{SD}^{[5]}$ with $E_{DS}^{[5]}$, and $E_{TD}^{[5]}$ with $E_{DT}^{[5]}$. However, this identity is not valid for $E_{QT}^{[5]}$ and $E_{TQ}^{[5]}$, due to the asymmetric nature of cluster equations, resulting in the disconnected energy contributions $E_{Tdc}^{[5]}$, $E_{Qdc}^{[5]}$ and $E_{dc}^{[5]}$ [110].

From these contribution, the CCSD energy includes $E_{SS}^{[5]}$, $E_{SD}^{[5]}$, $E_{DS}^{[5]}$, $E_{DD}^{[5]}$, $E_{DQ}^{[5]}$, $E_{Tdc}^{[5]}$, $E_{Qdc}^{[5]}$, and $E_{dc}^{[5]}$. The CCSDT energy has contributions of all the terms except for $E_{QT}^{[5]}$, and $E_{QQ}^{[5]}$, which require inclusion of connected quadruples.

Among these terms, only $E_{ST}^{[5]}$ will be important in further discussion. This term is larger than other fifth order contributions and plays a crucial role in the noniterative coupled clusters methods, particularly in CCSD(T), as will be shown in the following section.

2.4.5 Coupled clusters method with connected triples

The origin of the success of coupled cluster approaches is basically the fact that the dominant contribution of tetraexcitations is included even at the CCSD level. The perturbation analysis shows, that the $\frac{1}{2}\hat{T}_2^2$ term includes contributions of the second order, while $\hat{T}_4$ of the third order.

However, the situation with triple excitations is less favorable. Assuming the case of the Hartree-Fock reference wavefunction, the $\hat{T}_3$ term is of

the second order, while $\hat{T}_1\hat{T}_2$ of the third order. For the non-Hartree-Fock reference, both the terms are of the second order.

For a correct description of triple excitations, the inclusion of $\hat{T}_3$ is therefore inevitable, since this term is at least as important as $\hat{T}_1\hat{T}_2$. However, inclusion of triple excitations within the cluster operator increases the computational requirements of the method. The rigorous inclusion of connected triples is thus usually not the preferred way, and the connected triples are included in a noniterative way.

In the first part of this section, the full CCSDT method will be discussed, whereas in the latter two subsections, the discussion of approximate iterative and noniterative methods is given.

CCSDT

The CCSDT method is based on the straightforward inclusion of connected triples to the cluster operator

$$\hat{T} = \hat{T}_1 + \hat{T}_2 + \hat{T}_3. \tag{2.70}$$

Inserting the exponential ansatz with this truncation of the cluster operator leads to the following cluster equations:

$$D_i^a t_i^a = \langle (\Phi)_i^a \mid \hat{V}_N (\hat{T}_1 + \hat{T}_2 + \frac{1}{2}\hat{T}_1^2 + \hat{T}_1\hat{T}_2 + \frac{1}{3!}\hat{T}_1^3 + \hat{T}_3) \mid \Phi \rangle_C \tag{2.71}$$

for T$_1$ amplitudes,

$$D_{ij}^{ab} t_{ij}^{ab} = \langle (\Phi)_{ij}^{ab} \mid \hat{V}_N (1 \ + \ \hat{T}_1 + \hat{T}_2 + \frac{1}{2}\hat{T}_1^2 + \hat{T}_1\hat{T}_2 + \frac{1}{3!}\hat{T}_1^3 + \tag{2.72}$$
$$+ \ \frac{1}{4!}\hat{T}_1^4 \frac{1}{2}\hat{T}_2^2 + \frac{1}{2}\hat{T}_1^2\hat{T}_2 + \hat{T}_3 + \hat{T}_1\hat{T}_3) \mid \Phi \rangle_C$$

as the T$_2$ equation, and finally

$$D_{ijk}^{abc} t_{ijk}^{abc} = \langle (\Phi)_{ijk}^{abc} \mid \hat{V}_N (1 \ + \ \hat{T}_1 + \hat{T}_2 + \frac{1}{2}\hat{T}_1^2 + \hat{T}_1\hat{T}_2 + \frac{1}{3!}\hat{T}_1^3 + \frac{1}{4!}\hat{T}_1^4 +$$
$$+ \ \frac{1}{2}\hat{T}_2^2 + \frac{1}{2}\hat{T}_1^2\hat{T}_2 + \frac{1}{3!}\hat{T}_1^3\hat{T}_2 + \frac{1}{2}\hat{T}_1\hat{T}_2^2 +$$
$$+ \ \hat{T}_3 + \hat{T}_1\hat{T}_3 + \hat{T}_2\hat{T}_3 + \frac{1}{2}\hat{T}_1^2\hat{T}_3) \mid \Phi \rangle_C \tag{2.73}$$

as the T$_3$ equation.

Approximate iterative methods

By neglecting the computationally most expensive terms in the CCSDT cluster equations, it is possible to greatly reduce the computational cost and to obtain the n^7 scaling instead of n^8 of CCSDT. These approximations are called iterative, since the T$_3$ equation, although truncated, is being iterated throughout the calculation.

These methods are denoted as CCSDT-n and form a hierarchy of the approximations, with a decreasing number of terms included.

1. CCSDT-4
   In the CCSDT-4 method, all nonlinear terms that include $\hat{T}_3$, i.e. the $\hat{T}_1\hat{T}_3$, $\hat{T}_2\hat{T}_3$ and $\frac{1}{2}\hat{T}_1^2\hat{T}_3$ terms are neglected in the T$_3$ equation.

2. CCSDT-3
   The CCSDT-3 method is obtained by setting $\hat{T}_3 = 0$ on the right hand side of the T$_3$ equation. This means that all the terms on the right hand side of the T$_3$ equation that include connected triples are neglected.

3. CCSDT-2
   In the CCSDT-2 method both $\hat{T}_3$ and $\hat{T}_1$ are set to zero in the T$_3$ equation. Therefore, the right hand side of (2.73) includes only terms with $\hat{T}_2$.

4. CCSDT-1b
   The CCSDT-1b method is obtained from CCSDT-2 by neglecting of the $\frac{1}{2}\hat{T}_2^2$ term in the T$_3$ equation. Therefore, the only remaining term on the right hand side of (2.73) is $\hat{V}_N\hat{T}_2$.

5. CCSDT-1
   The least accurate approximation, CCSDT-1, is the same as CCSDT-1b, with one additional term omitted. This term is the $\hat{T}_1\hat{T}_3$ contribution to the T$_2$ equation. The wave operator is thus effectively restricted to $\hat{\Omega} = e^{\hat{T}_1+\hat{T}_2} + \hat{T}_3$.

Numerical studies have shown, that the energies obtained by CCSDT-1 and CCSDT-1b are usually very similar. This can be explained by the fact, that the energy expressions in these methods differ only by terms of sixth and higher orders of perturbation theory. CCSDT-2 and CCSDT-3 have

36

generally higher deviation from CCSDT and FCI results than CCSDT-1. To increase the accuracy beyond CCCSDT-1, it is necessary to include at least the linear contributions of the connected triples to the T_3 equation. Unlike the lower approximations, CCSDT-4 requires the storage of connected triple amplitudes, due to the intermediates including connected triples on the right hand side of (2.73).

However, due to the success of the noniterative approximations, and particularly CCSD(T), all these methods are of rather limited practical use and their importance lies mainly as historical predecessors of CCSDT and CCSD(T).

Approximate noniterative methods

The motivation for the noniterative approach in the inclusion of connected triple excitations is to greatly reduce the computational requirements of the method, while preserving the accuracy of the calculated energy. Since the general requirement for the energy is the accuracy up to the fourth order of perturbation theory, the scaling of these method cannot become lower than the n^7 scaling of the MBPT4 method. Since CCSDT-1 has the same scaling as MBPT4, further computational savings can only be achieved by the reduction of the number of the n^7 steps. Therefore, in the noniterative calculations, the CCSD calculation is carried out first, and subsequently the connected triples correction is included in one additional step.

The CCSD energy includes all contributions of second and third order, and also the fourth order terms $E_S^{[4]}$, $E_D^{[4]}$ and $E_Q^{[4]}$. The only remaining fourth order contribution, $E_T^{[4]}$, requires the inclusion of connected triples. It can be expressed as

$$E_T^{[4]} = \frac{1}{36} \sum_{abcijk} t_{ijk}^{abc[2]} D_{ijk}^{abc} t_{ijk}^{abc[2]} \tag{2.74}$$

where $t_{ijk}^{[2]abc}$ are connected triples amplitudes exact to the second order of the perturbation theory

$$\begin{aligned} D_{ijk}^{abc} t_{ijk}^{abc[2]} &= \sum_e P(i/jk)P(a/bc) t_{jk}^{ae[1]} \langle bc||ei \rangle \\ &- \sum_m P(i/jk)P(a/bc) t_{mi}^{bc[1]} \langle jk||ma \rangle. \end{aligned} \tag{2.75}$$

Here, $P(a/bc)$ is the antisymmetrisation operator, and the first order contri-

bution to connected doubles amplitudes is given by

$$t_{ij}^{ab[1]} = \frac{\langle ij \mid\mid ab \rangle}{D_{ij}^{ab}} \tag{2.76}$$

Numerical tests have shown that using converged doubles amplitudes in (2.75) instead of their first order approximations tends to give more accurate results. Since the final T_2 amplitudes are known when the triples correction is being evaluated, this procedure brings no additional computational costs.

In this way, the so called CCSD[T] method was developed. The energy here is given by

$$E(\text{CCSD}[T]) = E(\text{CCSD}) + E_T^{[4]} \tag{2.77}$$

where $E_T^{[4]}$ is obtained from (2.74) and (2.75) using converged connected doubles amplitudes.

However, the most commonly used approach, the CCSD(T) method, adds an additional fifth order contribution $E_{ST}^{[5]}$. The physical argument for this inclusion is, that this term becomes fourth order, when non-Hartree-Fock reference wave function is used; it is thus considerably larger than remaining fifth order contributions, and a more balanced treatment is achieved by including it.

The $E_{ST}^{[5]}$ term can be expressed as

$$E_{ST}^{[5]} = \sum_{ia} s_i^a t_i^a, \tag{2.78}$$

where the s_i^a intermediate is

$$s_i^a = \frac{1}{4} \sum_{bcjk} \langle bc \mid\mid jk \rangle t_{ijk}^{abc}. \tag{2.79}$$

The connected triples amplitudes in (2.79) are obtained again from (2.75).

The CCSD(T) energy is then given by

$$E(\text{CCSD}(T)) = E(\text{CCSD}) + E_T^{[4]} + E_{ST}^{[5]}. \tag{2.80}$$

For non-Hartree-Fock reference wavefunction, the offdiagonal Fock matrix elements are nonzero and the connected singles give a contribution to the first order energy, which leads to the presence of the $E_{DT}^{[4]}$ term

$$E_{DT}^{[4]} = \frac{1}{4} \sum_{abcijk} f_{kc} t_{ij}^{ab} t_{ijk}^{abc}, \tag{2.81}$$

and the CCSD(T) energy in this case becomes

$$E(\text{CCSD(T)}) = E(\text{CCSD}) + E_T^{[4]} + E_{ST}^{[5]} + E_{DT}^{[4]}. \qquad (2.82)$$

Since this expression includes terms with off-diagonal Fock matrix elements, the energy is no longer invariant to unitary occupied-occupied and virtual-virtual orbital transformations. To regain the invariance, it is necessary to either iterate the T_3 equation, or to use a special set of orbitals. The first possibility is not practical, since the iterations of T_3 equations would spoil the noniterative character of the method. The use of semicanonical orbitals has been introduced to solve this problem [23]. They are defined as orbitals yielding diagonal virtual-virtual and occupied-occupied blocks of the Fock matrix.

2.5 Multireference Brillouin-Wigner coupled clusters method

The state specific multireference Brillouin-Wigner coupled clusters method is one of multireference generalizations of the standard single reference coupled clusters method. As its name suggests, it is based on the multireference Brillouin-Wigner perturbation theory.

2.5.1 Basic concept of MR BWCC

For a correct description of quasidegenerate systems, it is necessary to account for the static correlation by the choice of reference wavefunction. The reference function Φ is taken in the form of a linear combination of several Slater's determinants, which are called reference configurations

$$\Phi = \sum_{\mu=1}^{M} C_\mu \Phi_\mu . \qquad (2.83)$$

For a given set of reference configurations, the reference wavefunction is restricted to the model space, which is a functional subspace of Hilbert space with the basis set consisting of reference configurations. The coefficients C_μ are a priori unknown and have to be determined in the subsequent calculation. Similarly to other Hilbert space multireference coupled clusters formalisms [42], the μ-th reference configuration Φ_μ acts as the μ-th Fermi vacuum.

Furthermore, let us define a projection operator on the μ-th reference configuration $\hat{P}_\mu$. Then the projection operator $\hat{P}$ on the whole reference space is the sum of the respective projection operators

$$\hat{P} = \sum_{\mu=1}^{M} \hat{P}_\mu \qquad (2.84)$$

The orthogonal complement of $\hat{P}$ will be denoted as $\hat{Q}$.

Next, let us define the effective Hamiltonian $\hat{H}^{\text{eff}}$ as the operator, which, when acting on the reference wafefunction, gives the exact energy

$$\hat{H}^{\text{eff}} \Phi = E\Phi. \qquad (2.85)$$

Of course, the effective Hamiltonian operator is a priori unknown and depends on the exact wavefunction, or equivalently on the wave operator $\hat{\Omega}$. When the intermediate normalization, $\hat{P}\hat{\Omega} = \hat{P}$, is obeyed, the effective Hamiltonian can be expressed as

$$\hat{H}^{\text{eff}} = \hat{P}\hat{H}\hat{\Omega}\hat{P}. \qquad (2.86)$$

To find the wave operator, the Brillouin-Wigner perturbation theory is employed, which requires that the wave operator fulfills the Bloch's equation (2.35). The wave operator is assumed to be in the form of Jeziorski--Monkhorst ansatz [41]

$$\hat{\Omega} = \sum_{\mu=1}^{M} e^{\hat{T}(\mu)} \hat{P}_\mu, \qquad (2.87)$$

which introduces the coupled clusters formalism to the MR BWCC method. The operator $\hat{T}(\mu)$ is the cluster operator corresponding to μ-th reference configuration, which plays the role of the μ-th Fermi vacuum for the creation and annihilation operators involved. The wave operator is thus uniquely determined by M sets of cluster amplitudes corresponding to M reference configurations in the expansion of the reference function.

Cluster amplitudes of excitations, transforming one reference configuration to another, are called internal amplitudes and have a special position in the scheme. To preserve the intermediate normalization, the internal amplitudes must be kept equal to zero for a complete model space. For an incomplete model space, these amplitudes must fulfill the C conditions [129,130].

40

Within the model space, the effective Hamiltonian is represented by a $M \times M$ matrix with elements $H^{\text{eff}}_{\mu\nu} = \langle \Phi_\mu \mid \hat{H}^{\text{eff}} \mid \Phi_\nu \rangle$. Using the Jeziorski--Monkhorst ansatz, we obtain

$$H^{\text{eff}}_{\mu\nu} = \langle \Phi_\mu \mid \hat{H} \mid \Phi_\mu \rangle \delta_{\mu\nu} + \langle \Phi_\mu \mid \hat{H}_N(\nu) e^{\hat{T}(\nu)} \mid \Phi_\nu \rangle. \qquad (2.88)$$

As suggested above, the knowledge of the effective Hamiltonian is sufficient to find the exact energy. Inserting the expansion of reference wavefunction (2.83) into the definition of effective Hamiltonian (2.85) and using the orthonormality of reference configurations, we obtain

$$\sum_\nu H^{\text{eff}}_{\mu\nu} C_\nu = E C_\mu. \qquad (2.89)$$

This is a non-hermitian matrix eigenvalue problem, and therefore the exact energy is found as the selected eigenvalue of the effective Hamiltonian matrix and the C_μ coefficients form the corresponding eigenvector. As noted before, the MR BWCC method is state specific, and therefore only the selected eigenvalue has a physical meaning.

Cluster equations

As noted above, the wave operator is uniquely determined by M sets of cluster amplitudes. These cluster amplitudes are obtained by solving cluster equations

$$(E - \langle \Phi_\mu \mid \hat{H} \mid \Phi_\mu \rangle) \langle \Phi_q \mid e^{\hat{T}(\mu)} \mid \Phi_\mu \rangle = \langle \Phi_q \mid \hat{H}_N \, e^{\hat{T}(\mu)} \mid \Phi_\mu \rangle, \qquad (2.90)$$

which are derived by inserting the Jeziorski-Monkhorst ansatz of the cluster operator (2.87) into the Bloch equation (2.35), and a subsequent projection of this equation to a general (excited) Slater's determinant Φ_q.

To obtain the T_1 equation, let us assume that the Slater determinant Φ_q is monoexcited with respect to μ-th Fermi vacuum

$$\Phi_q = (\Phi_\mu)^a_i. \qquad (2.91)$$

The left hand side of the equation (2.90) is simplified using

$$\langle (\Phi_\mu)^a_i \mid e^{\hat{T}(\mu)} \mid \Phi_\mu \rangle = t^a_i(\mu). \qquad (2.92)$$

The expression on the right hand side of the equation (2.90) is divided into connected, disconnected linked, and disconnected unlinked part.

$$\langle (\Phi_\mu)_i^a \mid \hat{H}_N e^{\hat{T}(\mu)} \mid \Phi_\mu \rangle = \langle (\Phi_\mu)_i^a \mid \hat{H}_N e^{\hat{T}(\mu)} \mid \Phi_\mu \rangle_C +$$
$$+ \langle (\Phi_\mu)_i^a \mid \hat{H}_N e^{\hat{T}(\mu)} \mid \Phi_\mu \rangle_{DC,L} + \quad (2.93)$$
$$+ \langle (\Phi_\mu)_i^a \mid \hat{H}_N e^{\hat{T}(\mu)} \mid \Phi_\mu \rangle_{DC,UL}$$

For the choice of $\Phi_q = (\Phi_\mu)_i^a$, the disconnected linked term yields zero contribution. The unlinked term can be factorized as

$$\langle (\Phi_\mu)_i^a \mid \hat{H}_N e^{\hat{T}(\mu)} \mid \Phi_\mu \rangle_{DC,UL} = t_i^a \langle \Phi_\mu \mid \hat{H}_N e^{\hat{T}(\mu)} \mid \Phi_\mu \rangle_C, \quad (2.94)$$

where $\langle \Phi_\mu \mid \hat{H}_N e^{\hat{T}(\mu)} \mid \Phi_\mu \rangle_C$ is recognized as a part of the diagonal element of the matrix of the effective Hamiltonian (2.88).

The final form of the T_1 equation thus reads

$$(E - H_{\mu\mu}^{\text{eff}}) t_i^a(\mu) = \langle (\Phi_\mu)_i^a \mid \hat{H}_N(\mu) e^{\hat{T}(\mu)} \mid \Phi_\mu \rangle_C. \quad (2.95)$$

Comparing this equation with the single reference coupled clusters one, the term $(E - H_{\mu\mu}^{\text{eff}}) t_i^a(\mu)$ is included on the left hand side of the equation.

The T_2 equation is derived analogously. It is obtained by substituting $\Phi_\vartheta = (\Phi_\mu)_{ij}^{ab}$ into the general cluster equation (2.93). Analogously to the T_1 equation, the $\langle (\Phi_\mu)_{ij}^{ab} \mid \hat{H}_N e^{\hat{T}(\mu)} \mid \Phi_\mu \rangle$ term is again divided into connected, disconnected linked, and unlinked parts. For the case of one reference configuration, the disconnected terms vanish.

The unlinked term has a similar structure to the corresponding term in the T_1 equation. Using the definition of $\tau_{ij}^{ab}(\mu)$

$$\langle (\Phi_\mu)_{ij}^{ab} \mid e^{\hat{T}(\mu)} \mid \Phi_\mu \rangle = t_i^a(\mu) t_j^b(\mu) - t_i^b(\mu) t_j^a(\mu) + t_{ij}^{ab}(\mu) \equiv \tau_{ij}^{ab}(\mu), \quad (2.96)$$

we obtain

$$\langle (\Phi_\mu)_{ij}^{ab} \mid \hat{H}_N e^{\hat{T}(\mu)} \mid \mu \rangle_{UL} = \tau_{ij}^{ab}(\mu) \langle \Phi_\mu \mid \hat{H}_N \hat{T}(\mu) \mid \Phi_\mu \rangle_C. \quad (2.97)$$

In contrast to the T_1 equation, the disconnected linked part is nonzero and must be included. It can be factorized into connected parts.

$$\langle (\Phi_\mu)_{ij}^{ab} \mid \hat{H}_N e^{\hat{T}(\mu)} \mid \Phi_\mu \rangle_{DC,L} = \mathcal{P}(ab)\mathcal{P}(ij) t_i^a(\mu) \langle (\Phi_\mu)_j^b \mid \hat{H}_N(\mu) e^{\hat{T}(\mu)} \mid \Phi_\mu \rangle_C,$$
$$(2.98)$$

where $\mathcal{P}(ij)$ is an antisymmetrization operator within the indices i and j.

The resulting T_2 equation reads

$$(E - H_{\mu\mu}^{\text{eff}})\tau_{ij}^{ab} = \langle (\Phi_\mu)_{ij}^{ab} \mid \hat{H}_N \, e^{\hat{T}(\mu)} \mid \Phi_\mu \rangle_C + \tag{2.99}$$
$$+ \mathcal{P}(ij)\,\mathcal{P}(ab)\,t_i^a(\mu)\,\langle (\Phi_\mu)_j^b \mid \hat{H}_N \, e^{\hat{T}(\mu)} \mid \Phi_\mu \rangle_C.$$

So far, no truncation of the cluster operator has been performed and all equations are valid for any truncation. In the MR BWCCSD case, only connected singles and doubles are included, i.e. $\hat{T}(\mu) = \hat{T}_1(\mu) + \hat{T}_2(\mu)$. In this case, the T_1 and T_2 cluster equations derived above are sufficient to determine all cluster amplitudes in the wave operator.

For higher approximations, additional cluster equations must be handled. The inclusion of connected triples, which requires the T_3 equation, is discussed in the two following chapters.

2.5.2 Size-extensivity corrections

The main drawback of the multireference Brillouin-Wigner coupled cluster method is the lack of size-extensivity. This size-inextensivity is caused by the inclusion of unlinked and disconnected terms within the cluster equations. However, these terms are responsible for a denominator shift, and thus for avoiding the intruder states problem.

To reduce or eliminate the size-inextensivity of the MR BWCCSD method, two corrections have been developed. Both approaches are based on the transition between the Brillouin-Wigner and the Rayleigh-Schrödinger perturbation theories. Let us multiply the Bloch equation in the Brillouin-Wigner scheme (2.35) by a parameter λ and the Bloch equation in the Rayleigh--Schrödinger scheme (2.34) by $(1 - \lambda)$, and add these two equations together. Here, the parameter λ is an arbitrary number between zero and one. In this way, the generalized Bloch equation [92] is obtained

$$\lambda E \hat{\Omega} \hat{P} + [(1 - \lambda)\hat{\Omega}\hat{H}_0 - \hat{H}_0\hat{\Omega}]\hat{P} = \hat{V}\hat{\Omega}\hat{P} - (1 - \lambda)\hat{\Omega}\hat{P}\hat{V}\hat{\Omega}\hat{P}. \tag{2.100}$$

The parameter λ scales the transition between the Brillouin-Wigner and the Rayleigh-Schrödinger perturbation theory. For $\lambda = 0$, the generalized Bloch equation corresponds to the Rayleigh-Schrödinger theory, and for $\lambda = 1$ to the Brillouin-Wigner theory.

By substituting the wave operator ansatz into the generalized Bloch equation and neglecting renormalization terms, the following cluster equation is

obtained

$$\lambda(E - H_{\mu\mu}^{\text{eff}})\langle\Phi_q|e^{T(\mu)}|\Phi_\mu\rangle = \langle\Phi_q|\hat{H}_N(\mu)e^{T(\mu)}|\Phi_\mu\rangle_{\text{C}} +$$
$$+ \lambda\langle\Phi_q|\hat{H}_N(\mu)e^{T(\mu)}|\Phi_\mu\rangle_{\text{DC,L}} \quad (2.101)$$

In all approaches, first the cluster amplitudes are converged with λ set to one. Then, two basic schemes are available. In the first one, one additional iteration is done, with the value of λ equal to zero. This leads to an approximate elimination of the size-inextensive terms in the cluster equations. This correction is called "a posteriori".

The other approach is the iterative correction, in which the parameter λ is reduced gradually from one to zero in a geometrical sequence, and the cluster equations are iterated accordingly. Therefore, the a posteriori correction can be viewed as a special case of the iterative one, with the transition involving only one step.

The aposteriori correction was found to have a good performance. Its advantage are the smaller computational demands. The iterative correction is more rigorous, but its drawbacks include large computational time needed and occasionally the numerical instability due to the reemerging intruder state problem.

Chapter 3

Iterative inclusion of connected triples

This chapter is devoted to various approaches towards iterative inclusion of connected triple excitations into the multireference Brillouin-Wigner coupled cluster method. The iterative approach, although computationally more demanding, is rigorous and conceptually straightforward.

Starting from the full MR BWCCSDT method, several additional approximations can be made. First, the simplification of the connected part of the cluster equations is possible, thus obtaining the multireference analogs of the CCSDT-n methods mentioned in the previous chapter. Second, we can neglect the disconnected and unlinked terms in the T_3 equation, which leads to so called α approximation.

3.1 First steps

Let us truncate the cluster operator to connected singles, doubles, and triples

$$\hat{T} = \hat{T}_1 + \hat{T}_2 + \hat{T}_3 \equiv \hat{T}_{123}. \tag{3.1}$$

In the following text the cluster operator within this truncation will be denoted as $\hat{T}_{123}$.

By substituting $\hat{T}_{123}$ into the general cluster equations of the multireference Brillouin–Wigner method, we obtain

$$(E - H_{\mu\mu}^{\text{eff}})\langle(\Phi_\mu)_i^a|e^{\hat{T}_{123}(\mu)}|\Phi_\mu\rangle = \langle(\Phi_\mu)_i^a|\hat{H}_N(\mu)e^{\hat{T}_{123}(\mu)}|\Phi_\mu\rangle_{\text{C}} \tag{3.2}$$

for connected singles,

$$(E - H^{\text{eff}}_{\mu\mu})\langle(\Phi_\mu)^{ab}_{ij}|e^{\hat{T}_{123}(\mu)}|\Phi_\mu\rangle = \langle(\Phi_\mu)^{ab}_{ij}|\hat{H}_N(\mu)e^{\hat{T}_{123}(\mu)}|\Phi_\mu\rangle_{\text{C}} +$$
$$+ \langle(\Phi_\mu)^{ab}_{ij}|\hat{H}_N(\mu)e^{\hat{T}_{123}(\mu)}|\Phi_\mu\rangle_{\text{DC,L}} \quad (3.3)$$

for connected doubles, and

$$(E - H^{\text{eff}}_{\mu\mu})\langle(\Phi_\mu)^{abc}_{ijk}|e^{\hat{T}_{123}(\mu)}|\Phi_\mu\rangle = \langle(\Phi_\mu)^{ab}_{ij}|\hat{H}_N(\mu)e^{\hat{T}_{123}(\mu)}|\Phi_\mu\rangle_{\text{C}} +$$
$$+ \langle(\Phi_\mu)^{ab}_{ij}|\hat{H}_N(\mu)e^{\hat{T}_{123}(\mu)}|\Phi_\mu\rangle_{\text{DC,L}} \quad (3.4)$$

for connected triples.

Let us compare these equations with those of MR BWCCSD method, given in the previous chapter. Of course, there is the T_3 equation, which was not present at the MR BWCCSD level. Moreover, connected triples contribute to T_1 and T_2 equations.

Let us postpone the discussion of unlinked and disconnected part of the T_3 equation and look firstly at the changes required for

1. the matrix elements of the effective Hamiltonian,

2. the connected part of cluster equations,

3. the unlinked part of the T_1 and T_2 cluster equations,

4. the disconnected linked part of the T_1 and T_2 cluster equations,

5. the denominators in the T_3 equation.

3.1.1 Connected part of the cluster equations

The determination of the connected part of the cluster equations is the computationally most expensive part of the calculation. Of course, the connected triples contribute significantly to these terms, which are fully analogous to their counterparts in the single reference CCSDT. These expressions can thus be evaluated directly by the routines used in the CCSDT part of the code. Since several reference configurations are included in the calculation, these routines have to be called for each of them and appropriate sets of amplitudes have to be given to them as input.

3.1.2 Elements of the effective Hamiltonian matrix

For the diagonal elements, only the first term on the right hand side of (2.88) is nonzero. This term can be viewed as the correlation energy corresponding to μ-th reference function. According to (2.42), the correlation energy within the coupled cluster scheme depends only on the connected singles and doubles, and the diagonal elements of effective Hamiltonian matrix are thus not directly affected by the inclusion of connected triples.

For the off-diagonal elements, only the second term of (2.88) is nonzero. This term generally includes contributions of connected triples. However, their inclusion is rather simple. As stated before, the current implementation of the multireference Brillouin-Wigner coupled cluster method is restricted to a model space, where the reference configurations are mutually monoexcited or biexcited. In this case, the offdiagonal elements of the $H_{\nu\mu}^{\text{eff}}$ matrix have the form $\langle (\Phi_\mu)_i^a | \hat{H}_N(\mu) e^{\hat{T}_{123}(\mu)} | \Phi_\mu \rangle_C$ for mutually monoexcited and $\langle (\Phi_\mu)_{ij}^{ab} | \hat{H}_N(\mu) e^{\hat{T}_{123}(\mu)} | \Phi_\mu \rangle_C$ for mutually biexcited pair of reference configurations and they correspond to the right hand sides of the T_1 and T_2 equations for respective internal excitations. As such, these terms are evaluated automatically when solving the T_1 and T_2 equation. As long as we restrict ourselves to a model space with references mutually no more than biexcited, no changes in the code are required. When expanding the program to allow mutually triexcited references, it will be necessary to perform a similar treatment for the T_3 equation.

To be precise, it should be noted, that the ACES II package does not compute explicitly the $\langle (\Phi_\mu)_i^a | \hat{H}_N(\mu) e^{\hat{T}_{123}(\mu)} | \Phi_\mu \rangle_C$ and $\langle (\Phi_\mu)_{ij}^{ab} | \hat{H}_N(\mu) e^{\hat{T}_{123}(\mu)} | \Phi_\mu \rangle_C$ terms, but instead of that the "true" right hand sides $\langle (\Phi_\mu)_i^a | \hat{V}_N(\mu) e^{\hat{T}_{123}(\mu)} | \Phi_\mu \rangle_C$ and $\langle (\Phi_\mu)_{ij}^{ab} | \hat{V}_N(\mu) e^{\hat{T}_{123}(\mu)} | \Phi_\mu \rangle_C$, where $\hat{V}_N$ was defined in (2.36). These expressions differ from the needed ones by $D_i^a t_i^a$ and $D_{ij}^{ab} t_{ij}^{ab}$ respectively. Therefore, these terms have to be added in so called "fixing" of the right hand sides. To distinguish these terms, let call the $\langle (\Phi_\mu)_i^a | \hat{H}_N(\mu) e^{\hat{T}_{123}(\mu)} | \Phi_\mu \rangle_C$ and $\langle (\Phi_\mu)_{ij}^{ab} | \hat{H}_N(\mu) e^{\hat{T}_{123}(\mu)} | \Phi_\mu \rangle_C$ fixed right hand sides, while the expressions $\langle (\Phi_\mu)_i^a | \hat{V}_N(\mu) e^{\hat{T}_{123}(\mu)} | \Phi_\mu \rangle_C$ and $\langle (\Phi_\mu)_{ij}^{ab} | \hat{V}_N(\mu) e^{\hat{T}_{123}(\mu)} | \Phi_\mu \rangle_C$ will be denoted as the right hand sides.

For a complete model space, the full right hand sides and the fixed ones are for internal amplitudes identical. This is due to the fact that internal amplitudes are equal to zero, and thus the difference between the two expressions vanishes.

3.1.3 Unlinked part of the T_1 and T_2 cluster equations

For the T_1 equation, the unlinked term reads as $(E - H_{\mu\mu}^{\text{eff}})\langle(\Phi_\mu)_i^a|e^{\hat{T}_{123}(\mu)}|\Phi_\mu\rangle$. In the first factor, there is the difference between the exact energy and diagonal element of the effective Hamiltonian. As shown above, no changes are required for $H_{\mu\mu}^{\text{eff}}$. The total correlation energy is obtained from the diagonalization of the effective Hamiltonian matrix, which is not affected by the presence of connected triples. The second part of the expression is identically equal to t_i^a, and therefore there are no contributions from connected triples.

For the T_2 equation, the situation is rather similar. The first factor of the $(E - H_{\mu\mu}^{\text{eff}})\langle(\Phi_\mu)_{ij}^{ab}|e^{\hat{T}_{123}(\mu)}|\Phi_\mu\rangle$ expression is the same as in the previous case, while the second factor is identically equal to the τ_{ij}^{ab} amplitude defined in (2.96), which consists only of connected singles and doubles.

3.1.4 Disconnected linked part of the T_2 cluster equation

The disconnected linked part of the T_2 cluster equation can be expressed as

$$\langle(\Phi_\mu)_{ij}^{ab}|\hat{H}_N(\mu)e^{\hat{T}_{123}(\mu)}|\Phi_\mu\rangle_{\text{DC,L}} = \tag{3.5}$$
$$= \mathcal{P}(ab)\mathcal{P}(ij)\left\{t_i^a(\mu)\langle(\Phi_\mu)_j^b \mid \hat{H}_N(\mu)\,e^{\hat{T}_{123}(\mu)} \mid \Phi_\mu\rangle_C\right\},$$

Connected triples do not affect directly the $t_i^a(\mu)$ amplitude, and therefore contribute through $\langle(\Phi_\mu)_j^b \mid \hat{H}_N(\mu)\,e^{\hat{T}_{123}(\mu)} \mid \Phi_\mu\rangle_C$ only. Since these quantities are already computed in the T_1 equation, the connected triples are included automatically.

3.1.5 Denominators in the T_3 equation

The D_{ijk}^{abc} denominators are constructed in an analogous way to the denominators in the T_1 and T_2 equation.

$$D_{ijk}^{abc} = f_{ii} + f_{jj} + f_{kk} - f_{aa} - f_{bb} - f_{cc}. \tag{3.6}$$

Since several reference configurations are taken into account, different spinorbitals are occupied in different references and it is necessary to reorder the diagonal elements of the Fock matrix, similarly as has been done already in MR BWCCSD for D_i^a and D_{ij}^{ab}.

3.2 MR BWCCSDTα approximation

In previous section, various aspects of the multireference generalization of CCSDT method were discussed. It has been shown, that apart of disconnected linked and unlinked terms in T_3 equation, very few changes in the ACES II package are required. This has lead to the MR BWCCSDTα approximation, where the disconnected linked and unlinked contributions to the T_3 equation are neglected. Otherwise, the connected triples are included fully in the description. This approximation leads to the following cluster equations

$$(E - H_{\mu\mu}^{\text{eff}})t_i^a(\mu) \;=\; \langle(\Phi_\mu)_i^a|\hat{H}_N(\mu)e^{\hat{T}_{123}(\mu)}|\Phi_\mu\rangle_C \tag{3.7}$$

for connected singles,

$$(E - H_{\mu\mu}^{\text{eff}})\tau_{ij}^{ab}(\mu) \;=\; \langle(\Phi_\mu)_{ij}^{ab}|\hat{H}_N(\mu)e^{\hat{T}_{123}(\mu)}|\Phi_\mu\rangle_C + \tag{3.8}$$
$$+ \; \mathcal{P}(ab)\mathcal{P}(ij)t_i^a(\mu)\langle(\Phi_\mu)_j^b \mid \hat{H}_N(\mu)\, e^{\hat{T}_{123}(\mu)} \mid \Phi_\mu\rangle_C$$

for connected doubles, and

$$0 \;=\; \langle(\Phi_\mu)_{ij}^{ab}|\hat{H}_N(\mu)e^{\hat{T}_{123}(\mu)}|\Phi_\mu\rangle_C \tag{3.9}$$

for connected triples.

The main motivation for this approximation was, of course, the easy implementation of the MR BWCCSDTα method. However, this approach faces several drawbacks. First of all, as the disconnected unlinked terms in T_3 are neglected, the method uses Rayleigh-Schrödinger denominators. This means, that the MR BWCCSDTα is sensitive to the intruder state problem. Furthermore, this method is not equivalent to the full configuration interaction for three–electron systems.

The α approximation is compatible with the multireference generalization of CCSDT-n methods. In this case, contributions of connected singles and triples to the connected parts of T_2 and T_3 equation are handled in the same way as in the single reference methods. This leads to MR BWCCSDT-$n\alpha$ methods, where $n = 1, 1b, 2, 3, 4$.

3.3 Disconnected terms in the T_3 equation

In the discussion of various aspects of the inclusion of connected triple excitations into the cluster operator, we have so far omitted the disconnected

linked and unlinked contribution to the T_3 cluster equation.

For a rigorous treatment it is, however, inevitable to include these terms. Also, with these terms the method is numerically more stable, due to the Brillouin-Wigner T_3 denominator shift.

3.3.1 Disconnected linked terms

Similarly to the MR BWCCSD case, the disconnected linked terms can be factorized into connected parts. Since we are concerned with contributions to the T_3 equation, the corresponding diagrams must have three pairs of external lines, which can be divided between the connected parts as $1 + 1 + 1$ or $2 + 1$.

The Hamiltonian $\hat{H}_N$ is included only once in disconnected terms, therefore only one of the connected parts includes the Hamiltonian and the remaining terms consist only of cluster amplitudes.

Let us first concentrate on the connected part which includes the Hamiltonian. As said before, it can have either one or two pairs of external lines. In the former case, all connected diagrams with one Hamiltonian, one pair of external lines and any number of cluster amplitudes contribute. However, these diagrams are precisely those contributing to $\langle (\Phi_\mu)_i^a | \hat{H}_N(\mu) e^{\hat{T}_{123}(\mu)} | \Phi_\mu \rangle_C$, which is the full right hand side of the T_1 equation. Therefore, this expression is available at almost no additional computational cost. Similarly, for diagrams with two pairs of external lines we get the $\langle (\Phi_\mu)_{ij}^{ab} | \hat{H}_N(\mu) e^{\hat{T}_{123}(\mu)} | \Phi_\mu \rangle_C$ T_2, which are multireference analogues of the T_2 right hand sides of the standard CCSD method.

Since the full right hand sides of the T_2 equation are not needed in the MR BWCCSD method, the "fixing" of T_2 right hand sides has to be performed in a new routine.

The remaining connected diagrams without the Hamiltonian can only be cluster amplitudes. The connected part with one pair of external lines is the T_1 amplitude, connected part with two pairs the T_2 amplitude.

The disconnected terms are shown in Figure 3.1. By the use of the definition of the τ_{ij}^{ab} amplitude (2.96), we can write it as

$$\langle (\Phi_\mu)_{ij}^{ab} | \hat{H}_N(\mu) e^{\hat{T}_{123}(\mu)} | \Phi_\mu \rangle_{DC,L} = \mathcal{P}(i/jk) \mathcal{P}(a/bc) \left\{ \langle (\Phi_\mu)_i^a | \hat{H}_N(\mu) e^{\hat{T}_{123}(\mu)} | \Phi_\mu \rangle_C \tau_{jk}^{bc} \right.$$
$$\left. + \; t_i^a \langle (\Phi_\mu)_{jk}^{bc} | \hat{H}_N(\mu) e^{\hat{T}_{123}(\mu)} | \Phi_\mu \rangle_C \right\}, \qquad (3.10)$$

Figure 3.1: Disconnected linked terms in the T_3 equation
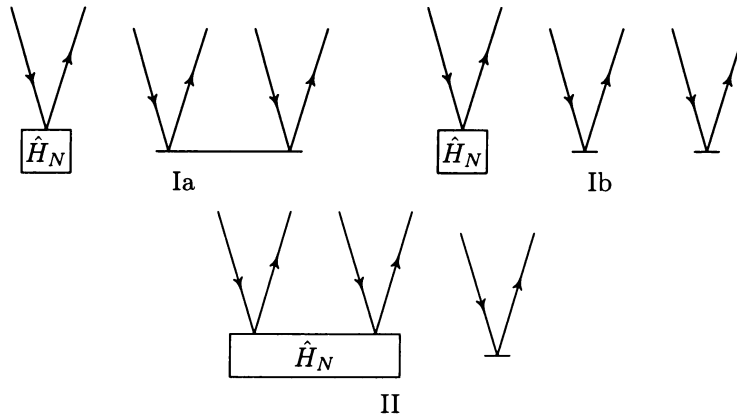
where $\mathcal{P}(i/jk)$ and $\mathcal{P}(a/bc)$ are antisymmetrization operators defined in [110].

From the computational point of view, both terms in (3.10) have the same structure. They consist of an antisymmetrized product of a two-index quantity, and four-index quantity. Therefore, they can be processed in the same way.

3.3.2 Unlinked terms

Analogously to the situation in the T_1 and T_2 equations, the unlinked part of the T_3 equation can be written as $(E - H^{\text{eff}}_{\mu\mu})\langle(\Phi_\mu)^{abc}_{ijk}|e^{\hat{T}_{123}(\mu)}|\Phi_\mu\rangle$.

The first part of this expression is the difference between the total energy and the respective diagonal element of the matrix of the effective Hamiltonian. However, the second part of this expression is more complicated.

$$
\begin{aligned}
\langle(\Phi_\mu)^{abc}_{ijk}|e^{\hat{T}_{123}(\mu)}|\Phi_\mu\rangle \;\equiv\;\; & \tau^{abc}_{ijk}(\mu) = t^{abc}_{ijk}(\mu) + \\
+\;\; & t^a_i(\mu)t^{bc}_{jk}(\mu) - t^a_j(\mu)t^{bc}_{ik}(\mu) + t^a_k(\mu)t^{bc}_{ij}(\mu) \\
-\;\; & t^b_i(\mu)t^{ac}_{jk}(\mu) + t^b_j(\mu)t^{ac}_{ik}(\mu) - t^b_k(\mu)t^{ac}_{ij}(\mu) \\
+\;\; & t^c_i(\mu)t^{ab}_{jk}(\mu) - t^c_j(\mu)t^{ab}_{ik}(\mu) + t^c_k(\mu)t^{ab}_{ij}(\mu) \\
+\;\; & t^a_i(\mu)t^b_j(\mu)t^c_k(\mu) - t^a_i(\mu)t^c_j(\mu)t^b_k(\mu) + t^b_i(\mu)t^c_j(\mu)t^a_k(\mu) \\
-\;\; & t^b_i(\mu)t^a_j(\mu)t^c_k(\mu) + t^c_i(\mu)t^a_j(\mu)t^b_k(\mu) - t^c_i(\mu)t^b_j(\mu)t^a_k(\mu)
\end{aligned}
\tag{3.11}
$$

51

In this expression, connected triple amplitude is added to the product of either three T_1 cluster amplitudes or one T_2 amplitude and one T_1 amplitude. It is possible to formally simplify this expression by introducing the τ_{ij}^{ab} amplitudes, which absorb the terms with three T_1 cluster amplitudes. It can be done in several ways, e.g.

$$
\begin{aligned}
\tau_{ijk}^{abc}(\mu) = t_{ijk}^{abc}(\mu) \quad &+ \quad t_i^a(\mu)\tau_{jk}^{bc}(\mu) - t_j^a(\mu)\tau_{ik}^{bc}(\mu) + t_k^a(\mu)\tau_{ij}^{bc}(\mu) \quad (3.12)\\
&- \quad t_i^b(\mu)t_{jk}^{ac}(\mu) + t_j^b(\mu)t_{ik}^{ac}(\mu) - t_k^b(\mu)t_{ij}^{ac}(\mu)\\
&+ \quad t_i^c(\mu)t_{jk}^{ab}(\mu) - t_j^c(\mu)t_{ik}^{ab}(\mu) + t_k^c(\mu)t_{ij}^{ab}(\mu)\\
= t_{ijk}^{abc}(\mu) \quad &+ \quad t_i^a(\mu)t_{jk}^{bc}(\mu) - t_j^a(\mu)t_{ik}^{bc}(\mu) + t_k^a(\mu)t_{ij}^{bc}(\mu)\\
&- \quad t_i^b(\mu)\tau_{jk}^{ac}(\mu) + t_j^b(\mu)\tau_{ik}^{ac}(\mu) - t_k^b(\mu)\tau_{ij}^{ac}(\mu)\\
&+ \quad t_i^c(\mu)t_{jk}^{ab}(\mu) - t_j^c(\mu)t_{ik}^{ab}(\mu) + t_k^c(\mu)t_{ij}^{ab}(\mu)\\
= t_{ijk}^{abc}(\mu) \quad &+ \quad t_i^a(\mu)t_{jk}^{bc}(\mu) - t_j^a(\mu)t_{ik}^{bc}(\mu) + t_k^a(\mu)t_{ij}^{bc}(\mu)\\
&- \quad t_i^b(\mu)t_{jk}^{ac}(\mu) + t_j^b(\mu)t_{ik}^{ac}(\mu) - t_k^b(\mu)t_{ij}^{ac}(\mu)\\
&+ \quad t_i^c(\mu)\tau_{jk}^{ab}(\mu) - t_j^c(\mu)\tau_{ik}^{ab}(\mu) + t_k^c(\mu)\tau_{ij}^{ab}(\mu)
\end{aligned}
$$

It is convenient to write this equation in a symmetric form. If we substitute in (3.11) all the T_2 amplitudes with corresponding τ_2 amplitudes, we would include the terms with three T_1 amplitudes three times. Defining the $\tilde{\tau}_{ij}^{bc}(\mu)$ amplitude as

$$
\tilde{\tau}_{ij}^{bc}(\mu) = t_{ij}^{bc}(\mu) + \frac{1}{3}\{t_i^a(\mu)t_j^b(\mu) - t_i^b(\mu)t_j^a(\mu)\}, \qquad (3.13)
$$

the $\tau_{ijk}^{abc}(\mu)$ amplitude can be consequently written as

$$
\begin{aligned}
\tau_{ijk}^{abc}(\mu) = \quad & t_{ijk}^{abc}(\mu) + t_i^a(\mu)\tilde{\tau}_{jk}^{bc}(\mu) - t_j^a(\mu)\tilde{\tau}_{ik}^{bc}(\mu) + t_k^a(\mu)\tilde{\tau}_{ij}^{bc}(\mu) \quad (3.14)\\
& - t_i^b(\mu)\tilde{\tau}_{jk}^{ac}(\mu) + t_j^b(\mu)\tilde{\tau}_{ik}^{ac}(\mu) - t_k^b(\mu)\tilde{\tau}_{ij}^{ac}(\mu)\\
& + t_i^c(\mu)\tilde{\tau}_{jk}^{ab}(\mu) - t_j^c(\mu)\tilde{\tau}_{ik}^{ab}(\mu) + t_k^c(\mu)\tilde{\tau}_{ij}^{ab}(\mu)
\end{aligned}
$$

or, using the antisymmetrization operators, as

$$
\tau_{ijk}^{abc}(\mu) = t_{ijk}^{abc}(\mu) + \mathcal{P}(i/jk)\mathcal{P}(a/bc)t_i^a(\mu)\tilde{\tau}_{jk}^{bc}(\mu) \qquad (3.15)
$$

52

3.4 Full MR BWCCSDT method

3.4.1 The T₃ equation in MR BWCCSDT

In the previous two paragraphs, the discussion of the disconnected linked and unlinked parts of T_3 cluster equation was presented. Now, it is appropriate to put all the terms together and present the final form of the T_3 equation. By substituting the expression for the disconnected linked (3.10) and unlinked (3.15) part into the T_3 equation (3.4), we obtain

$$
(E - H^{\text{eff}}_{\mu\mu}) \left(t^{abc}_{ijk}(\mu) + \mathcal{P}(i/jk)\mathcal{P}(a/bc)\{t^a_i(\mu)\tilde{\tau}^{bc}_{jk}(\mu)\} \right) =
$$
$$
= \langle (\Phi_\mu)^{abc}_{ijk} | \hat{H}_N(\mu) e^{\hat{T}_{123}(\mu)} | \Phi_\mu \rangle_{\text{C}} + \mathcal{P}(i/jk)\mathcal{P}(a/bc)\{
$$
$$
\langle (\Phi_\mu)^a_i | \hat{H}_N(\mu) e^{\hat{T}_{123}(\mu)} | \Phi_\mu \rangle_{\text{C}} \tau^{bc}_{jk} + t^a_i \langle (\Phi_\mu)^{bc}_{jk} | \hat{H}_N(\mu) e^{\hat{T}_{123}(\mu)} | \Phi_\mu \rangle_{\text{C}} \} \quad (3.16)
$$

Now, let us divide the Hamiltonian $\hat{H}_N$ into $\hat{V}_N$ and the part including diagonal elements of the Fock matrix. In a complete analogy to (2.46) and (2.47), we obtain

$$
\langle (\Phi_\mu)^{abc}_{ijk} | \hat{H}_N(\mu) e^{\hat{T}_{123}(\mu)} | \Phi_\mu \rangle_{\text{C}} = D^{abc}_{ijk} t^{abc}_{ijk} + \quad (3.17)
$$
$$
+ \langle (\Phi_\mu)^{abc}_{ijk} | \hat{V}_N(\mu) e^{\hat{T}_{123}(\mu)} | \Phi_\mu \rangle_{\text{C}}
$$

By inserting this expression into (3.16) we get

$$
(E - H^{\text{eff}}_{\mu\mu})(t^{abc}_{ijk}(\mu) + \mathcal{P}(i/jk)\mathcal{P}(a/bc)t^a_i(\mu)\tilde{\tau}^{bc}_{jk}(\mu)) = D^{abc}_{ijk} t^{abc}_{ijk}(\mu) + \quad (3.18)
$$
$$
+ \langle \Phi_{\mu\,ijk}^{\ abc} | \hat{V}_N(\mu) e^{\hat{T}_{123}(\mu)} | \Phi_\mu \rangle_{\text{C}} + \mathcal{P}(i/jk)\mathcal{P}(a/bc)\{
$$
$$
\left\{ \langle (\Phi_\mu)^a_i | \hat{H}_N(\mu) e^{\hat{T}_{123}(\mu)} | \Phi_\mu \rangle_{\text{C}} \tau^{bc}_{jk} + t^a_i \langle (\Phi_\mu)^{bc}_{jk} | \hat{H}_N(\mu) e^{\hat{T}_{123}(\mu)} | \Phi_\mu \rangle_{\text{C}} \right\}
$$

Let us put all the terms with t^{abc}_{ijk} on the left hand side of the equation, and all the remaining terms on the right one.

$$
(D^{abc}_{ijk} + E - H^{\text{eff}}_{\mu\mu}) t^{abc}_{ijk}(\mu) = - \langle \Phi_{\mu\,ijk}^{\ abc} | \hat{V}_N(\mu) e^{\hat{T}_{123}(\mu)} | \Phi_\mu \rangle_{\text{C}} + \quad (3.19)
$$
$$
+ \mathcal{P}(i/jk)\mathcal{P}(a/bc)\{ (E - H^{\text{eff}}_{\mu\mu}) t^a_i(\mu)\tilde{\tau}^{bc}_{jk}(\mu) +
$$
$$
+ \langle (\Phi_\mu)^a_i | \hat{H}_N(\mu) e^{\hat{T}_{123}(\mu)} | \Phi_\mu \rangle_{\text{C}} \tau^{bc}_{jk} + t^a_i \langle (\Phi_\mu)^{bc}_{jk} | \hat{H}_N(\mu) e^{\hat{T}_{123}(\mu)} | \Phi_\mu \rangle_{\text{C}} \}
$$

On the left hand side of the equation, there is a shift of the denominator by $(E - H^{\text{eff}}_{\mu\mu})$, which is characteristic for the Brillouin-Wigner theory and enables us to overcome the intruder state problem.

53

On the right hand side, apart from the standard connected part, there are three terms with the same structure. All these terms are antisymmetrized products of one quantity with one pair of external lines and one quantity with two pairs, and can thus be treated in an analogous manner.

3.4.2 Notes on the implementation

The denominator shift is performed in a routine called rmd314, which divides the right hand side of (3.19) by the denominator D_{ijk}^{abc}.

The inclusion of the disconnected linked and unlinked terms is done using the existing s1s214 and s1s223 routines. The first routine works for the spin cases $\alpha\alpha\alpha$ and $\beta\beta\beta$, i.e. for cluster amplitudes corresponding to excitations between spinorbitals with all α spin or β spin, respectively. The latter one is used for the spin cases $\alpha\alpha\beta$ and $\alpha\beta\beta$. These routines, which are used also for forming so called "disconnected triple amplitudes" in the analytic gradient of CCSD(T) and CCSD[T] method, perform generally the antisymmetrized product of a quantity with one pair of external lines and a quantity with such two pairs. These routines are called three times for each of the three contributions of disconnected linked and unlinked terms in equation (3.19).

In the CCSDT ACES II code, the T_3 cluster equations are solved before the T_1 and T_2 equations. Therefore, the T_1 and T_2 right hand sides from previous iterations are used. The same is true for the denominator shift $E - H_{\mu\mu}^{\text{eff}}$. The T_2 right hand sides $\langle (\Phi_\mu)_{ij}^{ab} | \hat{V}_N(\mu) e^{\hat{T}_{123}(\mu)} | \Phi_\mu \rangle_{\text{C}}$ are fixed by adding $D_{ij}^{ab} t_{ij}^{ab}$.

One potential difficulty is encountered, when doing a calculation with restricted Hartree Fock reference function. In this case, only the $\alpha\beta$ T_2 amplitudes are obtained by solving cluster equations, and the remaining $\alpha\alpha$ ones are calculated using the equation

$$t_{ij}^{ab} = t_{i\bar{j}}^{a\bar{b}} - t_{i\bar{j}}^{\bar{a}b} \tag{3.20}$$

Here, the indices without the bar indicate spinorbitals with the α spin and indexes with bar spinorbitals with the β spin. No right hand sides are thus computed for $\alpha\alpha$ and $\beta\beta$ amplitudes. However, the right hand sides fulfill an analogous equation to (3.20) and can be thus obtained by the same procedure as the corresponding cluster amplitudes.

Chapter 4

Noniterative inclusion of connected triples

This chapter is devoted to the noniterative inclusion of connected triple excitations into the multireference Brillouin-Wigner coupled cluster method.

4.1 Corrections to the effective Hamiltonian matrix

In the single reference CCSD(T) method, the effect of connected triples is handled as a perturbative correction obtained using an one-step approximation of connected triples amplitudes. In the multireference case, the situation is slightly more complicated. Firstly, the correlation energy is obtained by a diagonalization of the effective Hamiltonian. Secondly, for a calculation with more than one reference configurations, there are several sets of cluster amplitudes.

A natural way is thus not to calculate corrections to the correlation energy itself, but to the matrix elements of the effective Hamiltonian. The corrected energy is subsequently obtained by its diagonalization.

In the multireference Brillouin-Wigner coupled clusters method, the diagonal and off-diagonal elements of $\hat{H}^{\text{eff}}$ matrix elements are obtained in a different way. The diagonal elements are calculated formally as the "correlation energy" of the respective reference function. The off-diagonal elements are obtained as the full T_1 and T_2 right hand sides corresponding to internal excitations. The further discussion is correspondingly divided into two parts.

4.1.1 Correction to the diagonal $\hat{H}^{\text{eff}}$ matrix elements

As stated before, the diagonal element $\hat{H}^{\text{eff}}_{\mu\mu}$ formally corresponds to the correlation energy, calculated using the amplitudes of the μ-th reference configuration. Its triples correction is thus conceptually straightforward. The diagonal elements $\hat{H}^{\text{eff}}_{\mu\mu}$ are given by

$$
\begin{aligned}
H^{\text{eff}}_{\mu\mu}(\text{ MR BWCCSD(T)}) &= H^{\text{eff}}_{\mu\mu}(\text{ MR BWCCSD}) + E^{[4]}_T(\mu) \\
&\quad + E^{[5]}_{ST}(\mu) + E^{[4]}_{ST}(\mu),
\end{aligned} \tag{4.1}
$$

in an analogy to the single reference case.

In contrast to the case of MR CCSD(T) based on Rayleigh-Schrödinger perturbation theory [46], there are no renormalization terms present in the equations, and our expressions are fully analogous to the single reference theory. However, the formulas for non-Hartree-Fock references have to be used, since in a multireference theory the reference configurations are in general not Hartree-Fock ones.

To demonstrate the simplification of the formalism due to the lack of the renormalization terms, we first look at the first term in the MR CCSD(T) expression for $E^{[4]}_T(\mu)$ [46]

$$
\begin{aligned}
E^{[4]}_T(\mu) = &- \sum_{abcijk} \frac{1}{D^{abc}_{ijk}} \langle \Phi_\mu | [\sum_{\nu \neq \mu} \{\hat{T}_2(\mu)\hat{V}_N|\Phi_\nu\rangle\langle\Phi_\nu|\hat{T}_2(\mu)\} + \hat{T}_2(\mu)\hat{V}_N] |(\Phi_\mu)^{abc}_{ijk}\rangle_C \\
&\times \{\langle(\Phi_\mu)^{abc}_{ijk}|\hat{T}_2(\mu)\hat{V}_N|\Phi_\mu\rangle_C\}
\end{aligned} \tag{4.2}
$$

and for the connected triples amplitudes

$$
D^{abc}_{ijk}(\mu)t^{abc}_{ijk}(\mu) = \langle(\Phi_\mu)^{abc}_{ijk}|\hat{T}_2(\mu)\hat{V}_N|\Phi_\mu\rangle - \sum_{\nu \neq \mu}\langle(\Phi_\mu)^{abc}_{ijk}|\hat{T}_2(\nu)\hat{V}_N|\Phi_\nu\rangle H^{\text{eff}}_{\nu\mu}. \tag{4.3}
$$

The renormalization term in (4.3) is the second term. Without this term, the equation becomes

$$
D^{abc}_{ijk}(\mu)t^{abc}_{ijk}(\mu) = \langle(\Phi_\mu)^{abc}_{ijk}|\hat{T}_2(\mu)\hat{V}_N|\Phi_\mu\rangle, \tag{4.4}
$$

which is analogous to the T_3 equation of the single reference CCSD(T) and CCSDT-1 method.

Similarly, the first term in the expression for $E^{[4]}_T(\mu)$ (4.2) vanishes and the formula reduces to a symmetrical form analogous to the single reference CCSD(T) method

$$
E^{[4]}_T(\mu) = \frac{1}{36} \sum_{abcijk} t^{abc}_{ijk}(\mu)D^{abc}_{ijk}(\mu)t^{abc}_{ijk}(\mu), \tag{4.5}
$$

56

where we have used the equation for connected triples amplitudes (4.4)

For other terms, the situation is similar and we get

$$E_{ST}^{[5]}(\mu) = \sum_{ia} s_i^a(\mu) t_i^a(\mu), \tag{4.6}$$

$$E_{ST}^{[4]}(\mu) = \frac{1}{4} \sum_{abcijk} f_{kc}(\mu) t_{ij}^{ab}(\mu) t_{ijk}^{abc}(\mu), \tag{4.7}$$

where the s intermediate is given by

$$s_i^a(\mu) = \frac{1}{4} \sum_{bcjk} \langle bc||jk \rangle t_{ijk}^{abc}(\mu) \tag{4.8}$$

and the triple amplitudes are obtained by solving

$$\begin{aligned} D_{ijk}^{abc}(\mu) t_{ijk}^{abc}(\mu) &= \sum_e P(i/jk) P(a/bc) t_{jk}^{ae}(\mu) \langle bc||ei \rangle \\ &- \sum_m P(i/jk) P(a/bc) t_{mi}^{bc}(\mu) \langle jk||ma \rangle. \end{aligned} \tag{4.9}$$

All these equations differ from the CCSD(T) ones only by the index μ, corresponding to the respective reference configuration, from the corresponding equations (2.74), (2.75), (2.81), and (2.78) for the single reference CCSD(T) method.

4.1.2 Correction to the off-diagonal elements of the $\hat{H}^{\text{eff}}$ matrix

The situation concerning the off-diagonal matrix elements of the effective Hamiltonian is somewhat less clear.

Balková and Bartlett in their method [46] calculated this correction as the contribution of the connected triples to T_1 and T_2 right hand sides at the CCSDT-1 level. The justification for this argument was that CCSD(T) can be viewed as CCSD with one additional iteration of CCSDT-1. Li and Paldus argued in their work [103,104] that these corrections are not necessary, since they are already of the fifth or higher order of the perturbation theory. The validity of this statement, however, might be undermined by several factors. Firstly, for all reference configurations except the Hartree-Fock one, the Fock matrix has nonzero off-diagonal elements, and then the perturbation order of these contributions is reduced, due to the nonzero first order contribution

to connected singles amplitudes. Secondly, the number of the off-diagonal elements of effective Hamiltonian matrix grows quadratically with the size of the model space, and their influence thus increases with the number of reference configurations.

We have decided to implement both variants. In MR BWCCSD(T_d) there are no corrections to the off-diagonal $\hat{H}^{\text{eff}}$ matrix elements. In MR BWCCSD(T), they are given by

$$\begin{aligned}
H_{\nu\mu}^{\text{eff}}(\text{ MR BWCCSD(T)}) &= \langle\Phi_\nu|\hat{H}_N(\mu)e^{\hat{T}_{123}(\mu)}|\Phi_\mu\rangle_{\text{C}}^{\text{CCSDT}-1} \\
&= \langle\Phi_\nu|\hat{H}_N(\mu)(e^{\hat{T}_{12}(\mu)} + \hat{T}_3(\mu))|\Phi_\mu\rangle_{\text{C}} \quad (4.10)
\end{aligned}$$

4.2 The MR BWCCSD(T) method

As already mentioned, in single reference CCSD(T) the first step is a CCSD calculation, which is followed by the noniterative perturbative correction. In the case of multireference Brillouin-Wigner coupled clusters theory, the situation is the same. In the first step, MR BWCCSD calculation is performed. Subsequently, using the MR BWCCSD amplitudes, the triples corrections to the effective Hamiltonian are calculated, as suggested in the previous section. Finally, the correlation energy is obtained by the diagonalization of the effective Hamiltonian matrix.

However, there are several issues to be addressed. One of them is the size extensivity correction. Another is the lack of invariance of the method with respect to unitary transformations of orbitals.

4.2.1 Size-extensivity correction to MR BWCCSD(T)

The multireference Brillouin-Wigner coupled cluster method is not size extensive. Therefore, it is necessary to use size-extensivity corrections. The two most common types, the aposteriori and iterative correction, were mentioned already in the first chapter within the discussion of the MR BWCC theory.

However, in the case of methods with noniterative triple excitations the situation is more complex, which is true especially for the commonly used aposteriori correction. Here, not one, but two corrections are being performed - one for the effect of connected triples and the second for size-extensivity of the method. The question is, in what order to calculate these corrections.

In this work, the size-extensivity correction was always performed first, regardless of its type. It is assumed to be right to first partially remove the artifact of the method before using its result for a further calculation.

For the iterative correction, the situation is conceptually quite satisfactory, since the corrected amplitudes are a converged solution of respective cluster equations. However, in the case of aposteriori correction only one iteration of the cluster equations without the size-extensive terms is performed. Thus we are combining two noniterative corrections, which is at least potentially questionable, and has to be tested numerically.

However, since the MR BWCCSD has a n^6 scaling, while the triples correction has n^7 scaling, the computational expenses of the iterative correction are, when comparing relatively, considerably smaller.

For most systems, the use of size-extensivity correction is inevitable. However, for very small systems both the aposteriori and the iterative correction exhibit a very poor performance, while the uncorrected MR BWCC method, which is close to full configuration interaction for these systems, provides very accurate results. The use of MR BWCCSD(T) method without size--extensivity correction is thus in some situations inevitable.

Conceptually, the calculations without the size-extensivity correction reintroduce new problems. Since the size-extensivity correction is always performed before the triples correction, there is no need to include the disconnected linked and unlinked contributions to the T_3 equation, since all these terms are already neglected or scaled to zero by the size-extensivity correction. However, without this correction, all these terms remain and should be included.

At the moment, the inclusion of these terms is not implemented. The number of systems, where it is possible to use uncorrected MR BWCC is relatively small. Furthermore, this neglect is analogous to the α approximation from the iterative methods, and as will be shown later, the effect of the α approximation on the actual energies is rather limited, and the fundamental advantage of the full method is better convergence. Since here the connected triples are included noniteratively, this aspect loses its importance.

4.2.2 Noninvariance with respect to orbital rotations

One of the most important drawbacks of the MR BWCCSD(T) method is the lack of invariance with respect to unitary transformations within virtual–virtual and occupied-occupied blocks of orbitals. In the single reference the-

ory, CCSD(T) is noninvariant when a non-Hartree-Fock reference function is used. To remove this noninvariance, the semicanonical orbitals are employed [23].

As mentioned before, the semicanonical orbitals have diagonal occupied–occupied and virtual–virtual blocks of the Fock matrix. However, in the case of a multireference method, the orbitals in the active space are occupied for some reference configurations and virtual for other ones. The orbitals can thus be made semicanonical only with respect to one of the reference configurations. Therefore, the MR BWCCSD(T) is not invariant with respect to occupied–occupied and virtual–virtual transformations.

To ensure the invariance of the MR BWCCSD(T) towards virtual–virtual and occupied-occupied orbital rotations, it would be necessary to introduce a special set of orbitals that has not only diagonal virtual–virtual and occupied-occupied blocks Fock matrix, but is diagonal in the indexes corresponding to the active orbitals. No progress has been achieved yet in this field, and this problem remains open for further study.

Chapter 5

Applications

In the previous two chapters, the development of several new multireference Brillouin-Wigner coupled clusters methods was described. Here, we give the results of calculations employing these methods with the main aim to assess the performance of various aforementioned approaches. Parts of these results were published in [89, 131].

5.1 Study of the oxygen molecule

To assess the accuracy of the new methods, a study of the low-lying electronic states of the oxygen molecule has been performed. As noted before, the previous study showed that MR BWCCSD overestimates the harmonic vibrational frequencies by more than 100 cm^{-1} in comparison with the experimental values. The aim of this study was to find, whether this discrepancy would be significantly reduced, when connected triples are included in the description of the dynamic correlation, as was found for single reference methods.

5.1.1 Computational

The calculations of the oxygen molecule were performed using the model space spanned by four spin unrestricted reference configurations. They were formed by two electrons within the $1\pi_g^*$ antibonding orbital. Since this orbital is doubly occupied, it is possible to construct four reference configurations for the $M_S = 0$ spin component. The reference configurations are shown in Figure 5.1.

Figure 5.1: Four-reference model space for the oxygen molecule

$1\pi_g^*$ ↿ ⇂ $1\pi_g^*$ ⇂ ↿
Φ_1 Φ_2

$1\pi_g^*$ ⇅ — $1\pi_g^*$ — ⇅
Φ_3 Φ_4
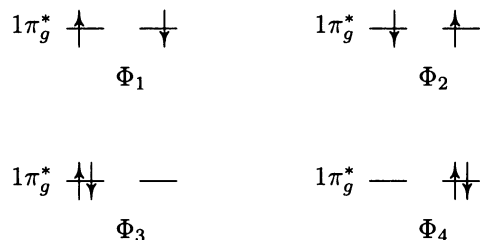
Within this model space, the first three electronic states of the oxygen molecule can be studied, because the effective Hamiltonian has three different eigenvalues, due to degeneracy. The ground state, $X^3\Sigma_g^-$, is not a genuine multireference system. Its $M_S = 0$ component is dominated by the symmetric combination of Φ_1 and Φ_2 references. However, the $M_S = 1$ component can easily be described using a single-reference approach. On the other hand, the first two excited states, $^1\Delta_g$ and $^1\Sigma_g^+$, benefit greatly from a multireference treatment. For the $^1\Delta_g$ state, the most important reference configurations are Φ_3 and Φ_4, while the $^1\Sigma_g^+$ state is dominated by an anti-symmetric combination of the Φ_1 and Φ_2 references. The $^1\Delta_g$ state is doubly degenerate.

In some calculations, an extended model space including eight reference configurations has been used. In the four additional reference configurations, the $1\pi_u$ orbital was occupied by two electrons and the $1\pi_g^*$ orbital by four electrons. This enlarged model space is complete, due to different symmetry of $1\pi_u$ and $1\pi_g^*$ orbitals.

In these calculations, the standard Dunning's correlation consistent basis sets were used. For all methods, cc-pVTZ was employed. For noniterative methods, calculations in cc-pVQZ are computationally feasible, and therefore have been performed. The 1s electrons were excluded from the correlation treatment, and the a posteriori correction for size-extensivity was used in all calculations.

For each of the states, the spectroscopic constants were obtained by Dunham-type polynomial expansion of the potential curve in the vicinity of the equilibrium interatomic distance. The energies of vertical excitations $X^3\Sigma_g^- \rightarrow\ ^1\Delta_g$ and $X^3\Sigma_g^- \rightarrow 1\Sigma_g^+$ were calculated at the experimental bond length of the $X^3\Sigma_g^-$ state, 1.20739 Å.

5.1.2 Results and discussion

For this study, the whole set of multireference Brillouin-Wigner coupled clusters methods, listed in previous chapters, has been used. Because of the number of different approaches, this section is divided into three parts.

Table 5.1: Spectroscopic constants of the $X^3\Sigma_g^-$ ground state of the oxygen molecule.

Method	r_e Å	ω_e cm^{-1}	$\omega_e x_e$ cm^{-1}	B_e cm^{-1}	α_e cm^{-1}
4R-BWCCSD[a]	1.199	1683.1	9.74	1.468	0.0140
8R-BWCCSD[a]	1.201	1661.4	9.98	1.461	0.0143
CCSD[a]	1.199	1679.1	9.73	1.467	0.0140
CCSD(T)[a]	1.211	1589.6	10.33	1.437	0.0150
MR BWCCSDT-1α	1.213	1580.8	14.20	1.432	0.0160
MR BWCCSDT-1bα	1.213	1576.8	13.71	1.432	0.0160
MR BWCCSDT-2α	1.211	1592.0	13.41	1.437	0.0158
MR BWCCSDT-3α	1.212	1591.8	13.22	1.436	0.0150
MR BWCCSDT-4α	1.211	1590.3	12.67	1.436	0.0157
MR BWCCSDT-α	1.211	1596.9	12.03	1.437	0.0151
8R-CISD[a]	1.198	1670.1	10.75	1.469	0.0148
Experiment[a]	1.20739	1580.361	12.0730	1.44566	0.01579

[a] Ref. [96]
[b] Ref. [132]

MR BWCCSDTα results

The results for the spectroscopic constants for the $X^3\Sigma_g^-$ state are given in Table 5.1. As mentioned before, the main focus of this study was to find, whether the inclusion of connected triples would lead to a significant improvement particularly of the vibrational frequency, and to a lesser extent of the anharmonicity.

Let us look first at the vibrational frequency ω_e. With the model space consisting of four reference configurations, the vibrational frequency is 1683.1 cm^{-1}, which which differs only by 4 cm^{-1} from the result of standard single reference CCSD method, due to the single reference nature of the $X^3\Sigma_g^-$ state. By increasing of the model space to eight reference configuration, only a

modest decrease of vibrational frequency of approximately 20 wavenumbers to 1661.4 cm^{-1} is achieved, which is still more than 80 cm^{-1} above the experimental value of 1580.361 wavenumbers.

When the connected triples are included, the situation is changed dramatically. The MR BWCCSDT-α method yields 1596.9 cm^{-1}, which is only about 17 cm^{-1} higher than the experimental value. Furthermore, all the approximative iterative methods MR BWCCSDT-$n\alpha$ provide very accurate values. The best agreement with experiment was obtained by the two computationally least expensive methods MR BWCCSDT-1α and MR BWCCSDT-1bα. The higher approximations yielded values in the range between 1490 and 1492 cm^{-1}.

However, it is necessary to stress that these calculations were performed only in the cc-pVTZ basis set, and therefore are hardly converged with respect to the basis set size. Particularly, the agreement of MR BWCCSDT-1α and MR BWCCSDT-1bα with the experiment must be assumed to be only a coincidence. As found by Tennyson and collaborators [133], to obtain vibrational frequencies with accuracy of one wavenumber, it is necessary to include also contributions of connected quadruples and quintuples, employ a nearly complete basis sets, and take into account relativistic effects.

Concerning anharmonicity $\omega_e x_e$, the inclusion of connected triples leads to a significant increase. While at CCSD or MR BWCCSD level the anharmonicity is about 10 cm^{-1}, the MR BWCCSDTα value 12.03 cm^{-1} is in an excellent agreement with experiment 12.0730 cm^{-1}. Again, this level of accuracy has to be regarded as numerical coincidence. Approximative MR BWCCSDT-$n\alpha$ methods all overestimate the anharmonicity. Unlike with the vibrational frequencies, the more advanced approximations yield in this case more accurate results.

The results also show, that the inclusion of connected triples leads to an elongation of the bond length r_e. While MR BWCCSD underestimates the bond length by 0.007 Å, MR BWCCSDTα overestimates this quantity by 0.004 Å. Among the MR BWCCSDT-$n\alpha$ methods, MR BWCCSDT-1α yields worst results, while the performance of the remaining approximations is almost the same. Also, the connected triples yield more accurate values of the rotation-vibration coupling constant α_e.

For the first excited electronic state, a$^1\Delta_g$, the situation is in many aspects similar. MR BWCCSD overestimates the vibrational frequency by approximately 120 cm^{-1}, underestimates the bond length by 0.01 Å and anharmonicity by 2.6 cm^{-1}. However, the a$^1\Delta_g$ state has a genuine multireference character, and therefore the increase of the size of the model space has

Table 5.2: Spectroscopic constants of the a$^1\Delta_g$ excited state of the O$_2$ molecule

Method	r_e Å	ω_e cm^{-1}	$\omega_e x_e$ cm^{-1}	B_e cm^{-1}	α_e cm^{-1}
4R-BWCCSD[a]	1.204	1628.4	10.27	1.453	0.0147
8R-BWCCSD[a]	1.210	1583.9	11.58	1.440	0.0156
MR BWCCSDT-1α	1.221	1515.6	14.68	1.414	0.0166
MR BWCCSDT-1bα	1.221	1511.1	13.64	1.414	0.0166
MR BWCCSDT-2α	1.219	1531.2	14.74	1.419	0.0161
MR BWCCSDT-3α	1.219	1525.0	11.29	1.419	0.0161
MR BWCCSDT-4α	1.219	1524.7	12.47	1.418	0.0165
MR BWCCSDT-α	1.219	1529.9	12.45	1.420	0.0167
8R-CISD[a]	1.208	1583.0	11.68	1.444	0.0160
Experiment[b]	1.2155	1509.3	12.90	1.4264	0.0171

[a] Ref. [96]
[b] Ref. [132]

a significant effect on the spectroscopic constants. The use of four additional reference configurations leads to a decrease of the vibrational frequency by approximately 45 cm^{-1}, increase of the bond length by 0.006 Å and increase of the anharmonicity by 1.2 cm^{-1}.

Similarly to the situation for the ground state, the inclusion of connected triples leads to a dramatic improvement of the vibrational frequency. MR BWCCSDTα result of 1529.9 cm^{-1} is only 20 cm^{-1} above the experimental value of 1509.3 cm^{-1}. Among the approximate methods, MR BWCCSDT-1α and MR BWCCSDT-1bα provide the best agreement with the experiment. However, the difference of only 6.3 and 1.8 cm^{-1} cannot be assumed to be anything but a numerical coincidence. The higher approximations give vibrational frequencies in between 1524 and 1532 cm^{-1}, which is in a good agreement with the full MR BWCCSDTα method.

For the bond length, the MR BWCCSDTα value 1.2185 Å is only 0.003 Å above the experiment, which is another significant improvement. The results of the approximative methods higher than MR BWCCSDT-1bα are very close to the MR BWCCSDTα value, while MR BWCCSDT-1α and MR BWCCSDT-1bα overestimate the bond length by 0.0055 Å. The anharmonicity is overestimated by MR BWCCSDT-1α and MR BWCCSDT-1bα and underestimed by the higher methods. The best performance is achieved

by MR BWCCSDT-4α and MR BWCCSDT-α.

Table 5.3: Spectroscopic constants of the $b^1\Sigma_g^+$ excited state of the O_2 molecule

Method	r_e Å	ω_e cm^{-1}	$\omega_e x_e$ cm^{-1}	B_e cm^{-1}	α_e cm^{-1}
4R-BWCCSD[a]	1.211	1576.1	10.72	1.436	0.0153
8R-BWCCSD[a]	1.222	1491.0	12.25	1.411	0.0169
MR BWCCSDT-1α	1.231	1443.5	15.40	1.390	0.0182
MR BWCCSDT-1bα	1.232	1441.5	14.56	1.390	0.0178
MR BWCCSDT-2α	1.229	1459.7	14.20	1.396	0.0175
MR BWCCSDT-3α	1.229	1458.1	13.19	1.396	0.0177
MR BWCCSDT-4α	1.228	1461.2	12.28	1.397	0.0175
MR BWCCSDT-α	1.229	1456.9	12.32	1.396	0.0181
8R-CISD[a]	1.220	1496.9	12.22	1.416	0.0170
Experiment[b]	1.22675	1432.687	13.950	1.40041	0.01817

[a] Ref. [96]
[b] Ref. [132]

The situation is similar for the $b^1\Sigma_g^+$ state as well, only the multireference character is even stronger. MR BWCCSD with four reference configurations overestimates the vibrational frequency by approximately 140 cm^{-1}, underestimates the bond length by 0.015 Å and anharmonicity by 3.2 cm^{-1}. The enlargement of the model space to eight reference configuration results in a decrease of the vibrational frequency by 85 cm^{-1}, an increase of the bond length by 0.01 Å, and an increase of anharmonicity by 1.5 Å.

The inclusion of connected triples has a similar effect as for the previous two states. The vibrational frequency obtained by MR BWCCSDTα method, which is 1456.9 cm^{-1}, is about 24 cm^{-1} above the experimental value of 1456.9 cm^{-1}. The results of MR BWCCSDT-$n\alpha$ for $n = 2, 3, 4$ are similar. Compared to the previous two states, the difference between MR BWCCSDTα and MR BWCCSDT-1α is only about 12 cm^{-1}.

Again, the bond length is overestimated by MR BWCCSDTα and all its approximations. The MR BWCCSDTα yields 1.2289 Å which is approximately 0.002 Å higher than the experiment. The performance of MR BWCCSDT-1α is for bond length worse than of the full MR BWCCSDTα method. The anharmonicity given by the MR BWCCSDTα method is 12.32cm^{-1}, which is 1.6 cm^{-1} below the experiment. When approximate

triples methods are used, anharmonicity increases as the less rigorous approximations are used.

Table 5.4: Comparison of the vertical transition energies computed for the O_2 molecule in the cc-pVTZ basis at the experimental equilibrium distance and harmonic 0-0 transition energies (in parenthesis)

Method	T_e ($X^3\Sigma_g^- \rightarrow a^1\Delta_g$) eV	T_e ($X^3\Sigma_g^- \rightarrow b^1\Sigma_g^+$) eV
DIP-STEOM-CCSD[a]	1.066	1.803
4R-BWCCSD[c]	1.058 (1.055)	1.902 (1.891)
8R-BWCCSD[c]	1.026 (1.023)	1.777 (1.761)
8R-CISD[c]	0.982 (0.980)	1.698 (1.684)
4R–BWCCSDT-1α	1.074 (1.070)	1.803 (1.795)
4R–BWCCSDT-1α [b]	1.067 (1.063)	1.792 (1.694)
4R–BWCCSDT-α	1.087 (1.083)	1.799 (1.790)
Experiment[d]	0.982	1.636

[a] Results obtained previously [96] employing the doubly ionized similarity transformed equation of motion CCSD method [73–76] implemented in the ACES II program [134].

[b] Computed in the aug-cc-pVTZ basis set.

[c] Ref. [96]

[d] Ref. [132]

From the performance of MR BWCCSD for the two excited states it is obvious, that the size of the model space has a significant effect on the accuracy of the spectroscopic constants. Calculations have been attempted with eight reference model space. However, they were not successful due to convergence problems. This can be explained by the sensitivity of the α approximation to the intruder state effect, due to the Rayleigh-Schrödinger denominators in the T_3 equation (3.9).

The results of vertical excitation energies are listed in Table 5.4. In contrast to the situation with the spectroscopic constants, there is no apparent improvement due to the inclusion of connected triples for both the $X^3\Sigma_g^-$ $\rightarrow a^1\Delta_g$ and $X^3\Sigma_g^- \rightarrow b^1\Sigma_g^+$ excitations. For $X^3\Sigma_g^- \rightarrow a^1\Delta_g$ vertical excitation, both MR BWCCSDTα and MR BWCCSDT-1α show a larger deviation from the experimental value than MR BWCCSD. In the case of $X^3\Sigma_g^-$ $\rightarrow b^1\Sigma_g^+$ the performance of MR BWCCSDTα and MR BWCCSDT-1α is slightly better than that of MR BWCCSD.

It was suggested, that the lack of improvement can be caused by the use of experimental geometry instead of the bond length calculated by the respective methods. Therefore, the vertical excitation energies were calculated also using these geometries and results are shown in parenthesis in Table 5.4. In all the cases, this leads to a better agreement with the experiment. However, the effect is very small, compared to the deviation from the experimental values.

It also has to be noted, that the data indicate that for vertical excitation energies, the size of the model space is much more important than the inclusion of connected triples.

Table 5.5: Spectroscopic constants of the $X^3\Sigma_g^-$ ground state of the O_2 molecule.

Method	r_e Å	ω_e cm^{-1}	$\omega_e x_e$ cm^{-1}	B_e cm^{-1}	α_e cm^{-1}
4R BWCCSDT-1α	1.213	1580.8	14.20	1.432	0.0160
4R BWCCSDT-4α	1.211	1590.3	12.67	1.436	0.0157
4R BWCCSDT-α	1.211	1596.9	12.03	1.437	0.0151
4R BWCCSDT-1	1.213	1578.1	11.89	1.431	0.0145
4R BWCCSDT-1b	1.214	1577.8	11.90	1.431	0.0145
4R BWCCSDT-2	1.211	1593.7	12.88	1.436	0.0156
4R BWCCSDT-3	1.212	1587.2	10.82	1.436	0.0157
4R BWCCSDT-4	1.213	1580.2	11.87	1.432	0.0145
4R BWCCSDT	1.211	1596.5	12.60	1.436	0.0148
8R BWCCSDT-1	1.213	1568.5	10.63	1.432	0.0159
8R BWCCSDT	1.211	1589.2	11.66	1.437	0.0161
Experiment[a]	1.20739	1580.361	12.0730	1.44566	0.01579

[a] Ref. [132]

MR BWCCSDT results

The results of spectroscopic constants, obtained at the MRBWCCSDT and MR BWCCSDT-n level, are presented in Table 5.5 for the $X^3\Sigma_g^-$ state, in Table 5.6 for the $a^1\Delta_g$ state and in Table 5.7 for the $b^1\Sigma_g^+$ state.

For most of the methods used, the inclusion of disconnected terms in T_3 equation has a very limited effect on both the bond length and the vibrational frequency. At the MR BWCCSDT-1 level, the vibrational frequency 1578.1

cm^{-1} is lowered by 2.7 cm^{-1} compared to the MR BWCCSDT-1-α value, while the bond length increased by 0.0002 Å. At the MR BWCCSDT level, the vibrational frequency decreased by only 0.4 cm^{-1} to 1596.5 cm^{-1}, and the bond length increased by 0.0001 Å.

The most significant shift was observed at the MR BWCCSDT-4 level. The MR BWCCSDT-4 vibrational frequency of 1580.2 cm^{-1} is lower by approximately 10 cm^{-1} than the MR BWCCSDT-4-α value of 1590.3 cm^{-1}. Also, the bond length is increased by 0.002 Å from 1.2114 Å to 1.2130 Å. The MR BWCCSDT-4 results are thus very similar to those of MR BWCCSDT-1 and MR BWCCSDT-1-α methods.

Perhaps the most important difference from the calculations with the α approximation was the increased numerical stability of the method, and consequently a faster convergence of the calculation procedure. Therefore, calculations with the eight reference model space have thus become possible.

The inclusion of eight reference configurations leads to a decrease of vibrational frequency and to an increase of the bond length. In some cases, this also leads to a larger deviation from experiment. However, as will be shown later, the use of larger basis set has the opposite effect on both of these quantities. It is necessary to bear in mind, that cc-pVTZ is far from being a complete basis set, and therefore a quantitative agreement with the experiment cannot be expected.

Similarly to the situation for the ground state, the results of vibrational frequency and the bond length of MR BWCCSDT method are very close to its α counterpart. The MR BWCCSDT-1 vibrational frequency decreased by 8.5 cm^{-1} to 1507.4 cm^{-1}, which is in an excellent agreement with the experimental value. The bond length was not affected by the inclusion of disconnected terms.

Furthermore, the MR BWCCSDT-4 bond length and vibrational frequency differ significantly from those obtained by the MR BWCCSDT-4-α method (i.e. 1.2197 Å vs. 1.2191 Å, 1524.7 cm^{-1} vs. 1524.7 cm^{-1}). In contrast to the ground state, the MR BWCCSDT-4 results lie between the MR BWCCSDT-1 and MR BWCCSDT values.

Similarly to the ground state, the extension of the model space results in a decrease of the vibrational frequency. For this state, its magnitude of this is larger, which is caused by a stronger multireference character of the a$^1\Delta_g$ state.

The situation for the b$^1\Sigma_g^+$ state is in many aspects analogous to the previous two states. The MR BWCCSDT results lie very close to the MR

69

Table 5.6: Spectroscopic constants of the $a^1\Delta_g$ excited state of the O_2 molecule

Method	r_e Å	ω_e cm^{-1}	$\omega_e x_e$ cm^{-1}	B_e cm^{-1}	α_e cm^{-1}
4R-BWCCSD	1.204	1628.4	10.27	1.453	0.0147
8R-BWCCSD	1.210	1583.9	11.58	1.440	0.0156
4R BWCCSDT-1α	1.221	1515.6	14.68	1.414	0.0166
4R BWCCSDT-4α	1.219	1524.7	12.47	1.418	0.0165
4R BWCCSDT-α	1.219	1529.9	12.45	1.420	0.0167
4R BWCCSDT-1	1.221	1507.4	11.03	1.413	0.0168
4R BWCCSDT-1b	1.221	1507.2	11.03	1.413	0.0168
4R BWCCSDT-2	1.219	1524.0	11.65	1.419	0.0168
4R BWCCSDT-3	1.219	1523.5	11.62	1.418	0.0168
4R BWCCSDT-4	1.220	1517.9	11.14	1.417	0.0166
4R BWCCSDT	1.218	1528.5	11.84	1.419	0.0170
8R BWCCSDT-1	1.224	1483.3	10.00	1.407	0.0156
8R BWCCSDT	1.220	1509.0	11.45	1.415	0.0169
Experiment[b]	1.2155	1509.3	12.90	1.4264	0.0171

[a] Ref. [96]
[b] Ref. [132]

BWCCSDT-α ones, while most of the MR BWCCSDT-n approaches provide significant decreases of vibrational frequency. The MR BWCCSDT-1 frequency is lower by 7 cm^{-1} compared to its α counterpart, while the most significant change is observed for the MR BWCCSDT-4 method.

The changes of the bond length have a larger magnitude than for the two lower states. The MR BWCCSDT-1 method provides a value of 1.2316 Å, which is larger by 0.0003 Å than that of MR BWCCSDT-1-α. The largest increase of the bond length was observed at the MR BWCCSDT-4 level, where the MR BWCCSDT-4 value lies 0.0021 Å above the MR BWCCSDT-4-α result.

Vibrational frequencies calculated within the eight reference model space are again significantly lower than those of four reference calculations.

The results of vertical excitation energies are listed in Table 5.8. The comparison shows only minimal differences between the full MR BWCCSDT method and its α approximation, when four reference configurations are used. However, with a model space consisting of eight reference configurations,

Table 5.7: Spectroscopic constants of the $b^1\Sigma_g^+$ excited state of the O_2 molecule

Method	r_e Å	ω_e cm^{-1}	$\omega_e x_e$ cm^{-1}	B_e cm^{-1}	α_e cm^{-1}
4R-BWCCSD[a]	1.211	1576.1	10.72	1.436	0.0153
8R-BWCCSD[a]	1.222	1491.0	12.25	1.411	0.0169
4R BWCCSDT-1α	1.231	1443.5	15.40	1.390	0.0182
4R BWCCSDT-4α	1.228	1461.2	12.28	1.397	0.0175
4R BWCCSDT-α	1.229	1456.9	12.32	1.396	0.0181
4R BWCCSDT-1	1.232	1437.9	15.22	1.389	0.0183
4R BWCCSDT-1b	1.232	1438.5	14.65	1.389	0.0181
4R BWCCSDT-2	1.229	1454.1	11.29	1.395	0.0175
4R BWCCSDT-3	1.229	1457.2	12.15	1.395	0.0175
4R BWCCSDT-4	1.231	1441.4	10.51	1.391	0.0174
4R BWCCSDT	1.229	1457.7	12.86	1.395	0.0179
8R BWCCSDT-1	1.238	1394.0	13.18	1.376	0.0175
8R BWCCSDT	1.233	1419.1	11.91	1.385	0.0183
Experiment[b]	1.22675	1432.687	13.950	1.40041	0.01817

[a] Ref. [96]
[b] Ref. [132]

the vertical energies are significantly decreased, which results in a better agreement with the experiment. At all calculation levels, the results for the $X^3\Sigma_g^- \rightarrow b^1\Sigma_g^+$ are more accurate than those for $X^3\Sigma_g^- \rightarrow a^1\Delta_g$ transition.

MR BWCCSD(T) results

The spectroscopic constants obtained are listed in Table 5.9 for the ground $X^3\Sigma_g^-$ state, in Table 5.10 for the $a^1\Delta_g$ state, and in Table 5.11 for $b^1\Sigma_g^+$.

For the ground state, there is no significant improvement of the results due to the multireference treatment. However, there is a dramatic improvement of vibrational frequencies due to the connected triples, regardless of the level at which they are included. The vibrational frequency of 1577.2 cm^{-1} obtained by MR BWCCSD(T) in cc-pVTZ basis set is incidentally in a very good agreement with the experimental value of 1580 cm^{-1}. The increase of the basis set size to cc-pVQZ leads to an increase of the vibrational frequency by approximately 10 cm^{-1}.

Table 5.8: Comparison of the vertical transition energies computed for the O_2 molecule in the cc-pVTZ basis at the experimental equilibrium distance

Method	T_e ($X^3\Sigma_g^- \rightarrow a^1\Delta_g$) eV	T_e ($X^3\Sigma_g^- \rightarrow b^1\Sigma_g^+$) eV
DIP-STEOM-CCSD[a]	1.066	1.803
4R-BWCCSD[b]	1.058	1.902
8R-BWCCSD[b]	1.026	1.777
4R-BWCCSDT-1α	1.074	1.803
4R-BWCCSDT-α	1.087	1.799
4R-BWCCSDT-1	1.075	1.802
4R-BWCCSDT	1.087	1.800
8R-BWCCSDT-1	1.043	1.745
8R-BWCCSDT	1.062	1.757
Experiment[c]	0.982	1.636

[a] Results obtained previously [96] employing the doubly ionized similarity transformed equation of motion CCSD method [73–76] implemented in the ACES II program [134].

[b] Ref. [96]

[c] Ref. [132]

Without the triples correction to the off-diagonal $\hat{H}^{\text{eff}}$ elements, the vibrational frequency is 1588.5 cm^{-1} in the cc-pVTZ basis set and 1599.8 cm^{-1} in cc-pVQZ. The value for cc-pVTZ basis set is almost identical to that of single reference CCSD(T).

Extending the model space to eight reference configurations yields only a minimal change of vibrational frequencies. This is hardly surprising, due to the single-reference character of the $X^3\Sigma_g^-$ ground state. However, these changes are significantly lower than in the case of the MR BWCCSD method.

For the $a^1\Delta_g$ state, the MR BWCCSD(T) vibrational frequency 1523 cm^{-1} is again close to the value 1529 cm^{-1} obtained by the iterative MR BWCCSDTα method and to the experimental value 1509 cm^{-1}. The increase of the basis set size leads to an increase of the vibrational frequency by 16.2 cm^{-1} to 1539.5 cm^{-1}. For both basis sets, the MR BWCCSD(T_d) results are approximately five wavenumbers below the values the MR BWCCSD(T) ones.

For the $a^1\Delta_g$ state, the multireference treatment starts to play an im-

72

Table 5.9: Spectroscopic constants of the $X^3\Sigma_g^-$ ground state of the O_2 molecule, 1s orbitals excluded from correlation treatment

Basis	Method	r_e Å	ω_e cm^{-1}	$\omega_e x_e$ cm^{-1}	B_e cm^{-1}	α_e cm^{-1}
cc-pVTZ	4R-BWCCSD[b]	1.199	1683.1	9.74	1.468	0.0140
cc-pVTZ	8R-BWCCSD[b]	1.201	1661.4	9.98	1.461	0.0143
cc-pVTZ	CCSD	1.199	1679.1	9.73	1.467	0.0140
cc-pVTZ	CCSD(T)	1.211	1589.6	10.33	1.437	0.0150
cc-pVTZ	4R BWCCSDT-1α	1.213	1580.8	14.20	1.432	0.0160
cc-pVTZ	4R BWCCSDT-α	1.211	1596.9	12.03	1.437	0.0151
cc-pVTZ	4R BWCCSD(T)	1.213	1577.3	11.54	1.433	0.0156
cc-pVTZ	8R BWCCSD(T)	1.213	1576.7	11.84	1.433	0.0159
cc-pVTZ	4R BWCCSD(T$_d$)[a]	1.212	1588.5	11.71	1.436	0.0156
cc-pVTZ	8R BWCCSD(T$_d$)[a]	1.212	1588.5	11.71	1.436	0.0156
cc-pVTZ	8R-CISD[b]	1.198	1670.1	10.75	1.469	0.0148
cc-pVQZ	4R BWCCSD(T)	1.209	1589.6	12.37	1.442	0.0159
cc-pVQZ	8R BWCCSD(T)	1.209	1589.7	12.38	1.442	0.0158
cc-pVQZ	4R BWCCSD(T$_d$)[a]	1.208	1599.8	11.78	1.445	0.0156
cc-pVQZ	8R BWCCSD(T$_d$)[a]	1.208	1599.8	11.77	1.445	0.0156
	Experiment[c]	1.2074	1580.36	12.073	1.4457	0.01579

[a] Triples correction only to diagonal elements of effective Hamiltonian matrix, for details see text.
[b] Ref. [96]
[c] Ref. [132]

portant role. Therefore, the increase of the size of the model space has a significant effect on the spectroscopic constants. For vibrational frequency it leads to the decrease of MR BWCCSD(T) value by almost 20 cm^{-1} to 1505 cm^{-1} in the cc-pVTZ and 1520.5 cm^{-1} in the cc-pVQZ basis set. In the case of MR BWCCSD(T$_d$), the decrease is only about 5 cm^{-1} in cc-pVTZ and 8 cm^{-1} in cc-pVQZ basis set.

Finally, in the $b^1\Sigma_g^+$ excited state the general picture is similar to the $a^1\Delta_g$ state. The MR BWCCSD(T) vibrational frequency 1454 cm^{-1} is only three wavenumbers lower than the MR BWCCSDTα result 1457 cm^{-1}. The cc-pVQZ value is larger by approximately 20 cm^{-1} compared to the cc-pVTZ one.

Table 5.10: Spectroscopic constants of the $a^1\Delta_g$ excited state of the O_2 molecule, 1s orbitals excluded from correlation treatment

Basis set	Method	r_e Å	ω_e cm^{-1}	$\omega_e x_e$ cm^{-1}	B_e cm^{-1}	α_e cm^{-1}
cc-pVTZ	4R-BWCCSD[b]	1.204	1628.4	10.27	1.453	0.0147
cc-pVTZ	8R-BWCCSD[b]	1.210	1583.9	11.58	1.440	0.0156
cc-pVTZ	4R BWCCSDT-1α	1.221	1515.6	14.68	1.414	0.0166
cc-pVTZ	4R BWCCSDT-α	1.219	1529.9	12.45	1.420	0.0167
cc-pVTZ	4R BWCCSD(T)	1.219	1523.2	11.32	1.418	0.0161
cc-pVTZ	8R BWCCSD(T)	1.221	1505.5	12.54	1.414	0.0172
cc-pVTZ	4R BWCCSD(T$_d$)[a]	1.220	1518.2	11.97	1.417	0.0167
cc-pVTZ	8R BWCCSD(T$_d$)[a]	1.221	1513.3	12.37	1.415	0.0160
cc-pVQZ	4R BWCCSD(T)	1.215	1539.5	12.63	1.429	0.0167
cc-pVQZ	8R BWCCSD(T)	1.217	1520.6	12.24	1.424	0.0168
cc-pVQZ	4R BWCCSD(T$_d$)[a]	1.215	1534.5	12.03	1.427	0.0167
cc-pVQZ	8R BWCCSD(T$_d$)[a]	1.216	1526.5	12.28	1.426	0.0170
	Experiment[c]	1.2155	1509.3	12.90	1.4264	0.0171

[a] Triples correction only to diagonal elements of effective Hamiltonian matrix, for details see text.
[b] Ref. [96]
[c] Ref. [132]

However, in this case the increase of the model space size has a dramatic effect on the vibrational frequency, leading to a decrease by 50 cm^{-1}. This effect is diminished slightly when a larger basis set is used or without triples correction to the non-diagonal effective Hamiltonian matrix elements.

Similarly to the $a^1\Delta_g$ state, the MR BWCCSD(T$_d$) results show a weaker dependence on the size of model space. With four reference configurations, the vibrational frequencies are 1449.6 wavenumbers in cc-pVTZ and 1470.3 wavenumbers in cc-pVQZ, while with eight reference configurations the results are 1411.8 and 1431.8 cm^{-1}, respectively. The differences between calculations with four and eight references are thus reduced by approximately 10 cm^{-1}.

The results of vertical excitation energies are listed in Table 5.12. The MR BWCCSD(T) values are close to those of the iterative methods. Using larger basis set, or larger model space leads to a decrease of the vertical excitation energies. The MR BWCCSD(T$_d$) results are close to the MR BWCCSD(T)

74

Table 5.11: Spectroscopic constants of the $b^1\Sigma_g^+$ excited state of the O_2 molecule, 1s orbitals excluded from correlation treatment

Basis	Method	r_e Å	ω_e cm^{-1}	$\omega_e x_e$ cm^{-1}	B_e cm^{-1}	α_e cm^{-1}
cc-pVTZ	4R-BWCCSD[b]	1.211	1576.1	10.72	1.436	0.0153
cc-pVTZ	8R-BWCCSD[b]	1.222	1491.0	12.25	1.411	0.0169
cc-pVTZ	4R BWCCSDT-1α	1.231	1443.5	15.40	1.390	0.0182
cc-pVTZ	4R BWCCSDT-1bα	1.232	1441.5	14.56	1.390	0.0178
cc-pVTZ	4R BWCCSDT-4α	1.228	1461.2	12.28	1.397	0.0175
cc-pVTZ	4R BWCCSDT-α	1.229	1456.9	12.32	1.396	0.0181
cc-pVTZ	4R-BWCCSD(T)	1.229	1454.1	12.15	1.395	0.0171
cc-pVTZ	8R-BWCCSD(T)	1.236	1405.9	12.59	1.380	0.0180
cc-pVTZ	4R-BWCCSD(T$_d$)[a]	1.230	1449.6	12.23	1.394	0.0175
cc-pVTZ	8R-BWCCSD(T$_d$)[a]	1.234	1411.8	12.76	1.384	0.0183
cc-pVTZ	8R-CISD	1.220	1496.9	12.22	1.416	0.0170
cc-pVQZ	4R-BWCCSD(T)	1.224	1472.7	12.64	1.407	0.0174
cc-pVQZ	8R-BWCCSD(T)	1.230	1426.8	13.27	1.394	0.0177
cc-pVQZ	4R-BWCCSD(T$_d$)[a]	1.224	1470.3	12.88	1.406	0.0171
cc-pVQZ	8R-BWCCSD(T$_d$)[a]	1.229	1431.8	13.60	1.396	0.0180
	Experiment[c]	1.2268	1432.69	13.950	1.4004	0.01817

[a] Triples correction only to diagonal elements of effective Hamiltonian matrix, for details see text.
[b] Ref. [96]
[c] Ref. [132]

ones for the $(X^3\Sigma_g^- \rightarrow b^1\Sigma_g^+)$ excitation, while for the $X^3\Sigma_g^- \rightarrow a^1\Delta_g$ there is a significant decrease of the excitation energy.

5.1.3 Conclusions

There has been a dramatic improvement of the vibrational frequencies due to the inclusion of connected triples methods. The differences between full MR BWCCSDT method and the α approximation were only modest. More significant differences were observed in the case of some of the approximative MR BWCCSDT-n level, especially MR BWCCSDT-4. Better numerical stability permitted calculations with eight reference configurations.

The MR BWCCSD(T) results were in a good agreement with both the experiment and the results of iterative methods. The greatly reduced com-

Table 5.12: Comparison of vertical transition energies computed for the O_2 moleand harmonic 0-0 transition energies (in parenthesis)

Method	T_e ($X^3\Sigma_g^- \rightarrow a^1\Delta_g$) eV	T_e ($X^3\Sigma_g^- \rightarrow b^1\Sigma_g^+$) eV
4R-BWCCSD[a]	1.058	1.902
8R-BWCCSD[a]	1.026	1.777
4R-BWCCSDT-1α	1.074	1.803
4R-BWCCSDT-α	1.087	1.799
4R-BWCCSD(T)	1.093	1.848
4R-BWCCSD(T$_d$)[e]	1.030	1.845
8R-BWCCSD(T)	1.074	1.774
8R-BWCCSD(T$_d$)[e]	1.038	1.804
4R-BWCCSD(T)[c]	1.074	1.826
4R-BWCCSD(T$_d$)[c,e]	1.011	1.827
8R-BWCCSD(T)[c]	1.050	1.747
8R-BWCCSD(T$_d$)[c,e]	1.016	1.779
Experiment[d]	0.982	1.636

[a] Results obtained previously [96]

[b] Computed in the aug-cc-pVTZ basis set.

[c] Computed in the cc-pVQZ basis set.

[d] Ref. [132]

[e] Triples correction only to the diagonal elements of effective Hamiltonian matrix, for details see text.

putational costs enabled us calculations with cc-pVQZ basis set.

5.2 Study of the perpendicular (C_{2v}) insertion pathway of Be into H_2

The perpendicular (also denoted as C_{2v}) insertion pathway of a beryllium atom into the hydrogen molecule is one of popular benchmarks for testing various multireference methods. However, it proceeds far from true transition state of the reaction [135], and has therefore little importance for chemistry. Nevertheless, it is very useful for assessing the performance of multireference methods [81, 88, 135–139].

76

This reaction path was designed by Purvis and collaborators [140], with the aim to include points with many different reference configurations. Very small model system has been chosen, in order to be able to perform full configuration interaction (FCI) calculations and make a rigorous comparison possible.

5.2.1 Computational

The reaction path includes ten points denoted as A-J. The geometries of these points are given in table (5.13). Among these points, G - J are located in the entrance of the Be + H_2 valley of the potential energy surface. At these geometries, the dominant configuration is $1a_1^2\, 2a_1^2\, 3a_1^2$. The points A-C, located in the exit of the valley, correspond to the linear structure of H-Be-H, where the dominant configuration is $1a_1^2\, 2a_1^2\, 1b_2^2$. In the transition between the two regions, the points D, E and F are located. At these geometries, both of the aforementioned configurations have an important contribution.

Table 5.13: Geometry of BeH_2 path along the reaction path

Point	Cartesian coordinates of hydrogen atoms		
	a.u.	a.u.	a.u.
A	0	±2.54	0.0
B	0	±2.08	1.0
C	0	±1.62	2.0
D	0	±1.39	2.5
E	0	±1.275	2.75
F	0	±1.16	3.0
G	0	±0.93	4.0
H	0	±0.7	4.0
I	0	±0.7	6.0
J	0	±0.7	20.0

[a] Beryllium atom is located at the origin of the set of coordinates.
[b] Ref [140]

The model space was spanned over the $1a_1^2\, 2a_1^2\, 3a_1^2$ and $1a_1^2\, 2a_1^2\, 1b_2^2$ configurations. The CAS SCF calculations indicate presence of other moderately significant configurations, but this treatment enables us to assess whether

the high level treatment of dynamic correlation satisfactorily substitutes the missing reference configurations.

Throughout the calculations, the basis set consisting of ten contracted Gaussian functions has been used [140],

Since the main goal of the study is a comparison with the full configuration interaction, all electrons are included in the correlation treatment. The previous study [88] found, that for such a small system the size-extensivity correction gives a poorer performance than uncorrected MR BWCCSD. We have thus performed without a size-extensivity correction. Unlike in [88], standard RHF orbitals were used throughout the calculations.

5.2.2   Results and discussion

The MR BWCCSDT and MR BWCCSDTα energies calculated in the smaller basis set [140] are presented in Table 5.14.

Table 5.14: Differences of MR BWCCSDT and MR BWCCSDTα energies from FCI for the BeH$_2$ molecule

| Point | Energy difference compared to FCI | | | FCI |
| | MR BWCCSDT[a] | MR BWCCSDTα[a] | MR BWCCSD[a] | FCI |
	kcal/mol	kcal/mol	kcal/mol	a.u.
A	0.014	not conv.	0.246	-15.779172
B	0.019	not conv.	0.239	-15.737225
C	0.012	0.020	0.257	-15.674818
D	0.055	0.095	0.111	-15.622884
E	0.184	0.266	-0.381	-15.602919
F	0.113	0.243	-0.083	-15.624964
G	0.091	0.145	0.135	-15.693195
H	0.114	0.133	0.162	-15.736689
I	0.165	0.165	0.180	-15.760878
J	0.168	0.168	0.171	-15.762903

[a] Without size-extensivity correction

For comparison, also the MR BWCCSD energies are given. These are different from those presented in [88], since RHF orbitals (instead of CAS SCF ones) were used throughout the study. The FCI energies [140] are given as a benchmark.

78

The performance of the MR BWCCSDT method in the exit part of the valley (i.e. points A - C) is highly satisfactory, with differences from FCI smaller than 0.02 kcal/mol. In this region, the description of dynamic correlation is the most critical aspect for achieving of high accuracy. Since the connected triples are included, and the system consists only of six electrons, the agreement of the energies with FCI results is very good.

In the region near the transition state (i.e. points D - F), the static correlation starts to play a dominant role. This results in an increase of the deviations to 0.055 kcal/mol for point D, 0.184 kcal/mol for point E, and 0.113 kcal/mol for point F. In contrast with the situation with the MR BWCCSD, all the deviations have a positive sign, which means that MR BWCCSDT energies lie above FCI for all studied geometries.

At the entrance to the valley, the deviation from FCI decreases, as the role of static correlation is diminished. Further increase of the beryllium-hydrogen interatomic distance and decrease of hydrogen-hydrogen bond length leads to an increase of the difference between MR BWCCSDT and FCI energies. This deviation is caused mainly by the size-inextensivity of the uncorrected MR BWCCSDT method. Comparing these values with the MR BWCCSD ones, it is clear that the role of connected triples is negligible. The reason for this trend is that when the molecule dissociates into a hydrogen molecule and a beryllium atom, which significantly reduces the role of dynamic correlation.

The results of MR BWCCSDT-α are generally close to those of MR BWCCSDT. Near the transition geometries, MR BWCCSDTα yields energy 0.04 to 0.12 kcal/mol higher, and thus further apart from the FCI. The larger differences were found at points D - E, where the multireference character of the system is strong and the neglected disconnected and unlinked terms in T_3 equation play a larger role. Also, MR BWCCSDTα was found to be numerically less stable than the full MR BWCCSDT method, failing to converge for geometries A and B.

Since the primary aim of this study is to assess the performance of the MR BWCC methods, the transition state region is the most interesting one. In Table 5.15, the results of previous studies for points D - F are listed the results, as well as the the difference of the deviations of point D and F are listed.

Among these methods, only MR CISD, MR BWCCSDT and its α counterpart overestimate the energy for all three geometries. However, the agreement of MR CISD energies with FCI is rather poor, with deviations ranging from 0.53 kcal/mol for point A to 1.93 kcal/mol for point F. MR AQCC provides a very good description for the point D, but considerably worse per-

Table 5.15: Comparison of MR BWCC with other multireference approaches

Method	ΔE in kcal/mol Geometry			
	D	E	F	$\Delta_{D-F}{}^f$
MR BWCCSD[a]	0.11	-0.38	-0.08	0.19
MR BWCCSD[abc]	-0.68	0.26	0.48	-1.13
MR BWCCSDT[a]	0.06	0.18	0.11	-0.05
MR BWCCSDTα[a]	0.10	0.27	0.24	-0.14
MR CISD[bd]	0.53	1.26	1.93	-1.40
MR AQCC[bd]	0.18	0.70	1.24	-1.06
MR ACPF[bde]	-0.56	-0.56	-0.33	-0.23
MR ACPF2[bd]	-0.07	0.28	0.25	-0.32

[a] Without size-extensivity correction.
[b] Using CAS SCF(2,2) orbitals.
[c] From reference [88].
[d] From reference [139].
[e] From reference [81].
[f] $\Delta_{D-F} = \Delta E(D) - \Delta E(F)$

formance for the two other states leads to a relatively large value of -1.04 kcal/mol for Δ_{D-F}. MR ACPF gives substantial, but very consistent, deviations from FCI, which results in a very low value of Δ_{D-F}. Further improvement is observed at MR ACPF2 level, where the largest deviation is only 0.28 kcal/mol for the point E. MR BWCCSD results with RHF reference are clearly superior to those obtained with CAS SCF orbitals. Most evident is the difference of the Δ_{D-F} values, where the use of RHF orbitals leads to only 0.19 kcal/mol and the use of CAS orbitals to 1.13 kcal/mol. Among these methods, the results of MR BWCCSDT method provide the best agreement with FCI, in terms of both the size of the deviations and their consistency.

5.2.3 Conclusions

The C_{2v} insertion pathway of a beryllium atom to a hydrogen molecule was studied by MR BWCCSDT and MR BWCCSDTα methods. The energies were compared to FCI. MR BWCCSDT provides very accurate results, while MR BWCCSDTα energies are generally close to the full MR BWCCSDT. However, for some geometries MR BWCCSDTα fails to converge. Perfor-

mance of both methods, compared to other multireference approaches, is very satisfactory. The use of RHF orbitals is justified by calculations at MR BWCCSD level.

5.3 Study of the XH_2 (X=C, Si) diradicals of the IV. A group

Diradicals are chemical compounds with two electrons in two orbitals with the same or nearly same energy. There are several classes of diradicals including $\sigma - \pi$ diradicals, nonconjugated diradicals, non-Kekulé structures and conjugated annulenes. For details see [141].

The $\sigma - \pi$ diradicals have one of the aforementioned partially filled orbitals of σ and one of π symmetry. Different symmetry of the two orbitals prevents their interaction. Carbenes and silylenes belong to this group.

With two electrons in two orbitals, six electron configurations can be constructed, as shown in Figure 5.2. Among these, four have the M_S component equal to zero. For methylene and silylene two geometry configurations are possible: a linear one and a bent one. The bent structure, which corresponds to the equilibrium geometry, has C_{2v} symmetry. For methylene, the five lowest molecular orbitals are- $1a_1$ $2a_1$ $1b_2$ $3a_1$ $1b_1$ with the two partially occupied orbitals being $3a_1$ and $1b_1$. The six electron configurations give rise to four states $^3B_1$, $^1A_1$, $^1B_1$ and $^1A_1$.

Figure 5.2: Possible references for two electrons in $3a_1$ and $1b_1$ orbitals

81
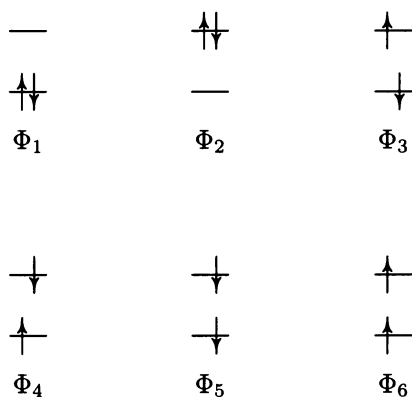
For linear geometry, the system has a $D_{\infty h}$ symmetry. The $1a_1$ and $2a_1$ orbitals become $1\sigma_g$ and $2\sigma_g$, $1b_2$ becomes $1\sigma_u$, and the $1b_2^2$ and $3a_1^2$ orbitals form s degenerate π_u orbital. This results in the electronic states $^3\Sigma_g^-$, $^1\Delta_g$, and $^1\Sigma_g^+$.

The relative ordering of these triplet and singlet states depends on the energy difference between $3a_1$ and $1b_1$ orbital. When these orbitals are degenerate, the triplet state is favored, according to Hund's rule. Any situation, which increases the energy difference, leads to the stabilization of the singlet. For methylene, the difference is relatively small and the ground state is triplet. In silylene, the energy gap between these orbitals is increased due to the smaller bond angle and different hybridization, and that results in a singlet ground state.

The spin multiplicity plays a key role in chemical reactivity, and therefore the knowledge of the energy differences between the lowest singlet and triplet state is important. The singlet state has a significant two–reference character, and the multireference treatment is thus beneficial.

Among the three studied systems, the methylene has been studied most extensively. Foster and Boyes configuration interaction study of methylene found a bent structure of the triplet state [142], in contrast to the results of Herzberg's photolysis experiment [143]. The experimental results were then refined several times [144–147].

Reviews of early quantum chemistry calculations can be found in [148–151]. Thanks to the small size of the system, various ab initio methods can be applied [93,151–160], including FCI [151–154].

The studies of the singlet–triplet gap in silylene are considerably less numerous [93,156,158,161].

5.3.1 Computational

Four electronic states were studied, the singlet states $^1A_1$ and $^1\Delta$, and the triplet states $^3B_1$ and $^3\Sigma^-$, depending on the symmetry.

Calculations of the singlet states were performed using the model space consisting of two reference configurations, as shown in Fig. 5.3. Due to the C_{2v} point group, the HOMO and LUMO orbitals have a different spatial symmetry and the monoexcited reference configurations are not necessary. The singlet state was studied by a variety of multireference Brillouin-
-Wigner coupled clusters approaches, which included MR BWCCSDT and MR BWCCSDT-1 and their α approximations, MR BWCCSD(T) and MR

BWCCSD(T_d), as well as MR BWCCSD calculations. Calculations were carried out with and without the posteriori size-extensivity correction. With the exception of iterative triples methods, the iterative size-extensivity correction was also deployed. All calculations were done using restricted Hartree Fock reference function. The calculations with noniterative triples used semicanonical orbitals of the Hartree-Fock reference.

Figure 5.3: Two reference model space for the singlet state of carbene

$$
\begin{array}{cc}
1b_2 \; \text{—} & 1b_2 \; \uparrow\downarrow \\
1a_1 \; \uparrow\downarrow & 1a_1 \; \text{—} \\
1b_1 \; \uparrow\downarrow & 1b_1 \; \uparrow\downarrow \\
2a_1 \; \uparrow\downarrow & 2a_1 \; \uparrow\downarrow \\
1a_1 \; \uparrow\downarrow & 1a_1 \; \uparrow\downarrow \\
\Phi_1 & \Phi_2
\end{array}
$$
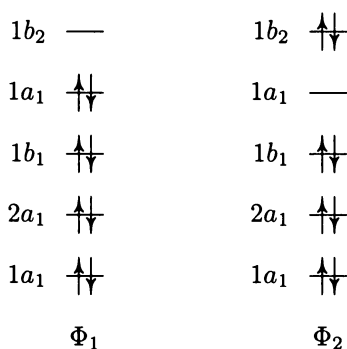
For the triplet state, standard single reference methods CCSD, CCSD(T), CCSDT-1, and CCSDT were used, due to its single reference character. Restricted open-shell Hartree Fock reference functions were used for CCSD(T) and CCSD, whereas CCSDT-1 and CCSDT used unrestricted Hartree Fock reference function, due to the program restrictions.

Standard Dunning's basis sets [162,163] cc-pVTZ, cc-pVQZ and cc-pV5Z were employed. Some of these basis sets were obtained from the EMSL library. Unless noted otherwise, spherical Gaussians were used. All structures were optimized in all basis sets used. Because of the lack of the analytical gradient for MR BWCC methods, most of the optimizations were carried out numerically. The 1s orbitals of all nonhydrogen atoms were excluded from the correlation treatment. All calculations were performed using the ACES II package.

The singlet-triplet gaps were calculated as the difference between the energetic minima of the respective states (i.e. adiabatically). On several places, the extrapolation to complete basis set were carried out using the $E_X = E_\infty + an^{-1}$ formula [164, 165], where n is the number of basis set functions.

5.3.2 Results and discussion

CH₂

Due to the multireference character, the main concern of this study are the singlet states. The equilibrium geometries and corresponding energies for the $^1A_1$ state are listed in Table 5.16 and for $^1\Sigma^-$ in Table 5.18. The values of singlet triplet gaps are presented in Table 5.17 for bent structure and in Table 5.19 for linear one.

Let us first concentrate on the geometries. In the cc-pVTZ basis set, the MR BWCCSD method yields the C-H bond length of 1.078 Å and the valence angle of 102.30°. The influence of the type of the size-extensivity correction is rather small, with the difference between the two approaches being only 0.0001 Å for the bond length, and 0.05° for the valence angle.

The inclusion of connected triples leads to an increase of the bond length by almost 0.002 Å to 1.1094 Å at MR BWCCSD(T), MR BWCCSD(T$_d$) and MR BWCCSDT-1 level. MR BWCCSDT gives a value larger by 0.0002 Å than the aforementioned methods. The difference between various noniterative MR BWCC approaches is small to negligible, as well as the influence of the α approximation. The valence angle decreases due to the inclusion of connected triples by 0.3-0.4 degrees.

The size of the basis set has a significant effect on the equilibrium geometry. The bond length decreases by approximately 0.002 Å, when the basis set is expanded to cc-pVQZ. The use of cc-pV5Z basis set decreases the C-H distance by additional 0.0008 to 0.0001 Å. Similarly, the valence angle increases by approximately 0.35° and 0.25°, respectively.

The differences between geometries calculated with a posteriori and iterative size-extensivity correction are relatively small. Calculations without size-extensivity correction yield bond length longer by approximately 0.001 Å and valence angle smaller by 0.25°.

The comparison with experiment shows that both MR BWCCSD(T) and MR BWCCSD underestimate the bond length and overestimate the valence angle, when a sufficiently large basis set is used. However, the inclusion of connected triples leads to a significant improvement. MR BWCCSD(T) in cc-pV5Z basis set underestimates the bond length by 0.0006 Å, while MR BWCCSD by 0.0032 Å. Similarly, MR BWCCSD in cc-pV5Z basis set overestimates the valence angle by 0.43°, while MR BWCCSD(T) by only 0.08°.

84

Table 5.16: The $^1A_1$ state of CH_2 diradical

Method[a]	Basis set	r_{C-H} (in Å)	α_{H-C-H}	Energy (in a. u.)
MR BWCCSD a.c.	cc-pVTZ	1.1072	102.30°	-39.058635
MR BWCCSD i.c.	cc-pVTZ	1.1071	102.35°	-39.058810
MR BWCCSD n.c.	cc-pVTZ	1.1077	102.15°	-39.057578
MR BWCCSD(T) a.c.	cc-pVTZ	1.1094	101.97°	-39.062623
MR BWCCSD(T_d) a.c.	cc-pVTZ	1.1094	102.03°	-39.062854
MR BWCCSD(T) i.c.	cc-pVTZ	1.1092	102.03°	-39.062786
MR BWCCSD(T_d) i.c.	cc-pVTZ	1.1093	102.08°	-39.063036
MR BWCCSD(T) n.c.	cc-pVTZ	1.1100	101.84°	-39.061590
MR BWCCSD(T_d) n.c.	cc-pVTZ	1.1101	101.87°	-39.061781
MR BWCCSDT-1 a.c.	cc-pVTZ	1.1094	101.97°	-39.062606
MR BWCCSDT-1-α a.c.	cc-pVTZ	1.1094	101.97°	-39.062606
MR BWCCSDT-1 n.c.	cc-pVTZ	1.1101	101.84°	-39.061613
MR BWCCSDT-1-α n.c.	cc-pVTZ	1.1101	101.84°	-39.061608
MR BWCCSDT a.c.	cc-pVTZ	1.1096	101.94°	-39.063029
MR BWCCSDTα a.c.	cc-pVTZ	1.1096	101.94°	-39.063029
MR BWCCSDT n.c.	cc-pVTZ	1.1102	101.79°	-39.062065
MR BWCCSDTα n.c.	cc-pVTZ	1.1103	101.82°	-39.062050
MR BWCCSD a.c.	cc-pVQZ	1.1050	102.63°	-39.068878
MR BWCCSD i.c.	cc-pVQZ	1.1048	102.69°	-39.069111
MR BWCCSD n.c.	cc-pVQZ	1.1059	102.47°	-39.067578
MR BWCCSD(T) a.c.	cc-pVQZ	1.1073	102.29°	-39.073354
MR BWCCSD(T_d) a.c.	cc-pVQZ	1.1073	102.36°	-39.073614
MR BWCCSD(T) i.c.	cc-pVQZ	1.1071	102.34°	-39.073576
MR BWCCSD(T_d) i.c.	cc-pVQZ	1.1073	102.39°	-39.073854
MR BWCCSD(T) n.c.	cc-pVQZ	1.1083	102.12°	-39.072100
MR BWCCSD(T_d) n.c.	cc-pVQZ	1.1083	102.18°	-39.072307
MR BWCCSDT-1 a.c.	cc-pVQZ	1.1074	102.31°	-39.073368
MR BWCCSDT-1-α a.c.	cc-pVQZ	1.1074	102.31°	-39.073364
MR BWCCSDT-1 n.c.	cc-pVQZ	1.1081	102.11°	-39.072176
MR BWCCSDT-1-α n.c.	cc-pVQZ	1.1081	102.11°	-39.072155
MR BWCCSD a.c.	cc-pV5Z	1.1039	102.83°	-39.072195
MR BWCCSD i.c.	cc-pV5Z	1.1038	102.87°	-39.072531
MR BWCCSD n.c.	cc-pV5Z	1.1055	102.53°	-39.070456
MR BWCCSD(T) a.c.	cc-pV5Z	1.1065	102.48°	-39.076833
MR BWCCSD(T_d) a.c.	cc-pV5Z	1.1064	102.51°	-39.077101
MR BWCCSD(T) i.c.	cc-pV5Z	1.1061	102.52°	-39.077156
MR BWCCSD(T_d) i.c.	cc-pV5Z	1.1062	102.59°	-39.077439
MR BWCCSD(T) n.c.	cc-pV5Z	1.1076	102.25°	-39.075182
MR BWCCSD(T_d) n.c.	cc-pV5Z	1.1076	102.25°	-39.075379
Experiment[a]		1.1070	102.4°	

[a] a.c. stands for a posteriori size–extensivity correction, i.c. for iterative one, n.c. for no correction

[b] Ref. [147]

85

Table 5.17: Singlet-triplet gap for bent CH_2

Method[a]	cc-pVTZ kcal/mol	cc-pVQZ kcal/mol	cc-pV5Z kcal/mol	CBS[b] kcal/mol
MR BWCCSD a.c.	9.86	9.08	8.63	8.19
MR BWCCSD i.c.	9.75	8.94	8.42	7.94
MR BWCCSD n.c.	10.52	9.90	9.72	9.36
MR BWCCSD(T) a.c.	9.53	8.74	8.28	7.83
MR BWCCSD(T_d) a.c.	9.39	8.58	8.11	7.65
MR BWCCSD(T) i.c.	9.43	8.60	8.08	7.6
MR BWCCSD(T_d) i.c.	9.27	8.43	7.90	7.42
MR BWCCSD(T) n.c.	10.18	9.53	9.32	8.95
MR BWCCSD(T_d) n.c.	10.06	9.40	9.19	8.82
MR BWCCSDT-1 a.c.	9.57	8.78		
MR BWCCSDT-1-α a.c.	9.57	8.78		
MR BWCCSDT-1 n.c.	10.19	9.53		
MR BWCCSDT-1-α n.c.	10.20	9.54		
MR BWCCSDT a.c.	9.58			
MR BWCCSDT-α a.c.	9.58			
MR BWCCSDT n.c.	10.18			
MR BWCCSDT-α n.c.	10.19			
Experiment[b]	9.032 ± 0.057			

[c] a.c. stands for a posteriori size–extensivity correction, i.c. for iterative one, n.c. for no correction

[b] Extrapolation to complete basis set were performed according to [164,165].

[c] Ref. [166]

For MR BWCCSD and MR BWCCSD(T), it is safe to extrapolate to a complete basis set. The MR BWCCSD(T) bond length calculated without size-extensivity correction is then 1.1066 Å while the valence angle is predicted as 102.41°, which is in an excellent agreement with experiment.

As far as the methods with iterative inclusion of triples are concerned, no cc-pV5Z data are available. Still, from the agreement between MR BWCCSD(T) and MR BWCCSDT-1 in smaller basis sets, it can be expected that the MR BWCCSDT-1 geometries will remain very close to the MR BWCCSD(T) ones.

Secondly, let us have a look at the values of total energies and the sin-

glet triplet gaps of methylene. In the cc-pVTZ basis set, MR BWCCSD yields the value of 9.86 kcal/mol for the singlet-triplet gap. The iterative correction reduces the gap by approximately 0.1 kcal/mol, the inclusion of connected triples by 0.3 kcal/mol, leading to the MR BWCCSDT-1 value of 9.58 kcal/mol and MR BWCCSDT value of 9.57 kcal/mol. The effect of the α approximation was found to be negligible.

However, significant differences have been found between the various methods with noniterative inclusion of connected triples. Let us first concentrate on the values of total energies. In the cc-pVTZ basis set, all the energies of the multireference methods with noniterative triples lie approximately in the region between the MR BWCCSDT and MR BWCCSDT-1 energies. The MR BWCCSD(T) energy lies closer to the MR BWCCSDT-1 one, while the MR BWCCSD(T_d) energy and results with the iterative correction closer to the MR BWCCSDT one. However, the MR BWCCSDT and MR BWCCSDT-1 results were obtained with the a posteriori correction, and as such should be compared with results obtained with the same size-extensivity correction.

As was stated already, CCSD(T) can be viewed as an one-step approximation of CCSDT-1. The same holds for their multireference Brillouin-Wigner analogues. By comparison with MR BWCCSDT-1, MR BWCCSD(T) differs by less than 20 μHartree, while MR BWCCSD(T_d) by approximately 250 μHartree. The same behavior has been observed in the cc-pVQZ basis set. From these results we can draw the conclusion, that in this case the performance of MR BWCCSD(T) is superior to that of MR BWCCSD(T_d).

This argument can also be confirmed by the values of singlet triplet gaps. While in the cc-pVTZ basis set MR BWCCSD(T) value differs from MR BWCCSDT-1 by only 0.03 kcal/mol and in cc-pVQZ by 0.04 kcal/mol, MR BWCCSD(T_d) results differ by 0.18 and 0.20 kcal/mol, respectively.

The use of the iterative size-extensivity correction lowers the results of MR BWCCSD(T) by 0.10, 0.14 and 0.20 kcal/mol, depending on the basis sets. For MR BWCCSD(T_d), these changes are 0.12, 0.14 and 0.21 kcal/mol. These values are very similar to the MR BWCCSD decreases of 0.09, 0.14 and 0.21 kcal/mol, obtained at MR BWCCSD level. Therefore, we can assume that the size extensivity corrections work at a similar level of accuracy with the use of connected triples as without them.

The calculations without size-extensivity correction lead in all cases to substantially higher values of singlet triplet gaps. In a complete analogy to calculations with size-extensivity correction, the MR BWCCSD provides largest values and the inclusion of connected triples leads to a decrease of

Table 5.18: The $^1\Sigma^-$ state of CH_2 diradical

Method[a]	Basis set	r_{C-H} (in Å)	Energy (in a. u.)
MR BWCCSD a.c.	cc-pVTZ	1.0634	-39.017869
MR BWCCSD i.c.	cc-pVTZ	1.0634	-39.018299
MR BWCCSD n.c.	cc-pVTZ	1.0632	-39.015827
MR BWCCSD(T) a.c.	cc-pVTZ	1.0644	-39.020702
MR BWCCSD(T_d) a.c.	cc-pVTZ	1.0645	-39.021329
MR BWCCSD(T) i.c.	cc-pVTZ	1.0644	-39.021136
MR BWCCSD(T_d) i.c.	cc-pVTZ	1.0645	-39.021766
MR BWCCSD(T) n.c.	cc-pVTZ	1.0641	-39.018638
MR BWCCSD(T_d) n.c.	cc-pVTZ	1.0641	-39.019256
MR BWCCSDT-1 a.c.	cc-pVTZ	1.0644	-39.020674
MR BWCCSDT-1-α a.c.	cc-pVTZ	1.0644	-39.020669
MR BWCCSDT-1 n.c.	cc-pVTZ	1.0645	-39.018679
MR BWCCSDT-1-α n.c.	cc-pVTZ	1.0642	-39.018652
MR BWCCSDT a.c.	cc-pVTZ	1.0646	-39.021320
MR BWCCSDTα a.c.	cc-pVTZ	1.0646	-39.021312
MR BWCCSDT n.c.	cc-pVTZ	1.0645	-39.019340
MR BWCCSDTα n.c.	cc-pVTZ	1.0644	-39.019315
MR BWCCSD a.c.	cc-pVQZ	1.0627	-39.029636
MR BWCCSD i.c.	cc-pVQZ	1.0627	-39.030168
MR BWCCSD n.c.	cc-pVQZ	1.0625	-39.027090
MR BWCCSD(T) a.c.	cc-pVQZ	1.0638	-39.032800
MR BWCCSD(T_d) a.c.	cc-pVQZ	1.0639	-39.033520
MR BWCCSD(T) i.c.	cc-pVQZ	1.0638	-39.033330
MR BWCCSD(T_d) i.c.	cc-pVQZ	1.0639	-39.034052
MR BWCCSD(T) n.c.	cc-pVQZ	1.0635	-39.030259
MR BWCCSD(T_d) n.c.	cc-pVQZ	1.0636	-39.030965
MR BWCCSDT-1 a.c.	cc-pVQZ	1.0638	-39.032791
MR BWCCSDT-1-α a.c.	cc-pVQZ	1.0638	-39.032808
MR BWCCSDT-1 n.c.	cc-pVQZ	1.0636	-39.030344
MR BWCCSDT-1-α n.c.	cc-pVQZ	1.0636	-39.030296
MR BWCCSD a.c.	cc-pV5Z	1.0625	-39.034068
MR BWCCSD i.c.	cc-pV5Z	1.0625	-39.034770
MR BWCCSD n.c.	cc-pV5Z	1.0624	-39.030389
MR BWCCSD(T) a.c.	cc-pV5Z	1.0635	-39.037047
MR BWCCSD(T_d) a.c.	cc-pV5Z	1.0635	-39.037800
MR BWCCSD(T) i.c.	cc-pV5Z	1.0635	-39.037743
MR BWCCSD(T_d) i.c.	cc-pV5Z	1.0635	-39.038499
MR BWCCSD(T) n.c.	cc-pV5Z	1.0633	-39.033486
MR BWCCSD(T_d) n.c.	cc-pV5Z	1.0633	-39.034217
Experiment[a]		1.070	

[a] a.c. stands for a posteriori size–extensivity correction, i.c. for iterative one, n.c. for no correction

[b] Ref. [167]

the gap, while MR BWCCSD(T) performs better than MR BWCCSD(T$_d$), when compared with results of iterative methods.

The comparison with the experimental value shows, that all multireference Brillouin-Wigner approaches underestimate the singlet triplet gap. Surprisingly, the best agreement was obtained at the MR BWCCSD level, which gave in cc-pV5Z a value lower by approximately 0.4 kcal/mol than the experiment. The MR BWCCSD(T) results was lower by further 0.3 kcal/mol.

However, the situation is completely different, when no size-extensivity correction is used. In this case, the MR BWCCSD overestimates in cc-pV5Z the singlet-triplet gap by 0.7 kcal/mol, while MR BWCCSD(T) and MR BWCCSD(T$_d$) by only 0.3 and 0.2 kcal/mol respectively.

For linear methylene, situation is in many aspects similar. All the multireference Brillouin-Wigner coupled clusters approaches significantly underestimate the bond length. Inclusion of connected triples leads to an improvement compared to MR BWCCSD by approximately 0.001 Å. Still, the deviation from the experiment remains significant, being 0.0065 Å at the MR BWCCSD(T) level in the cc-pV5Z basis set.

Unlike in the case of the $^1A_1$ state, there is no increase of the bond length, when no size-extensivity correction is used. For linear methylene, the bond length is lowered at all levels of theory by 0.0002 - 0.0003 Å, instead of a significant increase.

As far as the singlet-triplet gaps are concerned, the situation is again very much similar to the bent structure. The inclusion of connected triples leads to decrease of the gap size. While MR BWCCSD yields 29.36 kcal/mol in the cc-pVTZ basis set, the MR BWCCSDT gives 29.84 kcal/mol. In this case, the MR BWCCSDT-1 gap is higher by 0.1 kcal/mol than the MR BWCCSDT one. Similarly to the situation with bent geometry, there is an excellent agreement between MR BWCCSD(T) and MR BWCCSDT-1. The performance of MR BWCCSD(T) is again superior to MR BWCCSD(T$_d$).

The effect of the type of size-extensivity correction used is significantly larger than for the bent structure, as is the effect of the α approximation. This can be explained by significantly stronger multireference character of the linear methylene, compared to the bent one. However, the difference between the results obtained with a posteriori and iterative correction are almost identical for MR BWCCSD, MR BWCCSD(T) and MR BWCCSD(T$_d$). The omission of size-extensivity correction leads to an increase of the gap by approximately 1.3 kcal/mol, compared to the a posteriori correction.

Table 5.19: Singlet-triplet gap for linear CH_2

Method[a]	cc-pVTZ kcal/mol	cc-pVQZ kcal/mol	cc-pV5Z kcal/mol	CBS[b] kcal/mol
MR BWCCSD a.c.	29.36	27.77	26.68	25.74
MR BWCCSD i.c.	29.09	27.44	26.24	25.27
MR BWCCSD n.c.	30.65	29.37	28.98	28.24
MR BWCCSD(T) a.c.	29.92	28.45	27.58	26.72
MR BWCCSD(T_d) a.c.	29.53	28.00	27.10	26.20
MR BWCCSD(T) i.c.	29.65	28.12	27.14	26.24
MR BWCCSD(T_d) i.c.	29.56	27.70	26.67	25.58
MR BWCCSD(T) n.c.	31.22	30.05	29.81	29.14
MR BWCCSD(T_d) n.c.	30.83	29.60	29.35	28.64
MR BWCCSDT-1 a.c.	29.96	28.49		
MR BWCCSDT-1-α a.c.	29.94	28.48		
MR BWCCSDT-1 n.c.	31.19	30.03		
MR BWCCSDT-1-α n.c.	31.23	30.06		
MR BWCCSDT a.c.	29.84			
MR BWCCSDT-α a.c.	29.85			
MR BWCCSDT-α n.c.	31.09			
MR BWCCSDT n.c.	31.10			

[a] a.c. stands for a posteriori size–extensivity correction, i.c. for iterative one, n.c. for no correction

[b] Extrapolation to complete basis set were performed according to [164,165].

SiH₂

The equilibrium geometries and total energies for the $^1A_1$ and $^1\Sigma^-$ state are presented in Table 5.20 and 5.22, while the values of the singlet-triplet gaps are included in Tables 5.21 and 5.23.

In the cc-pVTZ basis set, MR BWCCSD provides the Si-H bond length of 1.5160 Å. The inclusion of connected triples leads to an increase of the bond length by approximately 0.002 Å. The differences between various methods with connected triples are relatively small, as is the influence of the α approximation and the type of size-extensivity correction.

The use of the cc-pVQZ basis set leads to a decrease of the bond length by approximately 0.0014 Å. The type of size-extensivity correction and the

90

Table 5.20: The $^1A_1$ state of SiH_2

Method	Basis set	r_{C-H} Å	α_{H-C-H}	Energy a. u.
MR BWCCSD a.c.	cc-pVTZ	1.5160	92.55°	-290.223590
MR BWCCSD i.c.	cc-pVTZ	1.5158	92.60°	-290.223719
MR BWCCSD n.c.	cc-pVTZ	1.1568	92.48°	-290.222922
MR BWCCSD(T) a.c.	cc-pVTZ	1.5180	92.36°	-290.228135
MR BWCCSD(T_d) a.c.	cc-pVTZ	1.5180	92.36°	-290.228381
MR BWCCSD(T) i.c.	cc-pVTZ	1.5180	92.36°	-290.228263
MR BWCCSD(T_d) i.c.	cc-pVTZ	1.5180	92.36°	-290.228531
MR BWCCSD(T) n.c.	cc-pVTZ	1.5186	92.23°	-290.227480
MR BWCCSD(T_d) n.c.	cc-pVTZ	1.5187	92.27°	-290.227673
MR BWCCSDT-1 a.c.	cc-pVTZ	1.5179	92.32°	-290.228070
MR BWCCSDT-1-α a.c.	cc-pVTZ	1.5179	92.32°	-290.228069
MR BWCCSDT-1 n.c.	cc-pVTZ	1.5187	92.25°	-290.2274945
MR BWCCSDT-1-α n.c.	cc-pVTZ	1.5187	92.25°	-290.227473
MR BWCCSDT a.c.	cc-pVTZ	1.5183	92.29°	-290.228667
MR BWCCSDT-α a.c.	cc-pVTZ	1.5183	92.29°	-290.228648
MR BWCCSDT n.c.	cc-pVTZ	1.5193	92.20°	-290.228114
MR BWCCSDT-α n.c.	cc-pVTZ	1.5193	92.20°	-290.228070
MR BWCCSD a.c.	cc-pVQZ	1.5025	92.76°	-290.221738
MR BWCCSD i.c.	cc-pVQZ	1.5022	92.80°	-290.221956
MR BWCCSD n.c.	cc-pVQZ	1.5037	92.65°	-290.220894
MR BWCCSD(T) a.c.	cc-pVQZ	1.5044	92.48°	-290.226656
MR BWCCSD(T_d) a.c.	cc-pVQZ	1.5045	92.52°	-290.226898
MR BWCCSD(T) i.c.	cc-pVQZ	1.5039	92.54°	-290.226878
MR BWCCSD(T_d) i.c.	cc-pVQZ	1.5039	92.54°	-290.227140
MR BWCCSD(T) n.c.	cc-pVQZ	1.5054	92.41°	-290.225834
MR BWCCSD(T_d) n.c.	cc-pVQZ	1.5052	92.44°	-290.226015
MR BWCCSDT-1 a.c.	cc-pVQZ	1.5044	92.47°	-290.226610
MR BWCCSDT-1-α a.c.	cc-pVQZ	1.5044	92.47°	-290.226606
MR BWCCSDT-1 n.c.	cc-pVQZ	1.5055	92.36°	-290.225875
MR BWCCSDT-1-α n.c.	cc-pVQZ	1.5052	92.40°	-290.225849
Experiment[b]		1.51403	91.9830°	

[a] a.c. stands for a posteriori size–extensivity correction, i.c. for iterative one, n.c. for no correction

[b] Ref. [168].

α correction play a larger role in the larger basis set, while the differences between MR BWCCSD(T) and MR BWCCSD(T_d) remain minimal, as far

91

as the bond length is concerned.

The inclusion of connected triples also results in an increase of the valence angle from 92.55° at the MR BWCCSD level to 92.36° of the MR BWCCSD(T) level, in cc-pVTZ. Again, the differences between various triples approaches are relatively small. In cc-pVQZ, the valence angle is increased by approximately 0.1°.

Table 5.21: Singlet-triplet gap of bent SiH_2

Method	cc-pVTZ kcal/mol	cc-pVQZ kcal/mol
MR BWCCSD a.c.	-20.47	-20.66
MR BWCCSD i.c.	-20.55	-20.79
MR BWCCSD n.c.	-20.05	-20.13
MR BWCCSD(T) a.c.	-20.69	-20.90
MR BWCCSD(T_d) a.c.	-20.84	-21.05
MR BWCCSD(T) i.c.	-20.77	-21.03
MR BWCCSD(T_d) i.c.	-20.94	-21.20
MR BWCCSD(T) n.c.	-20.28	-20.38
MR BWCCSD(T_d) n.c.	-20.40	-20.49
MR BWCCSDT-1 a.c.	-20.60	-20.80
MR BWCCSDT-1-α a.c.	-20.65	-20.80
MR BWCCSDT-1 n.c.	-20.24	-20.34
MR BWCCSDT-1-α n.c.	-20.22	-20.33
MR BWCCSDT a.c.	-20.54	
MR BWCCSDT-α a.c.	-20.53	
MR BWCCSDT n.c.	-20.20	
MR BWCCSDT-α n.c.	-20.17	
Experiment[b]	-20.99 ± 0.69	

[a] a.c. stands for a posteriori size–extensivity correction, i.c. for iterative one, n.c. for no correction.
[b] Ref. [169].

For the values of the singlet-triplet gaps, the connected triples play a relatively small role. In the cc-pVTZ basis set, the MR BWCCSD value of -20.47 kcal/mol is only 0.07 kcal/mol higher than the result of -20.54 kcal/mol of the MR BWCCSDT method. The MR BWCCSDT-1 value lies 0.06 and MR BWCCSD(T) value 0.16 kcal/mol below the MR BWCCSDT

Table 5.22: The $^1\Sigma^-$ state of SiH$_2$

Method	Basis set	r_{C-H} Å	Energy (in a. u.) a. u.
MR BWCCSD a.c.	cc-pVTZ	1.4499	-290.123022
MR BWCCSD i.c.	cc-pVTZ	1.4500	-290.123408
MR BWCCSD n.c.	cc-pVTZ	1.4495	-290.121516
MR BWCCSD(T) a.c.	cc-pVTZ	1.4525	-290.128654
MR BWCCSD(T$_d$) a.c.	cc-pVTZ	1.4529	-290.129172
MR BWCCSD(T) i.c.	cc-pVTZ	1.4528	-290.129112
MR BWCCSD(T$_d$) i.c.	cc-pVTZ	1.4532	-290.129631
MR BWCCSD(T) n.c.	cc-pVTZ	1.4519	-290.127022
MR BWCCSD(T$_d$) n.c.	cc-pVTZ	1.4523	-290.127535
MR BWCCSDT-1 a.c.	cc-pVTZ	1.4514	-290.128243
MR BWCCSDT-1-α a.c.	cc-pVTZ	1.4514	-290.128249
MR BWCCSDT-1 n.c.	cc-pVTZ	1.4513	-290.126765
MR BWCCSDT-1-α n.c.	cc-pVTZ	1.4513	-290.126768
MR BWCCSDT a.c.	cc-pVTZ	1.4520	-290.129117
MR BWCCSDT-α a.c.	cc-pVTZ	1.4520	-290.129119
MR BWCCSDT n.c.	cc-pVTZ	1.4518	-290.127637
MR BWCCSDT n.c.	cc-pVTZ	1.4518	-290.127647
MR BWCCSD a.c.	cc-pVQZ	1.4435	-290.120924
MR BWCCSD i.c.	cc-pVQZ	1.4437	-290.121456
MR BWCCSD n.c.	cc-pVQZ	1.4431	-290.119100
MR BWCCSD(T) a.c.	cc-pVQZ	1.4461	-290.127134
MR BWCCSD(T$_d$) a.c.	cc-pVQZ	1.4465	-290.127678
MR BWCCSD(T) i.c.	cc-pVQZ	1.4463	-290.127746
MR BWCCSD(T$_d$) i.c.	cc-pVQZ	1.4466	-290.128289
MR BWCCSD(T) n.c.	cc-pVQZ	1.4454	-290.125176
MR BWCCSD(T$_d$) n.c.	cc-pVQZ	1.4460	-290.125714
MR BWCCSDT-1 a.c.	cc-pVQZ	1.4451	-290.126697
MR BWCCSDT-1-α a.c.	cc-pVQZ	1.4451	-290.126690
MR BWCCSDT-1 n.c.	cc-pVQZ	1.4449	-290.124923
MR BWCCSDT-1-α n.c.	cc-pVQZ	1.4449	-290.124907

[a] a.c. stands for a posteriori size–extensivity correction, i.c. for iterative one, n.c. for no correction

result. The difference between MR BWCCSD(T) and MR BWCCSD(T$_d$) is about 0.15 kcal/mol, while the MR BWCCSD(T) value is closer to MR BWCCSDT-1. However, compared to methylene, the difference between MR BWCCSDT-1 and MR BWCCSD(T) is significantly higher. The influence of the α approximation is minimal, while the differences due to various types of size-extensivity correction are 0.1 kcal/mol or smaller.

The singlet-triplet gaps calculated in the cc-pVQZ basis set are about 0.2

kcal/mol below their cc-pVTZ counterparts.

For the $^1\Sigma^-$ state, the cc-pVTZ bond length 1.4520 Å calculated by MR BWCCSDT lies 0.0021 Å above the MR BWCCSD value. There are significant differences between results of methods with approximate inclusion of connected triples. The MR BWCCSDT-1 bond length is shorter by 0.0006 Å than MR BWCCSDT one, wheres MR BWCCSD(T) value is by 0.0005 Å longer. The results in the cc-pVQZ basis set are larger by 0.003–0.004 Å.

Table 5.23: Singlet-triplet gap of linear SiH_2

Method	cc-pVTZ kcal/mol	cc-pVQZ kcal/mol
MR BWCCSD a.c.	19.09	17.89
MR BWCCSD i.c.	18.85	17.56
MR BWCCSD n.c.	20.04	19.04
MR BWCCSD(T) a.c.	18.71	17.46
MR BWCCSD(T_d) a.c.	18.39	17.12
MR BWCCSD(T) i.c.	18.43	17.07
MR BWCCSD(T_d) a.c.	18.10	16.73
MR BWCCSD(T) n.c.	19.74	18.69
MR BWCCSD(T_d) n.c.	19.42	18.35
MR BWCCSDT-1 a.c.	19.02	17.80
MR BWCCSDT-1-α a.c.	19.01	17.80
MR BWCCSDT-1 n.c.	19.94	18.91
MR BWCCSDT-1-α n.c.	19.94	18.92
MR BWCCSDT a.c.	19.01	
MR BWCCSDT-α a.c.	19.01	
MR BWCCSDT n.c.	19.94	
MR BWCCSDT-α n.c.	19.93	

[a] a.c. stands for a posteriori size–extensivity correction, i.c. for iterative one, n.c. for no correction

For the singlet–triplet gaps, the effect of inclusion of connected triples is rather small, being smaller than 0.1 kcal/mol. There is very good agreement between MR BWCCSDT and MR BWCCSDT-1. The results of calculations with noniterative inclusion of connected triples lie significantly lower than those of more rigorous approaches. The effect of the type of size-extensivity correction is about 0.3 kcal/mol, wheres the influence of the α approximation

is minimal.

Compared to the $^1A_1$ state, the basis set dependence of the result of singlet-triplet gaps is much stronger, the cc-pVQZ values lie lower by 1.2–1.4 kcal/mol than their cc-pVTZ counterparts.

5.3.3 Conclusions

The inclusion of connected triples leads to a significant improvement geometries, while the effect on the energy differences is smaller and more questionable, especially for noniterative approach.

The comparison with MR BWCCSD(T) shows the performance of the MR BWCCSD(T) method is superior to MR BWCCSD(T_d).

The type of size-extensivity correction used has a large effect on the results obtained. For frozen core calculations of methylene (i.e. a six electron system), the best agreement with experiment is obtained when no correction is used.

5.4 Automerization barrier of cyclobutadiene

As an example of a study of moderately sized system, we have chosen to investigate the automerization barrier of cyclobutadiene. The scheme of this reaction is shown in Figure 5.4.

Figure 5.4: Automerization of cyclobutadiene
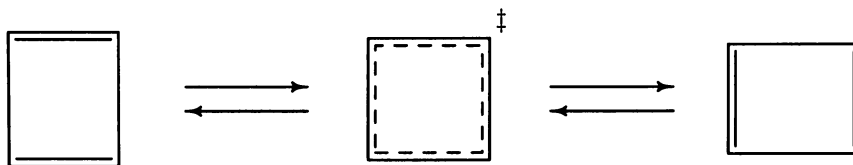
Cyclobutadiene is a classical example of an antiaromatic system, and as such has two carbon-carbon single bonds and two double bonds. Between the two rectangular structures lies the transition state with square geometry. The rate of interconversion of the two rectangular ground states, which can

be classified as a second order Jahn Teller distortion, is therefore determined by the height of the automerization barrier.

This system has been extensively studied by theoreticians [46, 100, 170–183] and experimentalists [184–187].

The transition structure of the cyclobutadiene is a typical two reference system. Therefore, single reference methods tend to significantly overestimate the automerization barrier, unless at least CCSDT, CISDTQ or higher method is used. Multireference treatment is thus highly beneficial. Among these studies is the article by Balková and Bartlett [46], who employed the MR CCSD and MR CCSD(T) method. Therefore, the comparison of various multireference coupled clusters approaches with or without connected triples is available.

5.4.1 Computational

Calculations were performed using standard cc-pVDZ and cc-pVTZ basis sets, as well as the [3s2p1d/2s] basis set [46], which has been used in earlier studies. For the transition state, the D_{4h} symmetry was slightly distorted by the change of two opposite C-C bond-length by 0.0001Å , in order to obtain "rectangular" orbitals [188] for the reference function. In all calculations, the 1s orbitals on carbon atoms and four highest molecular orbitals were excluded from the correlation treatment.

The system was studied at MR BWCCSD(T) and MR BWCCSD(T_d) level, with both the a posteriori and iterative size-extensivity correction. For comparison, MR BWCCSD results were also obtained.

The geometries were optimized numerically for all methods and basis sets. Optimization of the transition state was carried out by a successive interpolation of calculated energies under the constraint of square geometry.

In the square structure, the highest occupied molecular orbital is a pair of two degenerate π (e_g) orbitals ϕ_2 and ϕ_3 housed with two electrons. It is thus necessary to use a two-determinantal wavefunction, constructed from reference configurations $\phi_1^2\phi_2^2$ and $\phi_1^2\phi_3^2$, as the reference for the CC treatment (only the π-orbitals occupation is indicated). In the D_{2h} subgroup, the symmetries of ϕ_2 and ϕ_3 are b_{2g} and b_{3g}, respectively, and the singly excited configuration $\phi_1^2\phi_2\phi_3$ may be excluded on symmetry grounds and the two aforementioned references form a complete model space.

96

5.4.2 Results and discussion

The bond lengths and bond angles of the optimized geometries are listed in Table 5.24 for the rectangular optimal geometry, and in Table 5.25 for the square structure of the transition state.

Table 5.24: Optimum geometries of the ground state of cyclobutadiene

Method	Basis set	$r_{C=C}$ Å	r_{C-C} Å	r_{C-H} Å	α_{C-C-H}
MR BWCCSD	[3s2p1d/2s]	1.370	1.568	1.092	134.79°
MR BWCCSD	cc-pVDZ	1.364	1.570	1.093	134.86°
MR BWCCSD	cc-pVTZ	1.347	1.559	1.077	134.91°
MR BWCCSD[a]	[3s2p1d/2s]	1.371	1.567	1.092	134.80°
MR BWCCSD[a]	cc-pVDZ	1.365	1.570	1.092	134.86°
MR BWCCSD[a]	cc-pVTZ	1.347	1.558	1.077	134.91°
MR BWCCSD(T)	[3s2p1d/2s]	1.375	1.573	1.093	134.80°
MR BWCCSD(T)	cc-pVDZ	1.370	1.575	1.095	134.87°
MR BWCCSD(T)	cc-pVTZ	1.354	1.564	1.079	134.94°
MR BWCCSD(T_d)	[3s2p1d/2s]	1.377	1.571	1.093	134.80°
MR BWCCSD(T_d)	cc-pVDZ	1.372	1.574	1.095	134.87°
MR BWCCSD(T_d)	cc-pVTZ	1.355	1.563	1.079	134.92°
MR BWCCSD(T)[a]	[3s2p1d/2s]	1.377	1.572	1.094	134.81°
MR BWCCSD(T)[a]	cc-pVDZ	1.372	1.574	1.095	134.88°
MR BWCCSD(T)[a]	cc-pVTZ	1.354	1.563	1.079	134.92°
MR BWCCSD(T_d)[a]	[3s2p1d/2s]	1.378	1.570	1.094	134.81°
MR BWCCSD(T_d)[a]	cc-pVDZ	1.373	1.573	1.095	134.88°
MR BWCCSD(T_d)[a]	cc-pVTZ	1.356	1.562	1.079	134.92°

[a] Calculated using the iterative correction to size-extensivity.

The bond lengths have a decreasing trend with the size of the basis set for both structures and both MR BWCCSD and MR BWCCSD(T) methods, with the only exception being the single C-C bond length for the ground state. The magnitude of the changes of the bond lengths between results in the cc-pVDZ and the cc-pVTZ basis set is about $0.010 - 0.017$ Å for carbon-carbon bonds, and 0.016 Å for carbon-hydrogen bonds.

The difference between geometries obtained by MR BWCCSD(T) and MR BWCCSD(T_d) were found to be rather limited. Also, the type of size-

extensivity correction has a little effect on the equilibrium geometry.

Table 5.25: Optimum geometries of the transition state of cyclobutadiene

Method	Basis set	r_{C-C} Å	r_{C-H} Å
MR BWCCSD	[3s2p1d/2s]	1.462	1.091
MR BWCCSD	cc-pVDZ	1.459	1.092
MR BWCCSD	cc-pVTZ	1.444	1.076
MR BWCCSD[a]	[3s2p1d/2s]	1.463	1.091
MR BWCCSD[a]	cc-pVDZ	1.459	1.092
MR BWCCSD[a]	cc-pVTZ	1.444	1.076
MR BWCCSD(T)	[3s2p1d/2s]	1.468	1.092
MR BWCCSD(T)	cc-pVDZ	1.465	1.094
MR BWCCSD(T)	cc-pVTZ	1.451	1.078
MR BWCCSD(T_d)	[3s2p1d/2s]	1.469	1.093
MR BWCCSD(T_d)	cc-pVDZ	1.466	1.094
MR BWCCSD(T_d)	cc-pVTZ	1.452	1.078
MR BWCCSD(T)[a]	[3s2p1d/2s]	1.468	1.093
MR BWCCSD(T)[a]	cc-pVDZ	1.466	1.094
MR BWCCSD(T)[a]	cc-pVTZ	1.451	1.078
MR BWCCSD(T_d)[a]	[3s2p1d/2s]	1.469	1.093
MR BWCCSD(T_d)[a]	cc-pVDZ	1.466	1.093
MR BWCCSD(T_d)[a]	cc-pVTZ	1.452	1.078

[a] Calculated using the iterative correction to size-extensivity.

The inclusion of connected triples leads to an increase in the bond lengths. For the ground state, its is $0.005 - 0.007$ Å for the C=C bond, 0.005 Å for the C-C, and $0.001 - 0.002$ Å for the C-H bond. For the square structure, the increase is $0.005 - 0.006$ Å for C-C bond, and $0.001 - 0.002$ Å for the C-H bond. The effect on the C-C-H angle was found to be negligible. Again, both the type of size-extensivity correction and of the noniterative triples approach has little effect on the geometry.

The energies of both the rectangular and square structures are listed in the first two columns of Table 5.26. The third column contains the energy differences between the two states.

Similarly to geometries, there is a clear growing trend for the size of the energy gap between the two states with the basis set size and quality

of the method used. Larger basis sets lead to a larger value of ΔE, with the difference between the [3s2p1d/2s] and the cc-pVDZ basis set results 0.5 − 0.7 kcal/mol and difference between the cc-pVDZ and the cc-pVTZ basis set being 0.9 − 1.1 kcal/mol.

The MR BWCCSD(T) results of ΔE are consistently lower than those of MR BWCCSD, with the difference increasing with the size of the basis set from 0.2 kcal/mol for [3s2p1d/2s] to 0.6 kcal/mol for the cc-pVTZ basis set.

Table 5.26: The automerization barrier of cyclobutadiene

Method	Basis set set	E_{gs}^a ground state a.u.	E_{ts}^b transition state a.u.	ΔE kcal/mol
MR BWCCSD	[3s2p1d/2s]	-154.190896	-154.181697	5.8
MR BWCCSD	cc-pVDZ	-154.218996	-154.208680	6.5
MR BWCCSD	cc-pVTZ	-154.362879	-154.350776	7.6
MR BWCCSD^c	[3s2p1d/2s]	-154.191690	-154.183033	5.4
MR BWCCSD^c	cc-pVDZ	-154.219565	-154.209745	6.2
MR BWCCSD^c	cc-pVTZ	-154.363425	-154.351684	7.4
MR BWCCSD(T)	[3s2p1d/2s]	-154.211307	-154.202402	5.6
MR BWCCSD(T)	cc-pVDZ	-154.242451	-154.232711	6.1
MR BWCCSD(T)	cc-pVTZ	-154.397116	-154.385917	7.0
MR BWCCSD(T_d)	[3s2p1d/2s]	-154.212269	-154.204300	5.0
MR BWCCSD(T_d)	cc-pVDZ	-154.243409	-154.234616	5.3
MR BWCCSD(T_d)	cc-pVTZ	-154.397856	-154.387497	6.5
MR BWCCSD(T)^c	[3s2p1d/2s]	-154.212131	-154.203876	5.2
MR BWCCSD(T)^c	cc-pVDZ	-154.243043	-154.233899	5.7
MR BWCCSD(T)^c	cc-pVTZ	-154.397688	-154.386926	6.8
MR BWCCSD(T_d)^c	[3s2p1d/2s]	-154.213198	-154.205814	4.6
MR BWCCSD(T_d)^c	cc-pVDZ	-154.244097	-154.235846	5.2
MR BWCCSD(T_d)^c	cc-pVTZ	-154.398499	-154.388534	6.3

^{a} Energy of the ground state.
^{b} Energy of the transition state
^{c} Calculated using the iterative correction to size-extensivity.

Comparing the results of MR BWCCSD(T) and MR BWCCSD(T_d), the energies obtained by MR BWCCSD(T_d) are lower for both the ground state as well as for the square transition structure. However, the decrease of the energy is larger for the transition state, and therefore MR BWCCSD(T_d) pro-

vides values of ΔE lower by 0.5-0.6 kcal/mol, compared to MR BWCCSD(T) results. This situation is very similar to the methylene and silylene, where also gaps calculated by MR BWCCSD(T_d) were significantly lower than the MR BWCCSD(T) ones. From the experience from the previous section, the results of MR BWCCSD(T) should be regarded as more reliable.

The use of the iterative size-extensivity correction leads to a further decrease of the ΔE value. The magnitude of this change is 0.3-0.4 kcal/mol for the MR BWCCSD method and 0.2-0.4 kcal/mol for MR BWCCSD(T) and MR BWCCSD(T_d). Therefore, there has been found no increase of dependence of MR BWCCSD(T) and MR BWCCSD(T_d) on the type of the size-extensivity correction used, compared to MR BWCCSD.

5.4.3 Conclusions

The automerization barrier of cyclobutadiene was studied at MR BWCCSD, MR BWCCSD(T) and MR BWCCSD(T_d) levels. MR BWCCSD(T) values of the energy gaps were found to be 0.2-0.6 kcal/mol lower compared to MR BWCCSD, where the use of larger the basis sets corresponds to a larger difference in ΔE. MR BWCCSD(T_d) results of ΔE lie 0.5-0.6 kcal/mol below the MR BWCCSD(T) ones. The use of iterative correction of size-extensivity leads to further decrease of ΔE by approximately 0.2-0.4 kcal/mol for all the three methods used.

The size of the basis set used was found to have a crucial importance, as well as the necessity to optimize the geometries in the cc-pVTZ basis set, instead of using the cc-pVDZ geometries. Also, the type of size-extensivity correction is also important. The relative changes of energies due to the different size-extensivity corrections were found to be very similar for all the three methods. This is an argument justifying the use the a posteriori size-extensivity correction along with the noniterative inclusion of connected triples.

100

Chapter 6

Conclusions

Multireference Brillouin-Wigner coupled clusters with the inclusion of connected triple excitations has been developed and implemented in the ACES II program. The inclusion of connected triples was carried out in both iterative and noniterative way.

First of these approaches was the MR BWCCSDT-α method, which is a multireference generalization of the CCSDT method, with the omission of unlinked and disconnected terms in T_3 equation. It was found that the inclusion of connected triples has a dramatic positive effect on vibrational frequencies of the three electronic states of the oxygen molecule.

The remaining disconnected and unlinked terms have been added into the calculation procedure to obtain the full MR BWCCSDT method. The study of the oxygen molecule found results very close to MR BWCCSDT-α ones. The main improvement is an increased numerical stability, which enabled calculation with an extended model space.

The study of the C_{2v} insertion pathway of a beryllium atom to hydrogen molecule found a very good agreement of MR BWCCSDT and MR BWCCSDT-α methods with the full configuration interaction. The differences between the full method and its α approximation were largest in the region of the transition state. This is due to the strong multireference character of the system in this region, which results in larger values of disconnected and unlinked terms.

Finally, the noniterative inclusion of connected triples has been carried out in two different ways. Both approaches are based on triples correction to the matrix elements of the effective Hamiltonian. In MR BWCCSD(T_d), only the diagonal elements are corrected, whereas in MRBWCCSD(T) the

correction concerns all the elements.

For the oxygen molecule, results of both noniterative methods were found to be in a good agreement with both the experimental data and results of calculations with iterative connected triples.

By a comparison with MR BWCCSDT-1, the study of methylene and silylene has found a superior performance of the MR BWCCSD(T) method compared to MR BWCCSD(T_d). For the $^1A_1$ state, both of these methods gave results in an excellent agreement with the experiment, when a sufficiently large basis set was used and the calculation was carried out without size-extensivity correction, which is appropriate for very small systems.

The study of the automerization of cyclobutadiene was used to demonstrate the applicability of the MR BWCCSD(T) method to moderately sized systems. The reduced computational cost of the method enabled a full geometry optimization of the system in cc-pVTZ basis set. For the height of the energetic barrier, the inclusion of connected triples played a relatively minor role. The role of the basis set size was found to be more important. From comparison of results with different size-extensivity corrections, it was found that the differences remain almost constant at all calculation levels, which justifies the use of the a posteriori size-extensivity correction alongside with the noniterative inclusion of connected triples.

The development in this field is far from complete. Among the most important problems, that remain to be solved, are the investigation of numerical effects of the noninvariance of the MR BWCCSD(T) method with respect to unitary occupied-occupied and virtual-virtual orbital transformations, calculations with mutually triexcited reference configurations, and calculations with an incomplete model space.

However, the existing evidence suggests, that the inclusion of connected triples to the multireference Brillouin-Wigner coupled clusters theory yields a highly accurate method suitable for systems with quasidegenetate orbitals, and that the noniterative approach is applicable to a wide range of chemically interesting systems.

Bibliography

[1] F. Coester, Nucl. Phys. **7**, 421 (1958).

[2] F. Coester and H. Kümmel, Nucl. Phys. **17**, 477 (1960).

[3] H. Kümmel, Theor. Chim. Acta **80**, 81 (1991).

[4] M. Gell-Mann and F. Low, Phys. Rev. **84**, 350 (1951).

[5] J. Hubbard, Proc. Roy. Soc. (London) A **240**, 539 (1957).

[6] J. Čížek, J. Chem. Phys. **45**, 4256 (1966).

[7] R. J. Bartlett and G. D. Purvis III, Int. J. Quant. Chem. **14**, 561 (1978).

[8] J. A. Pople, R. Krishnan, H. B. Schlegel, and J. S. Binkey, Int. J. Quant. Chem. **14**, 545 (1978).

[9] G. D. Purvis and R. J. Bartlett, J. Chem. Phys. **76**, 1910 (1982).

[10] J. Noga and R. J. Bartlett, J. Chem. Phys. **86**, 7041 (1987).

[11] J. Noga and R. J. Bartlett, J. Chem. Phys. **89**, 3401 (1988).

[12] J. D. Watts and R. J. Bartlett, J. Chem. Phys. **93**, 6104 (1990).

[13] J. D. Watts and R. J. Bartlett, Int. J. Quant. Chem. Symp. **27**, 51 (1993).

[14] G. E. Scuseria and H. F. Schaeffer, Chem. Phys. Lett. **152**, 382 (1988).

[15] Y. S. Lee, S. A. Kucharski, and R. J. Bartlett, J. Chem. Phys. **81**, 5906 (1984).

[16] M. Urban, J. Noga, S. J. Cole, and R. J. Bartlett, J. Chem. Phys. **83**, 4041 (1985).

[17] G. E. Scuseria *et al.*, J. Chem. Phys. **86**, 2881 (1987).

[18] K. Raghavachari, J. Chem. Phys. **82**, 4607 (1985).

[19] T. J. Lee and G. E. Scuseria, in *Quantum Mechanical Electronic Structure Calculations with Chemical Accuracy*, edited by S. R. Langhoff (Kluwer Academic, Dordrecht, YEAR), pp. 47–108.

[20] K. Raghavachari, G. W. Trucks, J. A. Pople, and M. Head-Gordon, Chem. Phys. Lett. **157**, 479 (1989).

[21] R. J. Bartlett, J. D. Watts, S. A. Kucharski, and J. Noga, Chem. Phys. Lett. **165**, 513 (1990).

[22] J. Gauss *et al.*, Chem. Phys. Lett. **182**, 207 (1991).

[23] J. D. Watts, J. Gauss, and R. J. Bartlett, J. Chem. Phys. **98**, 8718 (1993).

[24] J. D. Watts, J. Gauss, and R. J. Bartlett, J. Chem. Phys. **98**, 8718 (1993).

[25] S. A. Kucharski and R. J. Bartlett, J. Chem. Phys. **97**, 4282 (1992).

[26] S. A. Kucharski and R. J. Bartlett, Theor. Chim. Acta **80**, 387 (1991).

[27] M. Musial, S. A. Kucharski, and R. J. Bartlett, J. Chem. Phys. **116**, 4382 (2002).

[28] M. Kállay, P. G. Szalay, and P. R. Surján, J. Chem. Phys. **117**, 980 (2002).

[29] J. Paldus, in *Methods in Computational Molecular Physics, NATO ASI Series*, edited by S. Wilson and G. H. F. Diercksen (Plenum, New York, 1992), pp. 99–194.

[30] J. Paldus, in *Theory and Applications of Computational Chemistry: The First 40 Years* (Elsevier, Amsterdam, The Netherlands, 2005), p. in press.

[31] J. Gauss, in *The Encyclopedia of Computational Chemistry*, edited by P. v. R. Schleyer *et al.* (Wiley, Chichester, 1998), pp. 615–636.

[32] R. J. Bartlett and J. Stanton, in *Reviews in Computational Chemistry*, edited by K. B. Lipkowitz and D. B. Boyd (VCH Publishers, New York, 1994), Vol. 5, pp. 65–169.

104

[33] R. J. Bartlett, in *Modern Electronic Structure Theory, Part I*, edited by D. R. Yarkony (World Scientific, Singapore, 1995).

[34] I. Lindgren, Int. J. Quant. Chem. **Symp. 12**, 33 (1978).

[35] I. Lindgren and D. Mukherjee, Phys. Rev. **151**, 93 (1987).

[36] D. Mukherjee and S. Pal, Adv. Quant. Chem. **20**, 292 (1981).

[37] B. Jeziorski and J. Paldus, J. Chem. Phys. **90**, 2714 (1989).

[38] K. Jankowski, J. Paldus, and I. G. nd K. Kowalski, J. Chem. Phys. **97**, 7600 (1992).

[39] U. Kaldor, Theor. Chim. Acta **80**, 427 (1991).

[40] K. Jankowski and P. Malinowski, J. Phys. B **27**, 829 (1994).

[41] B. Jeziorski and H. J. Monkhorst, Phys. Rev. A **24**, 1668 (1981).

[42] S. A. Kucharski and R. J. Bartlett, J. Chem. Phys. **95**, 8227 (1991).

[43] A. Balková, S. A. Kucharski, and R. J. Bartlett, Chem. Phys. Lett. **182**, 511 (1991).

[44] A. Balková and R. J. Bartlett, Chem. Phys. Lett. **193**, 364 (1992).

[45] A. Balková, S. A. Kucharski, L. Meissner, and R. J. Bartlett, J. Chem. Phys. **95**, 4311 (1991).

[46] A. Balková and R. J. Bartlett, J. Chem. Phys. **101**, 8972 (1994).

[47] U. S. Mahapatra, B. Datta, and D. Mukherjee, J. Chem. Phys. **110**, 6171 (1999).

[48] U. S. Mahapatra, B. Datta, and D. Mukherjee, Chem. Phys. Lett. **299**, 42 (1999).

[49] N. Oliphant and L. Adamowicz, J. Chem. Phys. **94**, 1229 (1991).

[50] P. Piecuch and L. Adamowicz, J. Chem. Phys. **100**, 5792 (1994).

[51] J. Padus, J. Čížek, and M. Takahashi, Phys. Rev. A **30**, 2193 (1984).

[52] J. Padus, M. Takahashi, and R. H. W. Cho, Phys. Rev. B **30**, 4267 (1984).

[53] M. Takahashi and J. Padus, Phys. Rev. B **31**, 5121 (1985).

[54] P. Piecuch, R. Toboła, and J. Padus, Phys. Rev. A **54**, 1210 (1996).

[55] S. M. Bachrach, R. A. Chiles, and C. E. Dykstra, J. Chem. Phys. **75**, 69 (1981).

[56] C. E. Dykstra *et al.*, Chem. Phys. Lett. **137**, 266 (1987).

[57] C. E. Dykstra and E. R. Davidson, Int. J. Quant. Chem. **78**, 226 (2000).

[58] J. Paldus and J. Planelles, Theor. Chim. Acta **89**, 13 (1994).

[59] L. S. Stolarczyk, Chem. Phys. Lett. **217**, 1 (1994).

[60] X. Li and J. Paldus, J. Chem. Phys. **107**, 6257 (1997).

[61] X. Li and J. Paldus, J. Chem. Phys. **108**, 637 (1998).

[62] X. Li and J. Paldus, J. Chem. Phys. **113**, 9966 (2000).

[63] X. Li and J. Paldus, J. Chem. Phys. **118**, 2470 (2003).

[64] X. Li and J. Paldus, J. Chem. Phys. **115**, 5759 (2001).

[65] X. Li and J. Paldus, J. Chem. Phys. **117**, 1941 (2002).

[66] X. Li and J. Paldus, J. Chem. Phys. **118**, 2470 (2003).

[67] K. Kowalski and P. Piecuch, J. Chem. Phys. **113**, 18 (2000).

[68] K. Kowalski and P. Piecuch, J. Molec. Struc. (Theochem) **547**, 191 (2001).

[69] H. Sekino and R. J. Bartlett, Int. J. Quant. Chem. Symp. **18**, 255 (1981).

[70] J. Geertsen, M. Rittby, and R. J. Bartlett, Chem. Phys. Lett. **164**, 57 (1989).

[71] D. Comeau and R. J. Bartlett, Chem. Phys. Lett. **207**, 414 (1993).

[72] J. Stanton and R. J. Bartlett, J. Chem. Phys. **98**, 7029 (1993).

[73] M. Nooijen, J. Chem. Phys. **104**, 2638 (1996).

[74] M. Nooijen and R. J. Bartlett, J. Chem. Phys. **106**, 6441 (1997).

[75] M. Nooijen and R. J. Bartlett, J. Chem. Phys. **107**, 6812 (1997).

[76] M. Nooijen and V. Lotrich, J. Chem. Phys. **113**, 494 (2000).

[77] W. D. Laidig, P. Saxe, and R. J. Bartlett, J. Chem. Phys. **86**, 887 (1987).

[78] P. G. Szalay and R. J. Bartlett, J. Chem. Phys. **213**, 481 (1993).

[79] P. G. Szalay and R. J. Bartlett, Chem. Phys. Lett. **103**, 3600 (1995).

[80] H. Lischka *et al.*, Phys. Chem. Chem. Phys. **3**, 664 (2001).

[81] R. J. Gdanitz and R. Ahlrichs, Chem. Phys. Lett. **143**, 413 (1988).

[82] P. J. A. Ruttink, J. H. van Lenthe, R. Zwaans, and G. C. Groenenboom, J. Chem. Phys. **94**, 7212 (1991).

[83] I. Hubač, in *New Methods in Quantum Theory, NATO ASI Series*, edited by A. Tsipis, V. S. Popov, D. R. Herschbach, and J. S. Avery (Kluwer, Dordrecht, 1996), pp. 183–202.

[84] I. Hubač *et al.*, in *Computational Chemistry. Reviews of Current Trends.*, edited by J. Leszczynski (World Scientific, Singapore, 1999), Vol. 3, pp. 1–48.

[85] J. Mášik and I. Hubač, Adv. Quant. Chem. **31**, 75 (1999).

[86] J. Pittner, P. Nachtigall, P. Čársky, and I. Hubač, J. Phys. Chem. A **105**, 1354 (2001).

[87] J. Pittner, J. Šmydke, P. Čársky, and I. Hubač, J. Molec. Struc. (Theochem) **547**, 239 (2001).

[88] J. Pittner, H. Valdes-González, R. J. Gdanitz, and P. Čársky, Chem. Phys. Lett. **386**, 211 (2004).

[89] J. Pittner and O. Demel, J. Chem. Phys. **122**, 181101 (2005).

[90] I. Hubač and S. Wilson, J. Phys. B **33**, 365 (2000).

[91] I. Hubač, J. Pittner, and P. Čársky, J. Chem. Phys. **112**, 8779 (2000).

[92] J. Pittner, J. Chem. Phys. **118**, 10876 (2003).

[93] J. Pittner *et al.*, J. Chem. Phys. **110**, 10275 (1999).

[94] O. Demel, J. Pittner, P. Čársky, and I. Hubač, J. Phys. Chem. A **108**, 3125 (2004).

[95] J. Brabec and J. Pittner, J. Phys. Chem. A submitted .

[96] J. Pittner, P. Čársky, and I. Hubač, Int. J. Quant. Chem. **90**, 1031 (2002).

[97] J. Pittner, O. Demel, P. Čársky, and I. Hubač, Int. J. Mol. Sci. **2**, 281 (2002).

[98] I. S. K. Kerkines *et al.*, J. Chem. Phys. **117**, 9733 (2002).

[99] V. I. Teberekidis *et al.*, Int. J. Quant. Chem. **102**, 762 (2005).

[100] J. C. Sancho-García, J. Pittner, P. Čársky, and I. Hubač, J. Chem. Phys. **112**, 8785 (2000).

[101] O. Rey-Puiggros *et al.*, Collect. Czech. Chem. Commun. **68**, 2309 (2003).

[102] T. H. Dunning Jr., Chem. Phys. **42**, 249 (1979).

[103] X. Li and J. Paldus, J. Chem. Phys. **124**, 034112 (2006).

[104] X. Li and J. Paldus, submitted (2005).

[105] N. Vaval, S. Pal, and D. Mukherjee, Theor. Chem. Acc. **99**, 100 (1998).

[106] M. Musial and R. J. Bartlett, J. Chem. Phys. **121**, 1670 (2004).

[107] A. Szabo and N. S. Ostlund, *Modern quantum chemistry* (McGraw-Hill Publishing Company, New York, 1989).

[108] T. Helgaker, P. Jørgensen, and J. Olsen, *Molecular Electronic-Structure Theory* (John Wiley & Sons, Chichester, 2000).

[109] J. Paldus, *Diagrammatic Methods for Many-Fermion Systems* (Lecture Notes, University of Nijmegen, 1981).

[110] S. A. Kucharski and R. J. Bartlett, Adv. Quant. Chem. **18**, 281 (1986).

[111] V. Kvasnička and S. Biskupič, *Diagramatické metody v kvantovej teórii molekul* (Veda, Bratislava, 1987).

[112] R. Polák and R. Zahradník, *Kvantová chemie* (SNTL, Prague, 1985).

[113] J. Fišer, *Úvod do kvantové chemie* (Academia, Praha, 1983).

[114] L. Skála, *Kvantová teorie molekul* (Karolinum, Praha, 1995).

[115] J. Goldstone, Proc. Roy. Soc. (London) A **239**, 267 (1957).

[116] N. M. Hugenholtz, Physica **23**, 481 (1957).

[117] B. H. Brandow, Adv. Quant. Chem. **10**, 187 (1977).

[118] F. A. Matsen and R. Paunz, *The unitary group in quantum chemistry* (Elsevier, Amsterdam, 1986).

[119] N. H. March, W. H. Young, and S. Sampanthar, *The Many Body Problems in Quantum Mechanics* (Cambridge Univ. Press, Cambridge, 1976).

[120] S. Raimes, *Many-Electron Theory* (North-Holland, Amsterdam, 1972).

[121] P. Čársky and M. Urban, *Lecture Notes in Chemistry* (No. 16 Springer Verlag, Berlin, 1980).

[122] H. P. Kelly, Adv. Chem. Phys. **14**, 129 (1969).

[123] I. Hubač, M. Urban, and V. Kellö, Chem. Phys. Lett. **62**, 584 (1979).

[124] M. Urban, I. Hubač, V. Kellö, and J. Noga, J. Chem. Phys. **72**, 3378 (1980).

[125] I. Lindgren and J. Morrison, *Atomic Many-Body Theory* (Springer Verlag, Berlin, 1986).

[126] R. J. Bartlett and I. Shavitt, Chem. Phys. Lett. **12**, 737 (1977).

[127] R. J. Bartlett and D. M. Silver, in *Quantum Science*, edited by J. L. Calais, O. Goscinski, J. Lindeberg, and Y. Öhrn (Plenum, New York, 1976), p. 393.

[128] R. J. Bartlett and G. D. P. III., Physica Scripta **21**, 255 (1980).

[129] X. Li and J. Paldus, J. Chem. Phys. **119**, 5320 (2003).

[130] X. Li and J. Paldus, J. Chem. Phys. **119**, 5334 (2003).

[131] O. Demel and J. Pittner, J. Chem. Phys. **124**, 144112 (2006).

[132] K. P. Huber and G. Herzberg, *Molecular spectra and molecular structure* (Van Nostrand Reinhold, New York, 1979), Vol. 4.

[133] O. L. Polyansky *et al.*, Science **299**, 539 (2003).

[134] ACES II is a program product of Quantum Theory Project, University of Florida, J. F. Stanton, J. Gauss, J. D. Watts, M. Nooijen, N. Oliphant, S. A. Perera, P. G. Szalay, W. J. Lauderdale, S. R. Gwaltney, S. Beck, A. Balková, D. E. Bernholdt, K.-K. Baeck, P. Rozyczko, H. Sekino, C. Huber, and R. J. Bartlett. Integral packages included are VMOL (J. Almloef and P. R. Taylor); VPROPS (P. R. Taylor); and ABACUS (T. Helgaker, H. J. Aa. Jensen , P. Joergensen, J. Olsen, and P. R. Taylor).

[135] S. B. Sharp and G. I. Gellene, J. Phys. Chem. A **104**, 10951 (2000).

[136] A. Barnjee and J. Simons, J. Chem. Phys. **81**, 281 (1983).

[137] R. K. Chaudhuri, J. P. Finley, and F. K. Freed, J. Chem. Phys. **106**, 4067 (1997).

[138] M. Kállay, P. G. Szalay, and P. R. Surján, J. Chem. Phys. **117**, 980 (2002).

[139] R. J. Gdanitz, Int. J. Quant. Chem. **85**, 281 (2001).

[140] G. D. Purvis, R. Shepard, F. B. Brown, and R. J. Bartlett, Int. J. Quant. Chem. **23**, 835 (1983).

[141] W. T. Borden, in *The Encyclopedia of Computational Chemistry*, edited by P. v. R. Schleyer *et al.* (Wiley, Chichester, 1998), pp. 485–497.

[142] J. M. Foster and S. F. Boys, Rev. Mol. Phys. **32**, 305 (1960).

[143] H. Herzberg and J. Shoesmith, Nature **183**, 1801 (1959).

[144] G. Herzberg and J. W. C. Johns, J. Chem. Phys. **54**, 2276 (1971).

[145] P. R.Bunker and P. Jensen, J. Chem. Phys. **79**, 1224 (1983).

[146] P. Jensen and P. R.Bunker, J. Chem. Phys. **89**, 1327 (1988).

[147] H. Petek *et al.*, J. Chem. Phys. **91**, 6566 (1989).

[148] I. Shavitt, Tetrahedron **41**, 1531 (1985).

[149] H. F. Schaefer, Science **231**, 1100 (1986).

[150] W. A. Goddard III, Science **227**, 917 (1985).

[151] C. D. Sherill, T. J. Van Huis, Y. Yamaguchi, and H. F. Schaefer III, J. Molec. Struc. (Theochem) **400**, 130 (1997).

[152] C. W. Bauschlicher, L. R. Langhoff, and P. R. Taylor, J. Chem. Phys. **87**, 387 (1987).

[153] C. D. Sherill, T. J. Van Huis, Y. Yamaguchi, and H. F. Schaefer III, J. Chem. Phys. **108**, 1040 (1998).

[154] A. G. Császár, M. L. Leininger, and V. Szalay, J. Chem. Phys. **118**, 10631 (2003).

[155] A. Neugebauer and G. Hafelinger, Int. J. Mol. Sci. **6**, 157 (2005).

[156] Y. Apeloig *et al.*, Organometallics **22**, 3250 (2003).

[157] K. A. Peterson and T. H. Dunning, J. Chem. Phys. **106**, 4119 (1997).

[158] A. Kalemos, T. H. Dunning, A. Mavridis, and J. F. Harrison, Can. J. Chem. **82**, 684 (2004).

[159] D. E. Woon and H. T. Dunning, J. Chem. Phys. **103**, 4572 (1995).

[160] D. C. Comeau, I. Shavitt, P. Jensen, and P. R. Bunker, J. Chem. Phys. **90**, 6491 (1989).

[161] P. G. Wenthold, Chem. Phys. Lett. **297**, 445 (1998).

[162] T. D. Jr., J. Chem. Phys. **90**, 1007 (1989).

[163] D. Woon and J. T.H. Dunning, J. Chem. Phys. **98**, 1358 (1993), basis sets were obtained from the Extensible Computational Chemistry Environment Basis Set Database, Version 02/25/04, as developed and distributed by the Molecular Science Computing Facility, Environmental and Molecular Sciences Laboratory which is part of the Pacific Northwest Laboratory, P.O. Box 999, Richland, Washington 99352, USA, and funded by the U.S. Department of Energy. The Pacific Northwest Laboratory is a multi-program laboratory operated by Battelle Memorial Institute for the U.S. Department of Energy under contract DE-AC06-76RLO 1830. Contact Karen Schuchardt for further information.

[164] R. Zahradník and L. Šroubková, Isr. J. Chem. **43**, 243 (2003).

111

[165] R. Zahradník and L. Šroubková, Int. J. Quant. Chem. **104**, 52 (2005).

[166] J. P. Gu *et al.*, J. Molec. Struct. **517+518**, 247 (2000).

[167] G. Duxbury, A. Alijah, B. D. McDonald, and C. Jungen, J. Chem. Phys. **108**, 2351 (1998).

[168] R. EScribano and A. Campargue, J. Chem. Phys. **108**, 6249 (1998).

[169] J. Berkowitz, J. P. Greene, H. Cho, and B. Ruscic, J. Chem. Phys. **86**, 1235 (1987).

[170] L. C. Snyder, J. Phys. Chem. **66**, 2299 (1962).

[171] R. J. Bunker and S. D. Peyerimhoff, J. Chem. Phys. **48**, 354 (1968).

[172] H. Kollmar and V. Staemmler, J. Am. Chem. Soc. **100**, 4303 (1978).

[173] J. A. Jafri and M. D. Newton, J. Am. Chem. Soc. **100**, 5012 (1978).

[174] M. J. S. Dewar, K. M. M. Jr., and J. J. P. Stewart, J. Am. Chem. Soc. **106**, 4040 (1984).

[175] H. Ångren, N. Correia, A. Flores-Riveros, and H. J. Å. Jensen, Int. J. Quant. Chem. **19**, 237 (1986).

[176] F. Fratav, V. Monev, and R. Janoschek, Tetrahedron **38**, 2929 (1982).

[177] P. Čársky *et al.*, J. Chem. Phys. **89**, 3080 (1988).

[178] P. Čársky, , J. W. Downing, and J. Michl, Int. J. Quant. Chem. **40**, 415 (1991).

[179] A. F. Voter and I. W. A. Goddard, J. Am. Chem. Soc. **108**, 2830 (1986).

[180] K. Nakamura, Y. Osamura, and S. Iwata, J. Chem. Phys. **36**, 67 (1989).

[181] V. Bonačič-Koutecký, K. Schöffel, and J. Michl, J. Am. Chem. Soc. **111**, 6140 (1989).

[182] J. C. Sancho-Garcia and F. Moscardo, J. Chem. Phys. **118**, 1054 (2003).

[183] S. V. Levchenko, T. Wang, and A. I. Krylov, J. Chem. Phys. **122**, (2005).

[184] B. Arnold and J. Michl, in *Kinetics and Spectroscopy of Carbenes and Biradicals*, edited by M. Platz (Plenum, New York, 1989), p. 1.

[185] A. M. Orendt *et al.*, J. Am. Chem. Soc. **110**, 2648 (1988).

[186] D. W. Whitman and B. K. Carpenter, J. Am. Chem. Soc. **105**, 6473 (1983).

[187] R. Lefevbre and N. Moiseyev, J. Am. Chem. Soc. **112**, 5052 (1990).

[188] W. T. Borden, E. R. Davidson, and D. Feller, J. Am. Chem. Soc. **103**, 5725 (1981).